Facultad de Biología

Departamento de Fisiología

TESIS DOCTORAL

Reacción glial tras el implante de precursores neurales en un modelo de lesión del sistema nervioso central

Rocío Talaverón Aguilocho

Sevilla, 2015

ESPERANZA R. MATARREDONA, Profesora titular del Dpto. de Fisiología de la Facultad de Biología, Universidad de Sevilla.

ÁNGEL M. PASTOR, Catedrático del Dpto. de Fiología de la Facultad de Biología, Universidad de Sevilla.

CERTIFICAN:

Que Dña. Rocío Talaverón Aguilocho, Licenciada en Biología por la Universidad de Sevilla, ha realizado bajo su dirección y supervisión el trabajo titulada "Reacción glial tras el implante precursores neurales en un modelo de lesión del sistema nervioso central", considerando que reúne todas las condiciones necesarias para ser presentado y defendido como Tesis Doctoral.

Sevilla, 26 de Junio de 2015.

Fdo: Esperanza R. Matarredona

Fdo: Ángel M. Pastor

ÍNDICE

ABREVIATURAS

aFGF: Factor acídico de crecimiento de fibroblastos

ATP: Trifosfato de adenosina

BDNF: Factor neurotrófico derivado del cerebro

BMP: Proteína morfogenética del hueso

BO: Bulbo olfatorio

CMR: Corriente migratoria rostral

CNTF: Factor neurotrófico ciliar

Cx: Conexina

CPNs: Células precursoras neurales

EGF: Factor de crecimiento epidérmico

EGFR: Receptor del factor de crecimiento epidérmico

ELA: Esclerosis lateral amiotrófica

FLM: Fascículo longitudinal medial

GDNF: Factor neurotrófico derivado de la glía

GFAP: Proteína glial fibrilar acídica

IGF: Factor de crecimiento parecido a la insulina

IL: Interleuquina

LIF: Factor inhibidor de leucemia

NAD^+: Nicotinamida adenina dinucleótido

NGF: Factor de crecimiento nervioso

NMOC: Núcleo motor ocular común

NMOE: Núcleo motor ocular externo

NP: Neuropilina

NT: Neurotrofina

PIGF: Factor de crecimiento de la placenta

PSA-NCAM: Molécula de adhesión neural polisializada

SNC: Sistema Nervioso Central

TGF-β: Factor de crecimiento transformante β

TNFα: Factor de necrosis tumoral α

Trk: Tropomiosina quinasa

VEGF: Factor de crecimiento derivado del endotelio vascular

VPF: Factor de permeabilidad vascular

ZSV: Zona subventricular

RESUMEN

En el cerebro adulto existen dos regiones con capacidad neurogénica, el giro dentado del hipocampo y la zona subventricular (ZSV). Las células precursoras neurales (CPNs) de la ZSV generan neuroblastos que migran al bulbo olfatorio donde se diferencian a interneuronas. Estas CPNs se pueden aislar y amplificar en cultivo. Se ha demostrado que el implante de CPNs en el cerebro lesionado tiene capacidad terapéutica, de manera que se restauran alteraciones morfológicas y fisiológicas derivadas de la lesión. Los efectos beneficiosos de estas células ante un daño en el cerebro se deben a diferentes factores, entre los que destacan su potencialidad como fuente de factores tróficos y su capacidad para integrarse e interaccionar con las células del tejido hospedador. Recientemente se ha descrito que el implante de CPNs de la ZSV en un modelo de lesión cerebral consistente en la axotomía de las neuronas internucleares del núcleo motor ocular externo produce la recuperación del patrón de disparo y de la cobertura sináptica inhibidora de las neuronas lesionadas. En esta Tesis Doctoral se han realizado implantes de CPNs provenientes de la ZSV en el mismo modelo de lesión, con el fin de profundizar en los mecanismos implicados en las funciones reparativas del implante. Concretamente se ha analizado el efecto del implante sobre la expresión de factores neurotróficos de las neuronas lesionadas y sobre la reacción glial derivada de la lesión. También se ha estudiado la posibilidad de comunicación mediante uniones gap entre las CPNs implantadas y las células gliales del hospedador pues existen evidencias previas de la participación de la comunicación mediante estas uniones en la integración de las células del implante y en los efectos beneficiosos del mismo. Hemos demostrado que los animales que recibieron implantes de CPNs tras la lesión incrementaron el contenido en el factor neurotrófico VEGF en las neuronas axotomizadas y que este factor que es expresado por las CPNs tras su implante. Respecto a la respuesta glial, las CPNs implantadas produjeron un aumento de la densidad de células de microglía en el lugar de la lesión y mostraron contactos directos con las mismas, además de con astrocitos reactivos. Tanto las CPNs como los astrocitos y microglía activada del hospedador expresaron la proteína de las uniones gap conexina 43. A nivel ultraestructural identificamos uniones gap entre las CPNs implantadas y las células gliales del hospedador. En experimentos *in vitro* realizados en

cocultivos de CPNs con astrocitos o con microglía demostramos también que las uniones gap establecidas entre estos tipos celulares fueron funcionales. Por tanto, los datos mostrados en esta Tesis Doctoral revelan que existen importantes interacciones celulares en el sitio de la lesión entre las CPNs implantadas y las células gliales del hospedador y planteamos la posibilidad de que estas interacciones intervengan tanto en la supervivencia de las células implantadas como en los efectos beneficiosos del implante.

INTRODUCCIÓN

1. CÉLULAS PRECURSORAS NEURALES

1.1 Neurogénesis en el cerebro postnatal y adulto

Se denomina neurogénesis al proceso de formación de nuevas neuronas. Hasta los años 60 se pensaba que los procesos de neurogénesis ocurrían solo durante el desarrollo embrionario y neonatal pero los estudios de Altman en los años 60 mostraron evidencias anatómicas de la existencia de células proliferativas que se convertían en neuronas en el giro dentado del hipocampo (Altman y Das, 1965).

Hoy día está establecido que la neurogénesis es un proceso continuo en la vida del individuo, aunque dicha actividad neurogénica ocurre primordialmente en dos regiones específicas del cerebro adulto, la capa subgranular del giro dentado del hipocampo (Eriksson et al., 1998) y la zona subventricular (ZSV) de la pared de los ventrículos laterales (Reynolds et al., 1992; Luskin, 1993; Doetsch y Alvarez-Buylla, 1996). También se ha propuesto la existencia de otras zonas neurogénicas en el cerebro adulto como la corteza cerebral, la sustancia negra o la zona subcallosa (Kornack and Rakic, 2001; Zhao et al., 2003; Seri et al., 2006) pero hasta el momento están menos consensuadas y caracterizadas. La existencia de neurogénesis en la etapa adulta ha planteado muchas dudas sobre su función y es un tema de actual debate, aunque en general se relaciona con procesos de plasticidad, aprendizaje y comportamientos afectivos (Nottebohm, 1985; Alvarez-Buylla et al., 1990; revisado en Ming and Song, 2011).

Durante el desarrollo embrionario, las células de la glía radial generadas a partir de células neuroepiteliales actúan como células precursoras neurales (CPNs) siendo capaces de generar todas las células de la estirpe neural: astrocitos, oligodendrocitos y neuronas. En las dos regiones neurogénicas mencionadas del cerebro adulto de mamíferos existe una población de CPNs con características similares a las células de la glía radial del desarrollo. Son células con capacidad de autorrenovación y de generar, en divisiones asimétricas, astrocitos, oligodendrocitos y precursores neuronales, a partir de los cuales se formarán las nuevas neuronas.

Mencionaremos ahora las características fundamentales de la capacidad neurogénica de la zona subventricular.

1.2 Células progenitoras neurales (CPNs) de la zona subventricular

La ZSV es una capa germinal que se forma durante el desarrollo embrionario adyacente a la zona ventricular que rodea los ventrículos laterales. La localización y la proliferación celular de la ZSV adulta sugieren que esta región deriva de la ZSV embrionaria de la eminencia ganglionar lateral aunque no se conoce realmente si los precursores neurales del embrión y de la ZSV adulta son equivalentes (García-Verdugo et al., 1998).

En la ZSV de mamíferos adultos existen células madre neurales con características de glía radial que generan células transitorias con alta capacidad proliferativa que a su vez dan lugar a los neuroblastos o precursores neuronales. Estos neuroblastos migran tangencialmente hacia el bulbo olfatorio (BO) a través de estructuras tubulares constituidas por astrocitos especializados, formando la llamada corriente migratoria rostral (CMR) (Figura 1). Una vez alcanzado su destino, inician una migración radial y se diferencian en interneuronas inhibitorias en las capas granular y periglomerular del bulbo olfatorio (Ghashghaei et al., 2007).

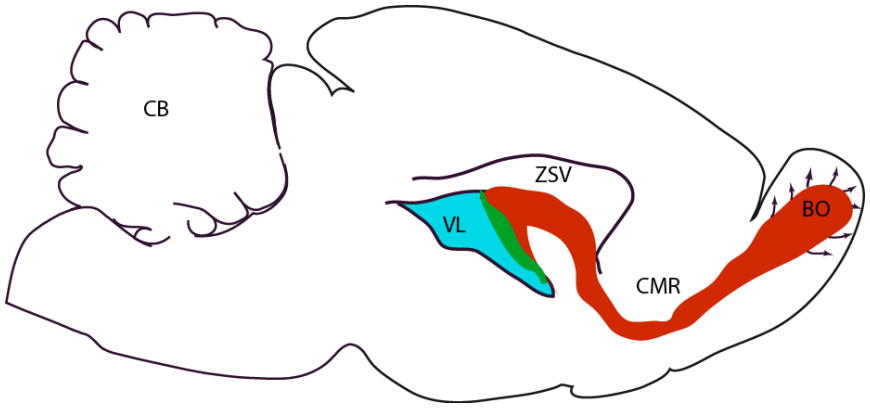

Figura 1: Esquema de la localización de la ZSV, corriente migratoria rostral y bulbo olfatorio en ratas adultas. Se muestra un esquema de un corte sagital de un cerebro de rata. La parte de la izquierda corresponde a la parte más caudal, como lo refleja la localización del cerebelo (CB). En azul se muestran un ventrículo lateral (VL), en verde observamos la zona subventricular (ZSV) y en rojo el camino migratorio rostral (CMR), la ruta que siguen los neuroblastos hasta el bulbo olfatorio (BO). Una vez en el BO los neuroblastos inician una migración radial (flechas) y se diferencian en interneuronas inhibitorias de las capas granular y periglomerular.

Por su morfología, ultraestructura y marcadores es posible distinguir varias poblaciones de células en la ZSV adulta (Figura 2B): las **células tipo B**, que son astrocitos con características de glía radial, pues algunos actúan como células madre neurales, las **células tipo C**, que son precursores neurales transitorios con alta capacidad proliferativa, las **células tipo A**, que son neuroblastos con capacidad migratoria, y las **células tipo E**, que son células ependimarias que tapizan los ventrículos laterales (Figura 2) (García-Verdugo et al., 1998). Todos estos tipos de células, junto con células de microglía, células endoteliales e incluso pericitos de la unión neurovascular, forman parte de lo que se conoce como el **nicho neurogénico** de la ZSV, que podemos definir como el conjunto de células y moléculas producidas por las mismas que forman un microambiente especializado en el mantenimiento y funcionalidad de la población de CPNs (revisado en Ming y Song, 2011; Crouch et al., 2015).

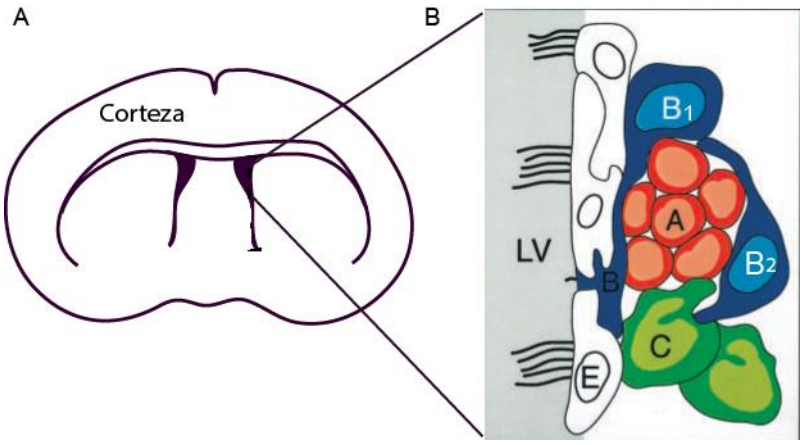

Figura 2: Esquema de la localización de la zona subventricular en cerebro de rata adulta y de los tipos celulares que presenta. En A observamos una representación esquemática de un corte coronal de cerebro de rata donde se resalta en un recuadro la localización de la zona subventricular adyacente a los ventrículos laterales. En B se representa un esquema de los tipos celulares de esta zona germinal: en contacto directo con los ventrículos (LV) se localizan las células ependimarias (E). En azul se identifican los astrocitos o células tipo B (B), que rodean a los neuroblastos o células tipo A (en rojo). En verde se representan los precursores neurales o células tipo C (C). Las células tipo B contactan con las tipo E, A y C, como se indica en el esquema. Modificado de Alvarez-Buylla y García-Verdugo, 2002.

Lo neuroblastos o células tipo A tienen capacidad migradora y proliferativa (Lois et al., 1996). Son positivos a marcadores como PSA-NCAM, β-III tubulina, doblecortina (Doetsch et al., 1999) y el factor de transcripción Dlx2.

La ultraestructura de las células tipo B indica que son astrocitos, son células que provienen de la glía radial embrionaria (Merkle et al., 2004) y que se han descrito como las células madre neurales de la ZSV, tanto durante procesos regenerativos como durante la homeostasis fisiológica (Doetsch and Alvarez-Buylla, 1996). En la ZSV se distinguen dos tipos de células B, llamadas B1 y B2. Las B1 se localizan entre los neuroblastos y las células ependimarias mientras que las B2 se sitúan entre los neuroblastos y el estriado (Figura 2B). Las células tipo B son positivas al marcador de astrocitos GFAP y tienen múltiples procesos con los que contactan con la luz del ventrículo, con los vasos sanguíneos y con otros tipos de células de la ZSV. En el camino migratorio rostral, las células B envuelven a las tipo A formando una especie de tubo glial que separa a los neuroblastos migradores del tejido circundante. En la migración de neuroblastos por el camino migratorio rostral intervienen factores liberados por los astrocitos del gliotubo y por la vasculatura que se dispone de forma paralela al trayecto del camino(Snapyan et al., 2009; Whitman and Greer, 2010; Bozoyan et al., 2012).

Las células tipo C son progenitores neurales de división rápida y constituyen la población celular más activa mitóticamente de la ZSV. Estas células expresan nestina y también el receptor del factor de crecimiento epidérmico, EGFR y el factor de transcripción Dlx2. La presencia de estos tres marcadores es lo que nos permite diferenciarlas del resto de células de la ZSV (Figura 3). Éstas son las células a partir de las cuales se van a generar los neuroblastos migradores (Doetsch et al., 1997).

La células ependimarias o células tipo E juegan un papel importante en la neurogénesis adulta, ya que estas células producen la proteína Noggin, que es fundamental en la formación de nuevas neuronas (Lim et al., 2000). Estas células son multiciliadas y el movimiento de sus cilios mantiene la dirección del flujo del líquido cefalorraquídeo; se ha demostrado que esto es importante para la orientación de las células tipo A en la corriente migratoria rostral hasta el bulbo olfatorio (Mirzadeh et al., 2009, 2010).

Se ha establecido una secuencia por la que las células tipo B se dividen para dar lugar a células tipo C que a su vez se dividen para amplificar la población y luego se diferencian a células tipo A que son las que migran y se convierten en neuronas en el bulbo olfatorio (Figura3) (Doetsch et al., 1999; Alvarez-Buylla and García-Verdugo, 2002).

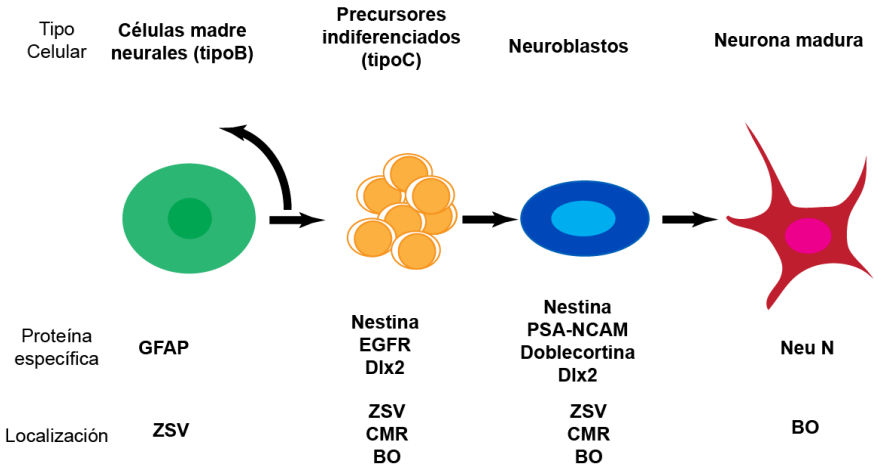

Figura 3: Esquema de las transiciones celulares desde célula madre neural a neurona madura en la ZSV adulta. En verde se representan los astrocitos (células tipo B) que actúan como célula madre neural y dan lugar a progenitores neurales tipo C (amarillo) o a nuevos astrocitos tipo B. Las células tipo C dan lugar a neuroblastos (azul) a partir de los cuales se formarán neuronas maduras (rojo). En la parte inferior de los tipos celulares representados se indican las proteínas que expresa selectivamente cada tipo celular y que permiten su caracterización mediante el empleo de anticuerpos específicos. También se indica la localización de cada tipo celular en sistema neurogénico de la zona subventricular-bulbo olfatorio. (Modificada de Estrada y Villalobo 2005).

1.3 Aislamiento y cultivo de CPNs de la ZSV como neuroesferas y su utilización como estrategia reparativa en lesiones cerebrales

Las CPNs de la ZSV pueden aislarse y amplificarse en cultivo en las condiciones adecuadas en forma de agregados esféricos conocidos como neuroesferas. Las células que forman las neuroesferas tienen alta capacidad proliferativa y al adherirse a un sustrato disminuyen su grado de proliferación y comienzan a diferenciarse a células de la estirpe neural (astrocitos, oligodendrocitos o neuronas) (Doetsch et al., 2002).

En los últimos años se han encontado pruebas convincentes de que las CPNs aisladas de la ZSV poseen una notable capacidad para mediar procesos reparativos tras su trasplante en diferentes tipos de lesiones del sistema nervioso como por ejemplo en modelos animales de la enfermedad de Parkinson, enfermedad de Huntington, esclerosis múltiple, en lesiones de la médula espinal o en accidente cerebrovascular (Cummings et al., 2005; Pluchino et al., 2005a, revisado en Taupin 2006).

La utilidad de estas células radica no sólo en que pueden sustituir neuronas dañadas y restablecer circuitos alterados, sino que sus mecanismos de reparación pueden incluir otros procesos como son la interacción con el sistema inmune o la producción de factores tróficos (Pluchino and Martino, 2005; Martino et al., 2006; Cusimano et al., 2012; Sabelström et al., 2013; Morado-Díaz et al., 2014).

Gran parte de los experimentos propuestos en esta Tesis Doctoral emplearán CPNs obtenidas de la ZSV de ratas postnatales con el fin de ser implantadas en animales con una lesión del sistema oculomotor.

2. EL SISTEMA OCULOMOTOR COMO MODELO EXPERIMENTAL

2.1 Anatomía del sistema oculomotor

El sistema oculomotor de vertebrados lo constituyen tres núcleos motores localizados en el tronco del encéfalo y los músculos extraoculares de cuya contracción dependen los movimientos de los ojos. A este sistema pertenece el núcleo motor ocular externo (NMOE) que se localiza en el puente dorsal, inmediatamente ventral a la rodilla del nervio facial. Este núcleo contiene dos poblaciones neuronales, las motoneuronas, que inervan el músculo recto externo homolateral, y una población de neuronas internucleares que proyectan a través del fascículo longitudinal medial (FLM) hacia el núcleo motor ocular común (NMOC) contralateral, donde establecen contacto sináptico excitador con las motoneuronas del músculo recto interno (Figura 5), (Delgado-Garcia et al., 1986a; b). La función de estas neuronas internucleares está relacionada con la coordinación de los movimientos de los ojos en el plano horizontal (Delgado-Garcia et al., 1986a; b). El núcleo troclear o patético se encuentra inmediatamente caudal al NMOC, a nivel del tubérculo cuadrigémino inferior.

Contiene motoneuronas que proyectan hacia el músculo oblicuo superior contralateral y homolateral (Miyazaki, 1985).

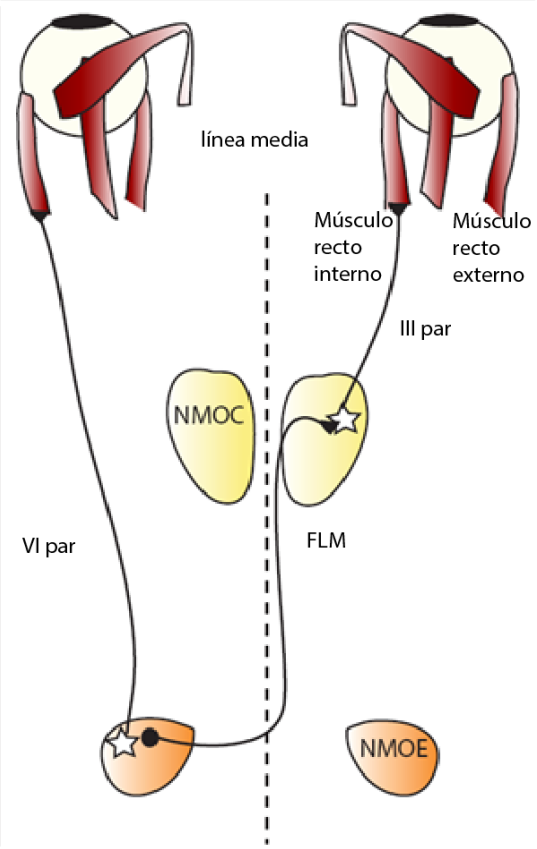

Figura 5: Representación simplificada del sistema oculomotor de mamíferos a ambos lados de la línea media cerebral. El núcleo motor ocular externo (NMOE) contiene motoneuronas que inervan el músculo recto externo homolateral formando el VI par craneal y neuronas internucleares (Int) que proyectan por el fascículo longitudinal medial (FLM) hacia la subdivisión del músculo recto interno en el núcleo del motor ocular común (NMOC) contralateral. Allí hacen sinapsis con las motoneuronas que inervan el músculo recto interno cuyos axones forman el III par craneal.

2.2 Lesión central por axotomía del fascículo longitudinal medial

La mayor parte de los experimentos que forman parte de esta Tesis Doctoral se han realizado en animales con una lesión mecánica consistente en la axotomía del FLM. En estudios previos se han caracterizado las alteraciones morfológicas y fisiológicas que produce esta lesión en gatos adultos y que se describen a continuación.

2.2.1 Cambios morfológicos debidos a la lesión del fascículo longitudinal medial

Se ha demostrado que tras la sección del FLM las células axotomizadas sobreviven a la lesión, al menos 3 meses después de la misma (Pastor et al., 2000). Aunque a nivel ultraestructural estas células presentan un citoesqueleto normal, en la superficie de membrana presentan una disminución de la cobertura sináptica. Identificando los axones de estas neuronas con un marcador anterógrado, la biocitina, se demostró que los axones lesionados en ningún caso consiguieron atravesar la cicatriz glial que se produce tras la lesión. Sin embargo, se pudo apreciar un recrecimiento abortivo de axones en busca de nuevas dianas caudales a la lesión. A nivel de microscopía electrónica, la gran mayoría de axones examinados carecían de un contacto neuronal diana, lo que indica ausencia de reinervación. En conjunto, estos datos indican que las interneuronas del NMOE sobreviven a la axotomía en el gato adulto y muestran alguna forma de rebrote axonal, incluso en ausencia de una conexión específica de destino (Pastor et al., 2000).

2.2.2 Cambios electrofisiológicos debidos a la lesión del fascículo longitudinal medial

La principal alteración observada tras la sección del FLM fue la disminución general de la tasa de disparo en las neuronas axotomizadas (de la Cruz et al. 2000), tanto la tasa de disparo asociada a la posición del ojo durante las fijaciones oculares, como la asociada a la velocidad del movimiento durante los movimientos sacádicos. Se observó que estas alteraciones se mantenían durante 3 meses postlesión, sin ningún signo de recuperación. Por lo tanto, la axotomía del FLM produce una reducción irreversible de los movimientos oculares y de la frecuencia de disparo de las neuronas causantes de los mismos (de la Cruz et al. 2000). Estas alteraciones pueden ser debidas a la ausencia de influencias tróficas derivadas de la diana.

2.3 Recuperación tras el implante de tejido cerebeloso embrionario

Las alteraciones morfológicas y electrofisiológicas de las neuronas del NMOE provocadas por la lesión del FLM se recuperaron cuando se implantó tejido cerebelar embrionario en la zona lesionada, de forma que los animales con estos implantes recuperaron tanto la frecuencia de disparo de las neuronas axotomizadas relacionada con la posición y la velocidad oculares como sus aferencias sinápticas (Benítez-Temiño et al., 2003). Además, se demostró el establecimiento de conexiones sinápticas entre

los axones lesionados y el implante. Probablemente, estas nuevas sinapsis permiten el tránsito retrógrado de factores tróficos a través de los axones lesionados hasta el soma de las neuronas internucleares en el NMOE, que podrían ser los responsables de la recuperación de las alteraciones inducidas por la axotomía.

2.4 Recuperación tras el implante de células precursoras neurales de la ZSV

Se han realizado también implantes de CPNs obtenidas de la ZSV de gatos postnatales en gatos adultos tras la axotomía del FLM. En estos experimentos se observó que las neuronas internucleares axotomizadas de los animales que recibieron los implantes mostraron una recuperación completa de la tasa de disparo relacionada con la posición del ojo y una recuperación parcial de la asociada a la velocidad ocular. Respecto a los estudios de cobertura sináptica, se analizó que los animales axotomizados con implante presentaban un restablecimiento total de las aferencias sinápticas inhibitorias y sólo una recuperación parcial de los botones sinápticos excitadores (Morado-Díaz et al., 2014). Además, se identificaron botones sinápticos sobre las CPNs implantadas, las cuales en su mayoría son inmunopositivas al factor de crecimiento del endotelio vascular (VEGF) (Morado-Díaz et al., 2014).

En conjunto, estos resultados sugieren que el apoyo neurotrófico de las CPNs podría intervenir en la recuperación de las propiedades de disparo y de las aferencias sinápticas de las neuronas lesionadas. Todo esto indica que estas células podrían proporcionar una estrategia prometedora para lesiones neuronales y que parte de su utilidad terapéutica podría ser debida a su capacidad para producir factores neurotróficos.

3. FACTORES NEUROTRÓFICOS

En 1982, Rita Levi-Montalcini y Stanley Cohen, trabajando en el laboratorio de Viktor Hamburger en Saint Louis, describieron que una molécula soluble producida por un sarcoma de ratón producía un crecimiento considerable de nervios simpáticos en embriones de pollo. A esta molécula la llamaron factor de crecimiento nervioso (NGF, del inglés *nerve growth factor*) (Levi-Montalcini, 1982) y por el descubrimento de los factores tróficos ambos recibieron el Premio Nobel de Fisiología o Medicina en 1986. Con este descubrimiento se demostró que la acción de los órganos diana sobre las

neuronas que los inervan está mediada por unas moléculas solubles denominadas **factores de crecimiento**, que son secretadas y producidas por estos órganos en cantidades limitantes.

Durante el desarrollo, solo las neuronas que reciben estos factores de sus células diana son capaces de sobrevivir y diferenciarse para adquirir las características de neuronas adultas. Hoy día se sabe que estos factores actúan en distintos aspectos de las neuronas, modulando la plasticidad, manteniendo y promoviendo la formación de sinapsis aferentes, potenciando cambios en la excitabilidad celular o protegiendo a las neuronas tras una lesión (Chao, 2003).

El NGF, junto al factor neurotrófico derivado del cerebro o BDNF (del inglés *brain derived neurotrophic factor*), la neurotrofina 3 (NT-3) y la neurotrofina 4/5 (NT-4/5), pertenecen a una importante familia de factores de crecimiento denominada **neurotrofinas**.

Además de la familia de las neurotrofinas, existen otras familias de factores tróficos con distintas funciones:

- La familia de las **neuroquinas**: donde destacan el CNTF (del inglés, *Ciliary Neurotrophic Factor*), el LIF (del inglés, *Leukaemia-Inhibitory Factor*), la interleuquina-6 y el VEGF (del inglés *Vascular Endothelial Growth Factor*).
- La superfamilia del **TGF-β** (del inglés, *Transforming Growth Factor*-β): engloba a la familia del TGF-β, a la familia del GDNF (del inglés, *Glial Cell-Derived Neurotrophic Factor*), a la familia de las BMP (del inglés, *Bone Morphogenetic Proteins*) y a la familia de las activinas.
- La superfamilia de los **factores de crecimiento no neuronales**: engloba al factor ácido de crecimiento de fibroblastos (aFGF; del inglés *Acidic Fibroblast Growth Factor*), el factor de crecimiento epidérmico (EGF; del inglés *Epidermal Growth Factor*) y al factor de crecimiento insulínico (IGF; *Insulin-like Growth Factor*) entre otros. Cada grupo de factores neurotróficos realiza sus efectos a través de receptores diferentes y específicos (Siegel y Chauhan, 2000).

Se ha descrito que los distintos tipos celulares de la ZSV expresan diversos factores neurotróficos entre los que se encuentran las neurotrofinas y el VEGF (Tonchev et al., 2007), motivo por el cual se van a describir con más detalle a continuación.

3.1 Neurotrofinas

3.1.1 Tipos de neurotrofinas

Como ya se ha mencionado, esta familia de factores neurotróficos incluye al NGF, al BDNF, la NT-3, la NT-4/5 y también la neurotrofina-6 (NT-6), aunque esta última no se ha encontrado en mamíferos.

El **NGF** fue el primer miembro de la familia de neurotrofinas descrito y se descubrió por sus efectos sobre la supervivencia de neuronas simpáticas y sensoriales en cultivo. Esta neurotrofina puede incrementar tanto el crecimiento como la ramificación dendrítica y es capaz de inducir la diferenciación de neuronas corticales, de neuronas colinérgicas estriatales y de neuronas de los ganglios basales (Kolb et al., 1997). Los ratones deficientes en NGF o en su receptor específico, presentan un descenso de la inervación colinérgica en el hipocampo (Terenghi, 1999) y graves defectos sensoriales caracterizados por deficiencias termorreceptivas y una pérdida completa de su capacidad nociceptiva (Barbacid, 1995).

El **NT-3** regula la supervivencia de neuronas simpáticas, vestibulares, espinales y motoneuronas (Rosenthal et al., 1990; Dechant et al., 1993). Ejerce un efecto trófico sobre neuronas sensoriales que inervan la médula espinal y sobre motoneuronas (Ernfors et al., 1994). Las neuronas que contienen NT-3 están localizadas fundamentalmente en el núcleo del trigémino y en los ganglios espinales cervicales y lumbares. De hecho, los ratones deficientes en NT-3 presentan pérdida de la arborización dendrítica en el trigémino (Barbacid, 1995). La administración continuada de esta neurotrofina restaura la conducción y la velocidad sensorial y motora alteradas tras la axotomía (Terenghi, 1999). Además dirige la migración de neuronas de la corteza y del cerebelo en el desarrollo (Maisonpierre et al., 1990).

El **BDNF** promueve la supervivencia de neuronas sensoriales (Davies et al., 1986) y de motoneuronas espinales (Oppenheim et al.1992). Además, en el adulto promueve la neurogénesis y supervivencia de los neuroblastos (Revisado en Bath and Lee, 2010), así

como la migración de neuronas de la corteza y del cerebelo en el desarrollo. Interviene en la diferenciación adecuada de las neuronas hacia el fenotipo noradrenérgico frente al colinérgico (Hayashida et al., 2008) Los ratones que presentan un déficit de esta neurotrofina manifiestan déficit en la coordinación de movimientos y en el mantenimiento del equilibrio, por atrofia y pérdida de neuronas vestibulares. Esta neurotrofina está también relacionada con un incremento de la efectividad sináptica en las neuronas hipocampales, proceso a su vez relacionado con el aprendizaje y la memoria (Falkenberg et al., 1992).

3.1.2 Receptores de neurotrofinas

Las neurotrofinas ejercen sus acciones uniéndose a dos tipos distintos de receptores transmembrana: receptores Trk de alta afinidad (del inglés "*tropomyosin receptor kinase*"), que pertenecen a una familia de receptores tirosina quinasas, y un receptor de baja afinidad, llamado p75 (p75NTR), miembro de la superfamilia del receptor del factor de necrosis tumoral (Yano y Chao, 2000; Hempstead y Salzer, 2002).

Se han identificado tres genes trk en mamíferos, trk A, trk B y trk C, a partir de los cuales se sintetizan tres receptores Trk funcionalmente distintos. Cada neurotrofina se une preferentemente a un receptor específico Trk; NGF se une a TrkA, BDNF y NT-4/5 a TrkB y NT-3 se une preferentemente a TrkC (revisado en Arévalo y Wu 2006).

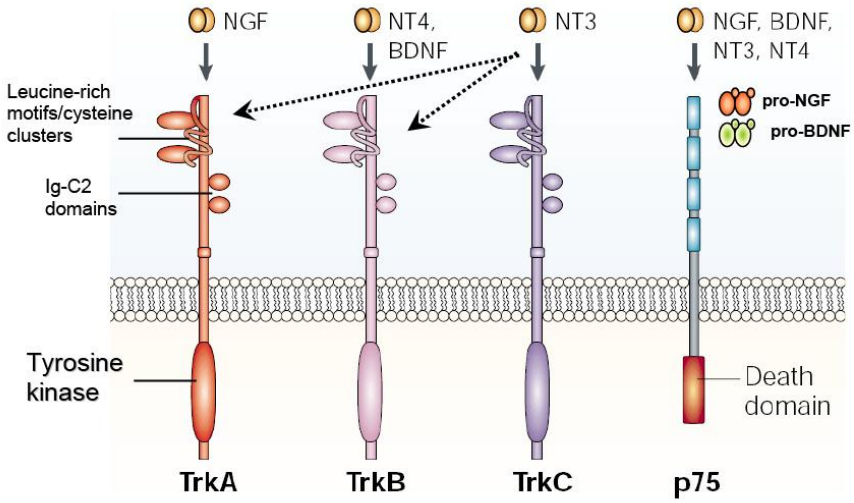

Figura 6: Modelos de receptores de neurotrofinas Trk y p75. Las distintas neurotrofinas se unen selectivamente a receptores específicos Trk, mientras que todas ellas se unen a p75. Los receptores Trk contienen dominios extracelulares de unión a ligando y una secuencia catalítica

tirosina quinasa en el dominio intracelular. Cada receptor activa varias vías de transducción. La porción extracelular de p75 contiene cuatro repeticiones ricas en cisteína y la parte intracelular contiene un dominio de inducción de muerte celular. Adaptado de Chao, 2003.

La acción de las neurotrofinas depende de:

1. El **receptor que se exprese y la ruta de señalización que se active**: el sistema dual de receptores de neurotrofinas da lugar a diferentes acciones de las mismas sobre la célula, debido a que cada receptor activa diferentes rutas de señalización que pueden producir efectos tan dispares como la supervivencia o la muerte celular. Además, la expresión tanto de un tipo de receptor como de otro está muy regulada y puede cambiar en situaciones tales como una lesión, el estrés oxidativo, el aumento de neurotransmisores, entre otros (Lewin y Carter, 2014).

2. La **maduración del receptor**: los receptores Trk presentan un dominio citoplasmático con actividad tirosina quinasa que en ocasiones puede faltar. Además, presentan dominios extracelulares comoC1 (cisteína), LRR1-3 (leucina), C2 (cisteína), Ig1, Ig2, que es el mayor punto de unión del ligando, y un inserto que a veces falta. La presencia o ausencia del inserto puede modificar la afinidad de las neurotrofinas al receptor (Lewin y Carter, 2014).

3. La **presencia de p75** puede disminuir la afinidad de NT-3 por TrkA y TrkB, y la afinidad de NT-4 por TrkB. Además, se ha observado que cuando p75 está presente junto con TrkA, los efectos del NGF sobre la neurona son diferentes revisado por (Arévalo y Wu, 2006).

4. También se pueden producir procesos de **transactivación** de otros receptores/canales iónicos por la interacción de cualquiera de los dos receptores (Trk o p75) con otras proteínas de membrana (revisado en Arévalo y Wu, 2006).

3.2 VEGF

En 1983, Senger y colaboradores lograron la purificación parcial de una proteína capaz de inducir proliferación vascular. Esta proteína se denominó “factor de permeabilidad vascular” (VPF, del inglés *Vascular Permeability Factor*) y se pensó que era un regulador específico de la permeabilidad de vasos sanguíneos en procesos tumorales,

más que un factor de crecimiento. En 1989, Ferrara y Henzel realizaron la purificación, homogeneización y secuenciación de dicha proteína, lo que supuso un primer paso para una mejor comprensión de la verdadera naturaleza de la misma, que se llamó a partir de entonces VEGF (Ferrara y Henzel, 2012). A la familia del VEGF pertenecen 5 factores homólogos: VEGF-A, VEGF-B, VEGF-C, VEGF-D y PIGF (del inglés *Placental Growth Factor*), siendo el VEGF-A el prototipo (Ferrara et al., 2003). De los tres primeros se han descrito funciones directas sobre las células neurales (revisado en Sathasivam, 2008).

El VEGF es el factor angiogénico más importante en el desarrollo embrionario de la vasculatura, en la angiogénesis patológica y también en la permeabilidad vascular. También tiene importantes acciones en el tejido nervioso, adquiriendo cada vez más relevancia a medida que se conocen mejor sus propiedades neuroprotectoras, neurotróficas y neurogénicas (Jin et al., 2002; Sköld y Kanje, 2008; Nowacka y Obuchowicz, 2012).

3.2.1 Receptores del VEGF

Los principales receptores para el VEGF son los receptores tirosina quinasa VEGFR-1 (Flt-1), VEGFR-2 (Flk-1) y VEGFR-3 (Flt-4), caracterizados por la presencia de siete dominios de tipo inmunoglobulina en el dominio extracelular, una sola región transmembrana y una secuencia consenso de la tirosina quinasa en el dominio intracelular (revisado en Ferrara et al. 2003).

El VEGFR-2 desempeña un papel crítico en la correcta diferenciación y organización de las células endoteliales en los lechos vasculares, siendo el mayor mediador de los efectos mitogénicos, angiogénicos y de aumento de permeabilidad del VEGF. Por otro lado, se cree que el VEGFR-1 regula negativamente la angiogénesis, evitando la unión del VEGF al VEGFR-2 (revisado en Ferrara et al. 2003). El receptor VEGFR- 3 está relacionado con la linfangiogénesis y la neurogénesis en la ZSV (Calvo et al., 2011).

Se ha descrito también que el VEGF se une a dos receptores que no pertenecen a la familia tirosina quinasa. Son los receptores neuropilina-1 (NP-1) y neuropilina-2 (NP-2), que están involucrados en el guiado axonal (revisado en Ferrara et al., 2003).

En la Figura 7 se muestra resumida la interacción de los miembros de la familia del VEGF con los distintos tipos de receptores.

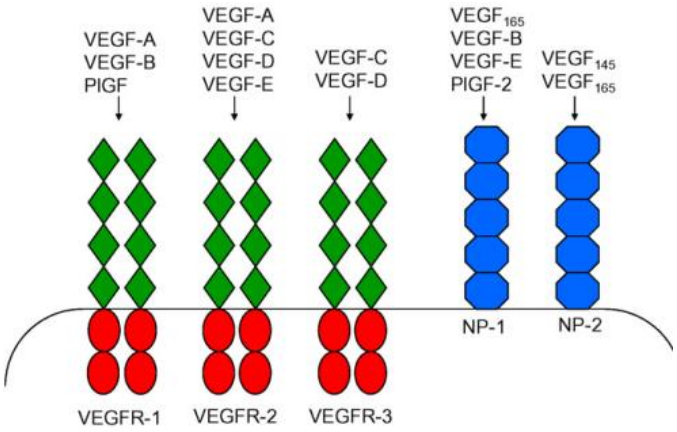

Figura 7: Interacción de los miembros de la familia VEGF con sus receptores. Interacción de los distintos miembros de la familia del VEGF con los tres tipos de receptores con actividad tirosina quinasa (VEGFR-1, VEGFR-2, y VEGFR-3) y con los receptores accesorios específicos neuropilina-1(NP-1) y neuropilina-2 (NP-2). Tomado de Sathasivam, 2008.

3.3 Sistema oculomotor y factores neurotróficos

3.3.1 Expresión de receptores de neurotrofinas en el sistema oculomotor

Benítez-Temiño y col., en 2004, examinaron la expresión de los tres receptores Trk (TrkA, TrkB y TrkC) en el sistema oculomotor de gatos adultos mediante técnicas inmunohistoquímicas, demostrando que los tres receptores están presentes en todas las poblaciones neuronales de los núcleos oculomotores. Esto sugiere que las neurotrofinas pueden ejercer una influencia en el funcionamiento normal de la circuitería de este sistema motor. Esto se corroboró en experimentos posteriores del grupo en los que se describió que tras la axotomía del VI par craneal se producían cambios en la expresión del ARNm de los receptores de neurotrofinas en las motoneuronas del NMOE. Así, tras la desconexión de su músculo diana, las motoneuronas del NMOE aumentan la expresión del ARNm de trkB y disminuyen la de trkC indicando que las neurotrofinas que se unen a estos receptores podrían estar implicadas de forma diferente en las respuestas de supervivencia y regeneración (Morcuende et al., 2011).

3.3.2 Administración exógena de neurotrofinas en el sistema oculomotor lesionado

Se ha descrito que la administración exógena de neurotrofinas en animales con lesión del sistema oculomotor es capaz de revertir propiedades fisiológicas y morfológicas alteradas por el daño causado. La axotomía de las motoneuronas del NMOE produce una disminución de la tasa de disparo responsable de los movimientos sacádicos y de las fijaciones oculares. Esta tasa de disparo se recupera por completo cuando se administran las neurotrofinas BDNF y NT-3 en el extremo distal de los axones seccionados (Davis-López de Carrizosa et al., 2009). Concretamente, el BDNF promueve la recuperación del disparo tónico de las motoneuronas axotomizadas y la NT-3 influye mayoritariamente en la recuperación del disparo fásico. Además, la administración conjunta de estas dos neurotrofinas produce también una recuperación de la cobertura sináptica de las motoneuronas lesionadas a nivel del soma y el neuropilo (Davis-López de Carrizosa et al., 2009).

La administración exógena de NGF en el extremo distal de los axones de las motoneuronas axotomizadas también es capaz de revertir las alteraciones inducidas por la axotomía. Concretamente el NGF fue capaz de restablecer el disparo tónico y fásico de las motoneuronas lesionadas a valores similares a cuando están inervando su músculo diana. Además, los estudios de cobertura sináptica demostraron que la administración de esta neurotrofina también produjo la recuperación de botones sinápticos tanto excitatorios como inhibitorios sobre las motoneuronas lesionadas (Davis-López de Carrizosa et al., 2010).

Por lo tanto, el sistema oculomotor de mamíferos adultos tiene receptores de neurotrofinas cuya expresión se modula en respuesta a la lesión y las neurotrofinas ejercen funciones implicadas en el mantenimiento de la tasa de disparo y de la cobertura sináptica de las motoneuronas.

3.3.3 VEGF en el sistema oculomotor

Estudios preliminares llevados a cabo en nuestro laboratorio indican que todas las motoneuronas oculomotoras expresan VEGF y el receptor VEGFR-2 (Flk-1) (Morcuende et al., 2014). Esto sienta una base anatómica para un posible papel del VEGF en la funcionalidad de las neuronas oculomotoras.

3.3.4 Administración exógena de VEGF en modelos animales de lesiones motoras

Por su capacidad angiogénica y neurogénica, el VEGF se ha utilizado como terapia contra distintos daños en el tejido nervioso. Concretamente, el VEGF se ha revelado en los últimos años como un factor importante para prolongar la supervivencia de motoneuronas en distintos modelos animales de degeneración o lesión de las mismas. Así, se ha descrito que la administración de VEGF retrasa la muerte de motoneuronas y mejora el comportamiento motor en distintos modelos animales de esclerosis lateral amiotrófica(Lambrechts et al., 2003; Azzouz et al., 2004; Storkebaum et al., 2005; revisado en Sathasivam 2008). La sobreexpresión neuronal de VEGF retarda la neurodegeneración y aumenta la supervivencia en ratones con ELA (Wang et al., 2007). También existen evidencias sobre el papel del VEGF en la reparación nerviosa tras una lesión de la médula espinal. Así, en ratas sometidas a una lesión de la médula espinal, el tratamiento con VEGF produjo un aumento en la densidad de vasos sanguíneos en la zona de la lesión, una disminución de la apoptosis celular y una mejora en el comportamiento motor (Widenfalk et al., 2003).

Otra función importante que se le ha atribuido recientemente al VEGF, es su papel en la transmisión sináptica. Se ha demostrado que el VEGF es capaz de inducir una depresión en la transmisión sináptica excitatoria en neuronas piramidales y granulares del hipocampo, y también en las motoneuronas del núcleo hipogloso (McCloskey et al.,2005; 2008).

3.4 Factores neurotróficos en la ZSV

3.4.1 Neurotrofinas en la ZSV

Tonchev y colaboradores describieron en un estudio en monos que los distintos tipos celulares de la ZSV expresan algunos factores neurotróficos y sus receptores (Tonchev et al., 2007). La neurotrofina NGF se expresa en los astrocitos de la ZSV, mientras que su receptor de alta afinidad TrkA está presente tanto en astrocitos como en neuronas inmaduras. La NT-3 y su respectivo receptor de alta afinidad, TrkC, se expresan en las células ependimarias. Los astrocitos de la ZSV expresan también BDNF y su receptor de alta afinidad TrkB. Este receptor TrkB también lo expresan las CPNs de la ZSV (Tonchev et al., 2007).

El BDNF es la neurotrofina de la que se han descrito más acciones en la ZSV. Los primeros estudios con los efectos de esta neurotrofina en la población de CPNs de la ZSV se realizaron en cultivo y demostraron que el BDNF promueve la supervivencia de estas células (Kirschenbaum y Goldman, 1995). Más tarde se demostró que la administración de BDNF en los ventrículos laterales aumentaba la neurogénesis en el bulbo olfatorio (Zigova et al., 1998). Estos datos han sido corroborados en numerosos estudios posteriores en los que además se demuestra un papel diferenciado de los distintos receptores de BDNF en la supervivencia y migración celular de la ZSV (revisado en Bath y Lee, 2010).

3.4.2 VEGF y ZSV

En el nicho neurogénico de la ZSV existe expresión de VEGF. En concreto, los astrocitos, los precursores neurales y las células endoteliales expresan VEGF y el receptor de VEGF VEGFR-1 (Flt-1) (Tonchev et al., 2007). Algunas evidencias recientes indican que este factor neurotrófico interviene en la neurogénesis de esta zona. Se ha descrito que la sobreexpresión de los receptores de VEGF de tipo VEGFR-3 estimulan la neurogénesis en la ZSV sin afectar a la angiogénesis y que tanto la supresión condicional de VEGFR-3 como el bloqueo de la señalización de VEGFR-3 con anticuerpos, reduce la neurogénesis de esta zona (Calvo et al., 2011). Estos resultados atribuyen un papel importante del VEGF en los procesos de neurogénesis a través de la señalización celular dependiente de VEGFR-3.

Además se ha demostrado que en la migración de neuroblastos por el CMR interviene también el VEGF producido por los astrocitos del gliotubo, el cual controla la formación y el crecimiento de los vasos sanguíneos que acompañan en paralelo a los neuroblastos a lo largo de todo el CMR (Bozoyan et al., 2012).

4. RESPUESTA GLIAL A LA LESIÓN POR AXOTOMÍA

4.1 Tipos de células gliales

Las células gliales son todas las células del sistema nervioso que no son neuronas, ni células sanguíneas, ni células endoteliales capilares. La principal diferencia de estas células con las neuronas es que no producen potenciales de acción. Son las células más

abundantes del tejido nervioso. De hecho, en el cerebro representan aproximadamente el 90% del total de células.

En el sistema nervioso central se identifican varios tipos de células gliales de origen neural (que derivan del ectodermo), a las que se denominan macroglía; los astrocitos, los oligodendrocitos y la glía positiva a NG2. Además existe otro tipo de célula glial de origen no neural, la microglía, cuyo origen es mesodérmico. En el sistema nervioso periférico el principal tipo de célula glial lo constituyen las células de Schwann que envuelven y mielinizan los axones periféricos (revisado en Verkhratsky y Butt, 2007).

4.2 Astrocitos

En 1893 el histólogo Michael von Lenhossek propuso el término astrocito para describir a este tipo de célula glial, por su forma estrellada. Los astrocitos son las células gliales más abundantes y diversas del cerebro. Como ya observó Lenhossek, esa morfología estrellada se debe a sus prolongaciones membranosas largas y estrechas, ricas en gliofilamentos. Estos filamentos están formados principalmente por una proteína denominada GFAP (del inglés *Glial Fibrillary Acidic Protein*).

Los astrocitos desempeñan funciones muy importantes en el sistema nervioso central. Intervienen en el metabolismo y el control del microambiente neuronal, en la formación de nuevas sinapsis, en la formación y regulación de la barrera hematoencefálica y en el control de la microcirculación cerebral. Además, los astrocitos son fundamentales para el desarrollo y la producción de nuevas células neurales (Mori et al., 2005). También se ha demostrado que intervienen en la formación de algunas sinapsis cerebrales participando como un componente activo de lo que se denomina “sinapsis tripartita” (Perea y Araque, 2010). Muy recientemente se han demostrado además importantes funciones de los astrocitos en los procesos de aprendizaje y memoria (Han et al., 2013).

4.3 Glía positiva a NG2

En 1980 William Stallcup y colaboradores identificaron una nueva población de células gliales en el SNC adulto (revisado en Verkhratsky y Butt, 2007). Estas células son positivas a un proteoglicano de condroitín sulfato denominado NG2. Las células NG2 son también positivas a la mayoría de los marcadores de progenitores de

oligodendrocitos pero no expresan marcadores de oligodendrocitos maduros ni tampoco GFAP. Tienen un soma pequeño con prolongaciones numerosas y delgadas y se encuentran tanto en la sustancia gris como en la sustancia blanca. La mayoría de las células positivas a NG2 se dividen muy lentamente con un ciclo celular de varias semanas, pero pueden aumentar su tasa de división como respuesta a un daño (revisado en Dimou y Götz, 2014).

Estas células actúan como progenitoras de oligondedrocitos, siendo capaces de generar oligodendrocitos maduros con la capacidad de mielinizar axones. En la sustancia blanca se localizan extendiendo sus procesos hasta los nodos de Ranvier, desde donde pueden detectar señales desde los axones que podrían desencadenar su diferenciación a oligodendrocitos maduros (Figura8)(Butt et al., 1999).

Además de esta función se ha descrito que en determinadas condiciones son capaces de generar neuronas y astrocitos (revisado en Belachew et al., 2003; Zhu et al., 2008; Rivers et al., 2013).

Son las únicas células gliales capaces de formar sinapsis eléctricas con neuronas (Bergles et al., 2000; Lin and Bergles, 2004). Así, se han descrito sinapsis funcionales entre neuronas y células NG2 en hipocampo, cerebelo, corteza, cuerpo calloso y el nervio óptico (Bergles et al., 2000; Lin y Bergles, 2004; Jabs et al., 2005; Lin et al., 2005; Kukley et al., 2007; Káradóttir et al., 2008; Tanaka et al., 2009). De hecho, por esta función a estas células gliales se las conoce también como sinantocitos (Butt et al., 2005).

La glía positiva a NG2 también establece contactos celulares con astrocitos, oligodendrocitos y macrófagos en sitios donde se ha producido una lesión, jugando un papel clave en la formación de la cicatriz glial (Butt et al., 2005).

4.4 Oligodendrocitos

Los oligodendrocitos fueron inicialmente descritos por Pío del Rio Hortega en 1928, el cual hipotetizó también que su función era la de producir la mielina que recubre a los axones de los nervios centrales., hecho que fue demostrado años más tarde.

Además de esta función principal, hoy día se sabe que los oligodendrocitos también participan en el desarrollo de los nodos de Ranvier (Kaplan et al., 2001). Existe también un tipo de oligodendrocitos, llamados “satélites”, que están presentes en la sustancia gris y cuya función es aún desconocida (revisado en Verkhratsky y Butt, 2007).

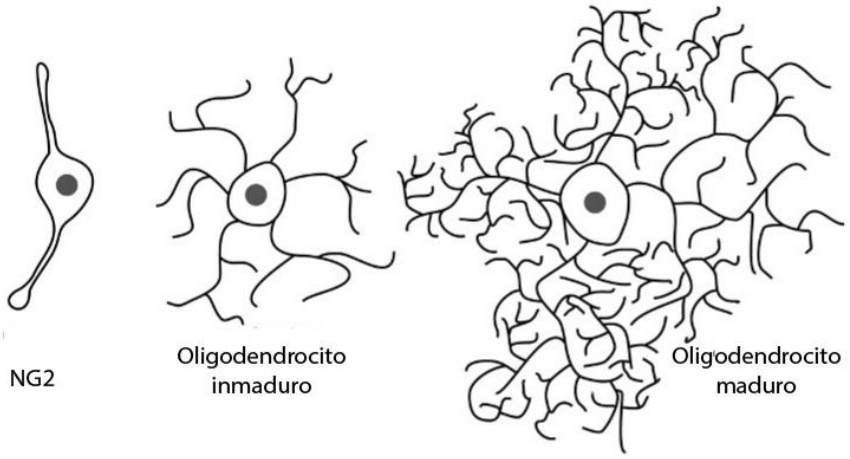

Figura 8: Linaje de oligodendrocitos. De izquierda a derecha observamos como cambia la morfología de una glia positiva a NG2 hasta un oligodendrocito maduro, la primera es una glía positiva a NG2. El segundo es un oligodendrocito inmaduro, caracterizado por tener pocas ramificaciones. El tercero es un oligodendrocito maduro, con muchas ramificaciones. (Adaptado de Verkhratsky and Butt, 2007)

4.5 Microglía

Pío del Rio Hortega fue quien propuso el termino microglía para caracterizar a esta población celular distinta de las neuronas y de la macroglía. Además, fue el primero en proponer que la microglía tiene un origen mesodérmico.

Las células de microglía se distribuyen por todo el cerebro, aunque se encuentran en mayor densidad en el hipocampo, telencéfalo olfativo, ganglios basales y en la sustancia negra (revisado en Verkhratsky y Butt, 2007). Representan aproximadamente el 10% del total de la glía del cerebro, constituyendo el sistema inmune del cerebro responsable de protegerlo frente a distintos tipos de daños y enfermedades.

Durante el desarrollo embrionario, los progenitores de las células de microglía acceden al tubo neural desde donde van completando su maduración y diseminación a lo largo del tejido nervioso (revisado en Saijo y Glass, 2011).

En condiciones fisiológicas, la microglía se encuentra en el cerebro en estado de reposo. En este estado, se caracteriza por tener un pequeño soma con numerosas y delgadas prolongaciones orientadas en todas direcciones (Figura 8). Cada célula de microglía con sus procesos ocupa su propio territorio (entre 15-30 μm) de forma que no suele solaparse con el territorio de células vecinas. Los procesos de las células de microglía en reposo están en continuo movimiento, de esta forma escanean constantemente sus territorios cerebrales (Saijo and Glass, 2011). Cuando detectan señales provenientes del daño neuronal adquieren un estado de activación intermedio. En este estado varía la morfología y la expresión de marcadores. Comienza la retirada de los procesos microgliales (Figura 9) y aumenta el tamaño del cuerpo celular hasta adquir una morfología ameboide en la que tienen capacidad fagocítica (Figura 9). En su estado activado la microglía puede adquirir distintos fenotipos en los que libera moléculas muy diversas según el tipo de daño que desencadena la activación (Goldmann y Prinz, 2013). Cuando existe una infección aguda o se activan por la entrada de un microrganismo, las células de microglía adquieren normalmente un estado de activación denominado M1 en el que producen moléculas asociadas a la respuesta inmune como citoquinas pro-inflamatorias, IL-1 (interleuquina 1), IL- 6 (interleuquina 6) o TNFα (factor de necrosis tumoral α) (Goldmann y Prinz, 2013). En otras circunstancias la microglía activada puede adquirir un estado denominado M2 en el que liberan citoquinas antiinflamatorias como IL-4 (interleuquina 4), IL10 (interleuquina 10) o TGF-β (factor transformante del cerebro β) y que tiene un papel importante en la remodelación del tejido, su reparación y su recuperación (Mathieu et al., 2010; Goldmann y Prinz, 2013).

El proceso de activación de la microglía es por tanto un proceso gradual y diferente dependiendo del tipo de patología y de las partes del cerebro que se vean afectadas (revisado en Kettenmann y Verkhratsky 2011).

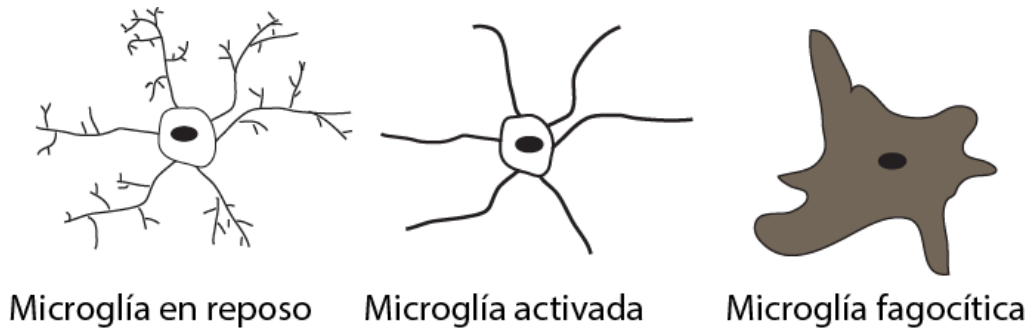

Figura 9: Morfología de las células de microglía según su estado de activación. De izquierda a derecha observamos cómo cambia la morfología de la microglía según su estado de activación, la primera es una microglía en reposo caracterizada por sus largos procesos con ramificaciones, en el centro observamos una microglía activada caracterizada por la pérdida de procesos. A la derecha observamos una microglía fagocítica con aspecto ameboide. Modificado de Verkhratsky y Butt, 2007.

4.6 Células gliales en el nicho neurogénico de la ZSV

Como ya se ha mencionado anteriormente, las células gliales juegan un papel fundamental en el nicho neurogénico de la ZSV. Así, las células ependimarias producen la proteína Noggin, que es fundamental en la formación de nuevas neuronas (Lim et al., 2000). Los astrocitos de la ZSV son considerados células madres neurales (Lim and Alvarez-buylla, 2014) y forman el gliotubo por el que migran los neuroblastos en el CMR (García-Verdugo et al., 1998).

En la ZSV adulta también existe una alta densidad de células de microglía en un estado activado (Goings et al., 2006). De hecho, este estado de activación la diferencia de la microglía presente en regiones no neurogénicas del cerebro adulto lo que sugiere que la microglía podría tener una función homeostática en la ZSV. Algunos artículos publicados recientemente corroboran este hecho. Por ejemplo, en animales postnatales, la microglía activada facilita la neurogénesis y oligodendrogénesis en la ZSV, mediante la producción de citoquinas como TNF-α y las interleuquinas IL-4, IL1β y IFN-γ (Shigemoto-Mogami et al., 2014). Además, la microglía es capaz de dirigir la migración de los precursores neurales (Aarum et al., 2003). Por otro lado, los precursores neurales de la ZSV también modulan la activación microglial (Mosher et al., 2012), de forma que está bien establecido que existe una comunicación bilateral entre CPNs y células de microglía en la ZSV.

4.7 Respuesta glial a la lesión por axotomía

Al producirse una lesión en el SNC por un daño mecánico, como una transección nerviosa, tiene lugar una fuerte reacción glial, siendo las primeras células gliales en actuar los astrocitos, que se dirigen a la zona de la lesión adquiriendo un estado activo y liberando mucopolisacáridos además de factores neurotróficos como NGF, BDNF y NT-3, así como diversas citoquinas e interleuquinas que pueden proteger a las neuronas dañadas de su muerte(Verkhratsky and Butt, 2007).

Como consecuencia de la liberación de mucopolisacáridos y del acúmulo de células gliales en la zona de la lesión, se forma una cicatriz glial que reemplaza la arquitectura tisular existente. Esta cicatriz previene de la extensión de la muerte neuronal secundaria pero también supone una barrera mecánica para la regeneración de los axones dañados (Figura 10).

A la zona de la lesión también acuden macrófagos (siempre que haya habido una rotura de la barrera hematoencefálica) y microglía, que se activa adquiriendo características fagocíticas y liberando sustancias citotóxicas (radicales libres de oxígeno) junto a citoquinas pro-inflamatorias como las interleuquinas 1 y 6 (IL-1 y IL-6) o el factor de necrosis tumoral-α (TNF-α) (Verkhrastsky y Butt, 2007). La glía positiva a NG2 también muestra una fuerte reacción después de una lesión traumática en el SNC, con un aumento rápido en la proliferación y en el tamaño celular (revisado en Dimou y Götz, 2014). Parte de estas células NG2 se diferencian a oligodendrocitos maduros, otras a células positivas a GFAP y muchas se mantienen como glía NG2, lo que indica un cierto grado de heterogeneidad en su reacción a la lesión (revisado en Dimou y Götz, 2014). Las células positivas a NG2 también forman parte de la cicatriz glial.

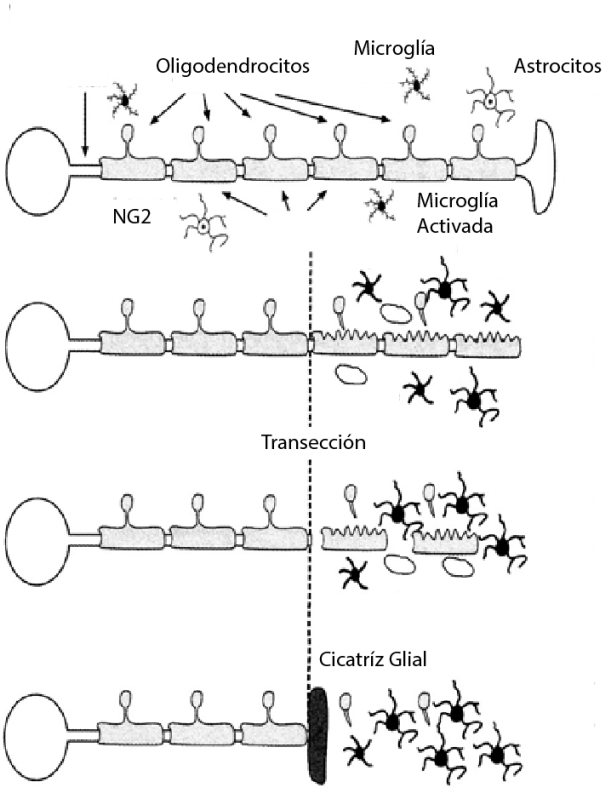

Figura 10: Esquema representativo de la respuesta glial asociada a una lesión en el SNC. En la imagen superior se muestra una neurona cuyo axón está intacto. Alrededor del axón se observan astrocitos, glía positivas a NG2 y microglía. En el esquema inmediatamente inferior se muestran las respuestas gliales que se desencadenan tras una axotomía: se activan los astrocitos, la glía positiva a NG2, la microglía y acuden macrófagos. Debajo se representa cómo se van fagocitando los restos del axón lesionado y al final se observa la formación de la cicatriz glial.

5. COMUNICACIÓN CELULAR MEDIANTE UNIONES GAP

Las uniones gap o uniones en hendidura ("gap junctions") son conglomerados de canales intercelulares a través de los cuales se permite el intercambio de iones, segundos mensajeros y pequeñas moléculas. Cada canal de unión en hendidura lo constituyen dos hemicanales, uno de cada una de las células implicadas en la unión. A su vez, cada hemicanal está formado por seis subunidades proteicas denominadas conexinas que se disponen alrededor de un poro central (Figura 11). La función de las uniones gap es la de coordinar procesos o respuestas metabólicas y eléctricas de células en contacto, ya que comunican los citoplasmas de dichas células, resultando fundamentales por ejemplo, para la contracción sincrónica del corazón o para la

función neuroprotectora que cumplen los astrocitos en el cerebro (Jalife et al., 1999; Contreras et al., 2004).

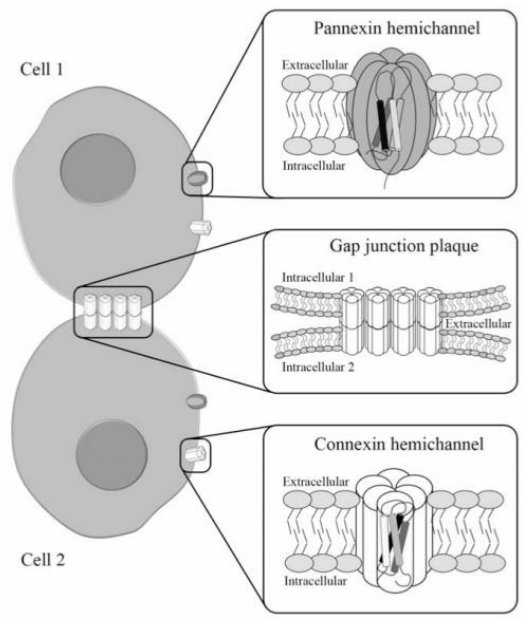

Figura 11: Uniones gap y hemicanales. En la parte superior se representa un hemicanal formado por panexinas; en el centro del diagrama, se representan uniones gap donde se aprecian en cada una de ellas dos hemicanales ensamblados, uno de cada célula; en la parte inferior se representa un hemicanal formado por Cxs (modificada de Orellana et al. 2009).

5.1 Conexinas

La familia de las conexinas (Cxs) está compuesta por 21 integrantes en humanos y 20 en ratones (Rackauskas et al., 2010). Las distintas isoformas de las Cxs se nombran según su peso molecular y presentan diferentes patrones de expresión en los tejidos. La Cx43, con un peso molecular de 43 kDa, es la isoforma más abundantemente expresada en los tejidos, incluido el SNC (Laird, 2006). Todas las Cxs comparten la misma topología en la membrana celular presentando cuatro dominios transmembrana, dos asas extracelulares, un asa intracelular y extremos amino y carboxilo localizados en el citosol (Figura 12). La mayor variabilidad entre las distintas isoformas se encuentra en el extremo C-terminal, que presenta distinta longitud y secuencia aminoacídica. El extremo C-terminal posee, además, varios residuos de serina, treonina y tirosina susceptibles de fosforilación, junto con dominios que detectan cambios de pH o redox y que se unen a distintas proteínas intracelulares incluyendo a algunas de andamiaje (revisado en Rackauskas et al., 2010).

Las células del cerebro expresan diferentes tipos de conexinas. Por ejemplo, las neuronas expresan Cx36, Cx45 y Cx57 (revisado en Orellana et al., 2009). Los astrocitos expresan sobre todo Cx43, aunque también expresan Cx26, Cx30, Cx40 y Cx45. Los oligodendrocitos expresan Cx29, Cx32 y Cx47 (revisado por Giaume et al., 2013). La microglía en condiciones no patológicas no expresa Cxs, pero se ha descrito que puede expresar Cx43 en condiciones que inducen inflamación(Eugenín et al., 2001; Garg et al., 2005).

Se ha descrito que los precursores neurales de la ZSV expresan Cx45. En ratones *knockout* para Cx45 se ha observado una disminución de la proliferación de estos precursores mientras que la sobreexpresión de esta proteína aumenta la proliferación de los mismos, lo cual sugiere un papel fundamental de esta proteína en la proliferación de esta población de células (Khodosevich et al., 2012).

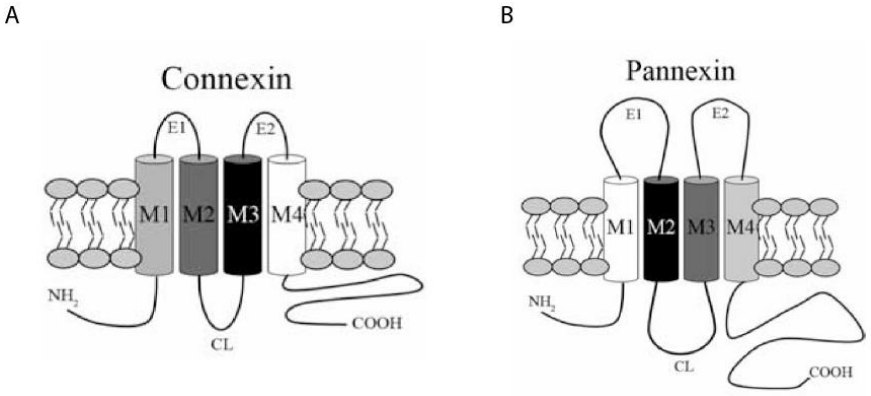

Figura 12: Representación esquemática de la topología en la membrana celular de una conexina y una panexina. En A se observa un esquema de una conexina y en B de una panexina, ambas con 4 dominios transmembrana (M1-4), 2 asas extracelulares (E1- E2) y un asa intracelular (CL). Además, las dos proteínas presentan sus extremos carboxilo y amino (-COOH, -NH_2) en la cara citosólica de la membrana celular.

Como ya se ha mencionado antes, la agrupación de seis conexinas alrededor de un poro central constituye un hemicanal. Los hemicanales, además de acoplarse con los de otras células para formar uniones gap, pueden abrirse en determinadas circunstancias fisiológicas y patológicas y permitir el intercambio de iones y pequeñas moléculas con el microambiente extracelular, lo que constituye una vía de comunicación intercelular autocrina/paracrina a tener en cuenta (revisado en Orellana

et al. 2009). Entre los estímulos que regulan su apertura se encuentran: alteraciones en la concentración de Ca^{2+} intra y extracelular, estímulos mecánicos, cambios de potenciales de membrana, alcalinización extracelular, acidificación intracelular, disminución del potencial redox y cambios del estado de fosforilación (Saez et al., 2003; Bennett et al., 2012).

Los hemicanales de Cxs están también involucrados, al igual que las uniones gap, en la propagación de las señales de calcio entre astrocitos que tiene lugar por ejemplo en las sinapsis tripartitas (revisado en Giaume et al., 2013).

5.2 Panexinas

En vertebrados, los hemicanales pueden estar también formados por otras proteínas distintas a las conexinas, las panexinas. A diferencia de los hemicanales de conexinas, los formados por panexinas no se ensamblan para formar uniones gap (revisado en Giaume et al., 2013).

Se han identificado 3 genes denominados Panexinas (Panx) 1-2-3 que codifican para estas proteínas. Estos genes son homólogos a las inexinas, proteínas responsables de la formación de uniones gap en invertebrados. Las Panxs tienen la misma topología que las Cxs (Figura 12), sin embargo, al comparar las secuencia de aminoácidos de Panxs y Cxs solo se aprecia un 16% de homología (Orellana et al., 2009).

Panx 1 se expresa en diferentes tejidos de mamíferos. En el tejido nervioso, se ha descrito su expresión en la médula espinal, el hipocampo y el cerebelo, entre otros. Se encuentra en distintos tipos neuronales como las células mitrales del bulbo olfativo, las células de Purkinje del cerebelo o neuronas dopaminérgicas y colinérgicas (Bruzzone et al., 2003; Ray et al., 2005; Zappalà et al., 2006). Los hemicanales de Panx1 son permeables a Ca^{2+} y a pequeñas moléculas como ATP o moléculas exógenas como calceína (revisado en Orellana et al., 2009). Se ha demostrado también la expresión de Panx 1 en CPNs de la ZSV, donde juega un papel importante en la proliferación celular (Wicki-Stordeur et al., 2012).

Panx2 se expresa únicamente en algunas zonas del cerebro como son el bulbo olfatorio, cerebelo, sustancia negra y en la médula espinal. En los astrocitos del hipocampo se expresa solo en caso de isquemia (revisado en Orellana et al., 2009).

5.3 Acoplamiento celular en la ZSV

Los primeros estudios de acoplamiento de colorante realizados en rodajas de cerebro a nivel de la ZSV, demostraron la existencia de comunicación a través de uniones gap en la ZSV y sugerían un gradiente de acoplamiento celular, siendo éste mayor en la zona más caudal y menor en la más cercana al bulbo olfatorio, lo que coincide con el patrón de proliferación de los neuroblastos (Menezes et al., 2000). Lacar y colaboradores describieron posteriormente (Lacar et al., 2011) que el acoplamiento celular en esta zona tiene lugar entre las células ependimarias y los astrocitos B1 y B2, entre los astrocitos y entre las NPCs. Las funciones concretas de este alto grado de acoplamiento celular en esta región neurogénica quedan aún por determinar aunque estudios previos indican que al menos estaría involucrado en la migración de los neuroblastos a través del CMR (Menezes et al. 2002; Marins et al; 2009).

5.4 Uniones gap en CPNs tras su implante en el cerebro lesionado

En un estudio publicado en 2010 se describió por primera vez que cuando se implantan CPNs en un modelo de lesión del cerebelo caracterizado por la degeneración de las células de Purkinje, éstas forman uniones gap con neuronas del hospedador y que la comunicación mediante estas uniones gap es esencial para los efectos beneficiosos del implante (Jäderstad et al., 2010). Otro artículo posterior en el que se realizaron implantes de CPNs en médula espinal lesionada mostró que las CPNs con fenotipo no diferenciado forman uniones gap con macrófagos que acuden a la zona de la lesión y son capaces de modular la respuesta inmune de la zona hacia la producción de moléculas con acción neuroprotectora (Cusimano et al., 2012).

En este trabajo hemos analizado si las CPNs provenientes de la ZSV de animales postnatales son capaces de formar uniones gap con células gliales tras su implante e cerebro lesionado.

OBJETIVOS

El objetivo general del estudio es el de estudiar la expresión de factores neurotróficos y la respuesta glial que se produce en el cerebro lesionado tras el implante de CPNs así como las interacciones celulares que pueden establecerse entre las CPN implantadas y las células del hospedador. Pensamos que estas interacciones pueden afectar positivamente tanto a la integración de las células como a los efectos beneficiosos del implante. El estudio se realizará en ratas adultas con transección del FLM tras la cual se procederá al implante de CPNs procedentes de la ZSV. Bajo este abordaje los objetivos específicos son:

1.- Analizar si el contenido en factores neurotróficos de neuronas axotomizadas se modifica en animales que han recibido implante de CPNS.

2.- Analizar si la respuesta glial a la lesión se modifica en animales que han recibido implante de CPNs.

3.- Analizar la relación anatómica entre las CPNs implantadas y las células gliales del hospedador.

4.- Analizar la existencia de uniones gap entre las CPNs implantadas y astrocitos y microglía activada del hospedador.

Paralelamente, en estudios *in vitro* con cultivos de células procedentes de la ZSV y con cultivos conjuntos de CPNs con astrocitos y con microglía pretendemos profundizar en los mecanismos de comunicación entre estas poblaciones de células para lo que llevaremos a cabo estos objetivos:

5.- Analizar el grado de acoplamiento a colorante entre cultivos de CPNs de la ZSV así como la existencia en las mismas de hemicanales funcionales.

6.- Analizar el grado de acoplamiento a colorante entre CPNs y astrocitos y entre CPNs y microglía.

RESULTADOS

ARTÍCULO 1

Neural Progenitor Cell Implants Modulate Vascular Endothelial Growth Factor and Brain-Derived Neurotrophic Factor Expression in Rat Axotomized Neurons

OPEN ACCESS Freely available online

PLOS ONE

Neural Progenitor Cell Implants Modulate Vascular Endothelial Growth Factor and Brain-Derived Neurotrophic Factor Expression in Rat Axotomized Neurons

Rocío Talaverón, Esperanza R. Matarredona, Rosa R. de la Cruz, Angel M. Pastor*

Laboratorio de Fisiología y Plasticidad Neuronal, Departamento de Fisiología, Facultad de Biología, Universidad de Sevilla, Sevilla, Spain

Abstract

Axotomy of central neurons leads to functional and structural alterations which largely revert when neural progenitor cells (NPCs) are implanted in the lesion site. The new microenvironment created by NPCs in the host tissue might modulate in the damaged neurons the expression of a high variety of molecules with relevant roles in the repair mechanisms, including neurotrophic factors. In the present work, we aimed to analyze changes in neurotrophic factor expression in axotomized neurons induced by NPC implants. For this purpose, we performed immunofluorescence followed by confocal microscopy analysis for the detection of vascular endothelial growth factor (VEGF), brain-derived neurotrophic factor (BDNF), neurotrophin-3 (NT-3) and nerve growth factor (NGF) on brainstem sections from rats with axotomy of abducens internuclear neurons that received NPC implants (implanted group) or vehicle injections (axotomized group) in the lesion site. Control abducens internuclear neurons were strongly immunoreactive to VEGF and BDNF but showed a weak staining for NT-3 and NGF. Comparisons between groups revealed that lesioned neurons from animals that received NPC implants showed a significant increase in VEGF content with respect to animals receiving vehicle injections. However, the immunoreactivity for BDNF, which was increased in the axotomized group as compared to control, was not modified in the implanted group. The modifications induced by NPC implants on VEGF and BDNF content were specific for the population of axotomized abducens internuclear neurons since the neighboring abducens motoneurons were not affected. Similar levels of NT-3 and NGF immunolabeling were obtained in injured neurons from axotomized and implanted animals. Among all the analyzed neurotrophic factors, only VEGF was expressed by the implanted cells in the lesion site. Our results point to a role of NPC implants in the modulation of neurotrophic factor expression by lesioned central neurons, which might contribute to the restorative effects of these implants.

Citation: Talaverón R, Matarredona ER, de la Cruz RR, Pastor AM (2013) Neural Progenitor Cell Implants Modulate Vascular Endothelial Growth Factor and Brain-Derived Neurotrophic Factor Expression in Rat Axotomized Neurons. PLoS ONE 8(1): e54519. doi:10.1371/journal.pone.0054519

Editor: Tim Douglas Aumann, Florey Institute of Neuroscience & Mental Health, Australia

Received October 2, 2012; **Accepted** December 12, 2012; **Published** January 18, 2013

Funding: The study was funded by grants in Spain BFU2009-07121 and BFU2012-33975 from MEC-FEDER and CVI-6053 from Junta de Andalucía-FEDER. The funders had no role in study design, data collection and analysis, decision to publish, or preparation of the manuscript.

Competing Interests: The authors have declared that no competing interests exist.

* E-mail: ampastor@us.es

Introduction

Axotomy of adult CNS neurons leads to severe morphofunctional alterations which include synaptic stripping and reduced firing rate [1,2]. When neurotrophic factors are delivered to the distal stump of lesioned nerves, these alterations are largely prevented and neuronal function is restored [3,4,5,6], which suggests that physiological changes induced by axotomy are, at least in part, due to the lack of target-derived trophic support. Neurotrophic dependence of adult neurons is also evidenced by the axotomy-induced regulation in the expression of growth factors and/or their receptors [7,8,9], which might compensate for the loss of retrograde trophic support through alternative pathways, such as anterograde, paracrine or autocrine [10].

By using the oculomotor system as the experimental model, we have previously described that the transection of the medial longitudinal fascicle (MLF) induces profound alterations in the axotomized internuclear neurons of the abducens nucleus, which are left disconnected from their target [2,11]. The abducens nucleus is composed of motoneurons that innervate the ipsilateral lateral rectus muscle, and a group of premotor cells, the abducens internuclear neurons, whose axons course through the MLF to establish synaptic contacts with medial rectus motoneurons in the contralateral oculomotor nucleus [12]. After their axotomy, abducens internuclear neurons show a marked reduction in firing rate, a significant decrease in eye position and velocity sensitivities and a noticeable stripping of synaptic afferences [2,11]. Moreover, when a new target (embryonic tissue) is provided, lesioned abducens internuclear neurons are able to restore their firing properties and synaptic afferences [13,14]. It was suggested that neurotrophic factors released by the implanted tissue probably mediate the re-establishment of these axotomy-induced alterations, a hypothesis supported by the fact that abducens internuclear neurons express the different types of trk receptors for neurotrophins [15].

As a further step, we have explored in our central axotomy model the effects of neural progenitor cell (NPC) implants based

on the reported efficacy of this cell population in promoting functional improvement of damaged CNS neurons [16,17,18]. Thus, axotomized abducens internuclear neurons largely recover their morphophysiological properties following the implant of NPCs at the lesion site in the MLF, as we have shown recently in the cat [19]. Several mechanisms have been proposed to be likely involved in the benefitial effects of the NPC implants after CNS injury: secretion of neurotrophic and/or angiogenic factors, restoration of synaptic transmitter release by providing local reinnervation, re-establishment of functional afferent and efferent connections, or change in the brain microenvironment towards more favourable conditions for both the lesioned neurons to survive and the implanted progenitors to integrate [20,21]. In line with this, recent evidence suggests that implanted NPCs establish a "cross-talk" or bilateral communication with host tissue cells of relevant importance for the neuroprotective action of the implants [22,23].

NPCs used in our study were obtained from the subventricular zone (SVZ) of postnatal animals. In their neurogenic niche, SVZ cells have been described to express the angiogenic factor vascular endothelial growth factor (VEGF) and the neurotrophic factors brain-derived neurotrophic factor (BDNF), nerve growth factor (NGF) and neurotrophin-3 (NT-3) [24]. More precisely, SVZ astrocytes express all the mentioned angionenic and neurotrophic factors whereas SVZ neural progenitors selectively express VEGF [24]. The neurobiological interest for VEGF is sharply increasing nowadays since in addition to its well known angiogenic activity, VEGF also exhibits neurotrophic and neuroprotective properties [25,26,27,28]. Moreover, a role in synaptic transmission has also been attributed to this factor. In particular, VEGF is able to induce a depression in excitatory synaptic transmission onto pyramidal and granule neurons of the hippocampus and also on hypoglossal motoneurons [29,30]. On the other hand, the neurotrophins BDNF, NT-3 and NGF, also expressed in the SVZ niche, have been demonstrated to induce benefitial effects in lesioned neurons after different types of brain damage [3,5,6].

In the present work, we aimed to investigate possible modifications of neurotrophic factor expression in central injured neurons following NPC implants which could be involved in the physiological recovery induced by these implants. For this purpose, we transected the MLF in adult rats and implanted NPCs at the lesion site. Changes induced by the lesion and/or the implant in the expression of VEGF, BDNF, NT-3 and NGF were analyzed in the axotomized population of abducens internuclear neurons. In addition, we also evaluated the expression of these neurotrophic molecules by the implanted NPCs. The findings of this study indicate that axotomy induces changes in the expression of neurotrophic factors by injured central neurons that can be differentially modulated by NPC implants. We propose that the neurotrophic regulation promoted by NPCs might contribute to the restorative effects of NPC implants.

Materials and Methods

Experiments were performed in adult and 7 day postnatal (P7) Wistar rats in accordance with the guidelines of the European Union (86/609/EU) and Spanish law (R.D. 120/2005 BOE 252/34367-91, 2005) for the use and care of laboratory animals. Surgical procedures used in this study were approved by the ethics committee of Universidad de Sevilla.

Neural Progenitor Cell Culture and Infection

Neural progenitors were isolated from the SVZ of postnatal rats (P7) and were expanded in the form of neurospheres essentially as reported [31]. Briefly, the lateral walls of the lateral ventricles were removed and enzymatically dissociated with 1 mg/ml trypsin at 37°C for 15 min. The tissue was then centrifuged at 150 g for 5 min, rinsed in Dulbecco's modified Eagle's medium/F12 medium 1:1 (DF-12) and centrifuged again in the same conditions. Then, the cells were resuspended in DF-12 containing 0.7 mg/ml ovomucoid, and mechanically disaggregated with a fire polished Pasteur pipette. The dissociated cells were centrifuged, resuspended in defined medium (DM: DF-12 containing B-27 supplement, 2 mM glutamine, 100 units/ml penicillin, 100 μg/ml streptomycin and 0.25 μg/ml amphotericin B) supplemented with 20 ng/ml EGF and 10 ng/ml FGF-2, and maintained in an atmosphere of 5% CO_2, at 37°C. After 1–2 days, cell aggregates known as neurospheres were formed (Figure 1A). Cells were subcultured 48 hours after isolation and then every 3–4 days. Neurosphere-derived cells were immunopositive for the neural precursor marker nestin and were able to generate glial and neuronal cells when they were induced to differentiate after plating on adhesive substrate (supporting information S1 and Figure S1).

Neurospheres were infected with a lentiviral vector containing a reporter gene encoding for the green fluorescent protein (GFP) under the control of the cytomegalovirus (CMV) promoter (generously provided by Dr. David Macías, Hospital Universitario Virgen del Rocío, University of Seville; lentivirus titer: 3×10^6 IFU/ml) with a multiplicity of infection of 3. Neurosphere-derived cells were incubated for 8 hours with virus-added DM in T25 flasks containing 250,000 cells. Virus-containing medium was then removed and replaced with fresh DM. After 48–72 hours of virus incubation, cells from neurospheres expressed GFP as confirmed by direct visualization in a Zeiss LSM 7 DUO confocal microscope (Figure 1B). The phenotype of the neurosphere-derived cells was not affected by the infection since they maintained the same ability to generate neurons and glial cells in differentiating conditions (data not shown).

Transection of the Medial Longitudinal Fascicle and Neural Progenitor Cell Implantation

Under general anesthesia (4% chloral hydrate, 1 ml/100 g, i.p.), adult rats were placed on a stereotaxic frame and a window trephined in the occipital bone. The right MLF was transected by means of a 750-μm width microblade aimed with a 45° anterior angle at the following stereotaxic coordinates: 3.5 mm caudal to lambda and 0 mm lateral [32]. Figure 1C shows the site of axotomy in a schematic drawing of a rat brainstem parasagittal section. Then, lesioned rats were divided into two groups according to the type of procedure performed after the axotomy: the implanted group and the axotomized group. Rats of the implanted group received an injection of GFP-expressing neurosphere-derived cells (one μl of a suspension of 50,000 viable cells/μl prepared in DF-12). Cells were injected with a Hamilton microsyringe coupled to a glass capillary in the same coordinates of the lesion (Figures 1C–E). Rats from the axotomized group received only vehicle injection (one μl of DF-12) after the MLF transection.

The unilateral transection of the right MLF disrupts the axons of the internuclear neurons of the left abducens nucleus. As the left MLF was not transected, right side abducens internuclear neurons remained unlesioned and were used as control neurons throughout this study.

Eight weeks after lesion followed by cell implant or vehicle injection, animals were perfused transcardially under deep anesthesia (sodium pentobarbital, 50 mg/kg, i.p.) with 100 ml of physiological saline followed by 250 ml of 4% paraformaldehyde in 0.1 M sodium phosphate buffer, pH 7.4. The brainstem was

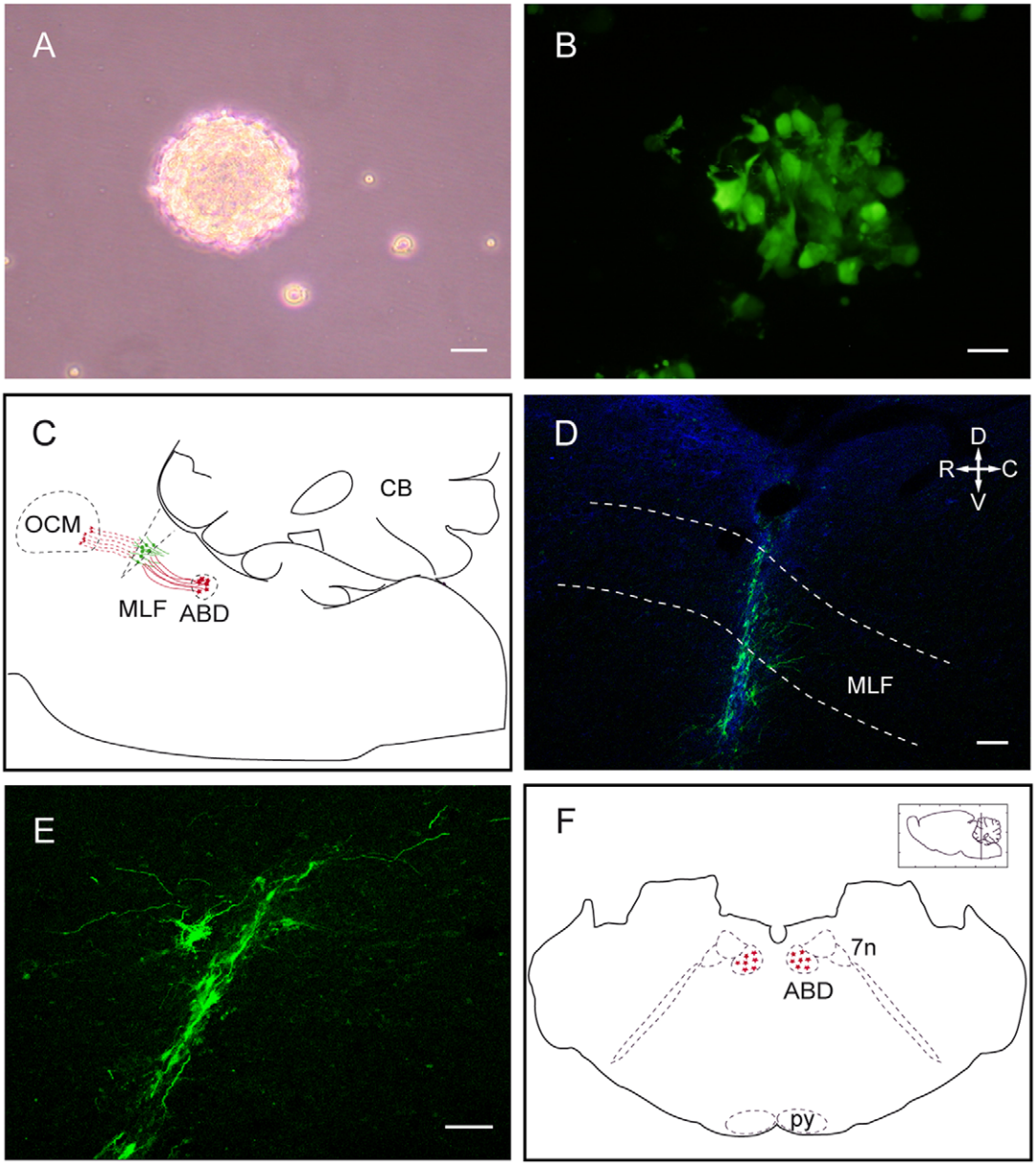

Figure 1. Neural progenitor cell culture, axotomy and cell implant. A. Floating neurosphere obtained from neural progenitors of the postnatal rat subventricular zone (SVZ). Scale bar: 25 µm. B. GFP-expressing cells (in green) in a SVZ-derived neurosphere. Scale bar: 25 µm. C. Schematic drawing of a rat parasagittal brainstem section showing the location of the medial longitudinal fascicle (MLF) transection and cell implant. Abducens internuclear neurons are represented in red and implanted neural progenitor cells in green. Axons of abducens internuclear neurons (red lines) course through the MLF towards the contralateral oculomotor nucleus. The distal stump of disrupted axons are represented in red dashed lines. D. Confocal microscopy image of a parasagittal brainstem section showing the implanted cells labeled with GFP (in green) at the site of axotomy. Dashed lines indicate the approximate dorso-ventral limits of the MLF. Scale bar: 100 µm. E. Higher magnification image of implanted GFP-labeled cells. Dorso-ventral and rostro-caudal orientation as in D. Scale bar: 50 µm. F. Schematic representation of a rat coronal section through the pons showing the abducens nucleus location. Abducens internuclear neuron somata are represented in red. **Abbreviations:** ABD: abducens nucleus; C: caudal; CB: cerebellum; D: dorsal; GFP: green fluorescent protein; MLF: medial longitudinal fascicle; OCM: oculomotor nucleus; py: pyramidal tract; R: rostral; V: ventral; 7n: facial nerve.
doi:10.1371/journal.pone.0054519.g001

removed and cryoprotected by immersion in a solution of 30% sucrose in sodium phosphate-buffered saline (PBS) until it sank. Then, for cryostat sectioning, the brainstem was cut in two pieces: the more rostral one, containing the site of lesion in the MLF, was sectioned sagitally (Figure 1C–E) and the caudal one, containing the abducens nucleus, was sectioned coronally (schematically represented in Figure 1F). All the sections were 40-µm thick. Sections were divided in parallel series to be processed for different immunostainings.

Immunohistochemistry

After washing in PBS, coronal sections containing the abducens nucleus were incubated with 1% sodium borohydride for 10 min for antigen retrieval. They were rinsed again in PBS and incubated

for 1 hour in a blocking solution consisting of 5% normal donkey serum in PBS with 0.01% Triton X-100 (PBS-T). Following the blocking treatment, sections were incubated overnight at room temperature with one of the following primary antibodies: rabbit anti-VEGF (Santa Cruz Biotechnology, sc-507, 1:100), rabbit anti-BDNF (Santa Cruz Biotechnology, sc-546, 1:400) or rabbit anti-NT-3 (Santa Cruz Biotechnology, sc-547, 1:400), prepared in blocking solution. After several rinses in PBS, sections were incubated with a biotinylated secondary antibody in PBS-T (biotinylated anti-rabbit IgG Jackson ImmunoResearch, 1:500), washed again and finally transferred for 45 minutes to a solution containing streptavidin-FITC (Jackson ImmunoResearch, 1:800). Then, in order to identify abducens internuclear neurons, subsequent immunohistochemistry for the detection of calretinin was performed since this protein is selectively expressed within the abducens nucleus by this population of neurons [33]. The primary antibody was a goat anti-calretinin from Swant (1:500) and the antibody binding was made visible by incubation with an anti-goat-TRITC (Jackson ImmunoResearch, 1:100). In other experiments, when the detection of abducens motoneurons was required, a goat anti-choline acetyltransferase (ChAT) antibody (Millipore, 1:500) followed by anti-goat-TRITC incubation was used. Sections were then washed for several times, mounted on glass slides and coverslipped with a 0.1 M solution of propyl gallate prepared in glycerol:PBS (9:1).

The immunohistochemical protocol for NGF varied slightly since a different antigen retrieval method was needed, which consisted of incubating the sections in 0.01 M sodium citrate buffer, pH 6, at 74°C for 40 min. The remaining protocol was the same as described above except that incubation with the primary antibody (rabbit anti-NGF; Santa Cruz Biotechnology, sc- 548, 1:100) lasted for 72 hours at 4°C. Finally, calretinin immunohistochemistry and mounting on slides were performed as described above.

It is important to point out that, in order to avoid differences in immunostaining intensity due to methodological procedures, series of sections from implanted and axotomized groups were always processed simultaneously for each neurotrophic factor.

To analyze neurotrophic factor expression by implanted cells, parasagittal sections containing the lesion and implant site were processed for single immunohistochemistry for VEGF, BDNF, NT-3 or NGF, following the same described procedure but a streptavidin-DyLight649 was used (Jackson ImmunoResearch, 1:800) instead of a FITC-coupled streptavidin, since implanted cells were already labeled in green by their GFP expression.

Antibody Characterization

For positive controls, the immunohistochemistry protocol was performed in brain sections that contained areas previously reported as immunopositive for each of the neurotrophic factors used in this study.

Negative controls carried out by omission of the primary antibodies resulted in absence of staining in all cases. Additional negative controls were performed by preadsorption of the antibodies with their blocking peptides. Specifically, each antibody and its corresponding immunizing peptide were mixed for 2 hours at a 1:20 proportion before being used for the immunohistochemical protocol. Sections incubated with this preadsorbed solution showed no specific staining.

For the VEGF primary antibody, a blocking peptide was not available by the provider. Then, as negative control, the primary antibody incubation was replaced by incubation with normal rabbit IgG (Jackson ImmunoResearch) at the same concentration than the primary antibody. Again, no specific labeling was found.

Confocal Microscopy and Optical Density Quantification

Confocal microscopy images of abducens neurons were captured in order to analyze differences between groups in the intensity of the VEGF, BDNF, NT-3 and NGF immunostainings.

For each neurotrophic factor, all abducens neurons identified in one out of three coronal sections from each animal were captured with a confocal laser scanning microscope (Zeiss LSM 7 DUO) at 63X magnification and 8-bit resolution. Different focal planes containing the cell nucleus and separated 2 μm in the z axis were scanned by exciting the FITC and TRITC fluorophores with 488-nm argon and DPSS 561-nm lasers, respectively, with a pinhole aperture of 1 Airy Unit. Before scanning, gray scales were adjusted to maximize their dynamic range. Acquisition settings were kept constant during the image capture of neurons from the left (lesioned) and right (unlesioned) abducens nucleus of the same section.

Captured images were analyzed with ImageJ (NIH). In order to determine the intensity of the immunostaining, we calculated the mean gray value of the cell immunolabeling (i.e., the optical density) by manually outlining the cell cytoplasm in the corresponding scanned images. Optical density measurements have been demonstrated to correlate significantly with the amount of protein present in the brain tissue [34] and have been widely used by other authors to compare protein levels between groups [35,36,37,38]. Optical density values for VEGF, BDNF, NT-3 and NGF immunoreactivies were determined for neurons of the lesioned and the unlesioned (control) sides of both axotomized and implanted animals and data were finally expressed as percentages relative to the control side.

Statistics

Comparisons between groups were carried out in Sigma Plot 11 (Systat Software) by using one-way ANOVA followed by post-hoc multiple comparisons (Dunns method) at a significant level of $p<0.05$.

Results

Antibody Characterization

Positive and negative controls were carried out to test the specificity of the antibodies used in this study for the immunoidentification of the neurotrophic factors BDNF, NT-3, NGF and VEGF.

Initially, the immunohistochemistry protocol and the antibody titration were established in sections containing brain regions in which the expression of each factor has been previously described in the literature [30,39,40,41,42,43]. Thus, immunoreactivity for BDNF was found in rat hippocampus and the immunostaining was not evident when the antibody was preadsorbed with its immunizing peptide (Figures 2A and 2A'). Positive results were obtained for NT-3 immunostaining in cerebellar Purkinje cells (Figure 2B) and in hippocampus (not shown), and specific staining was absent when sections were incubated with the preadsorbed antibody (Figure 2B'). NGF immunodetection required a more intense antigen retrieval method after which its expression was evident in cerebellum (Figure 2C) and in hippocampus (not shown). Again, preincubation with the blocking peptide led to negative staining (Figure 2C').

VEGF expression was conspicuous in Purkinje cells of the cerebellum (Figure 2D) and in many other brain regions such as cortex or hippocampus (not shown). As the VEGF blocking peptide was not available (see Materials and Methods), sections were preincubated with normal rabbit IgG instead of the rabbit-

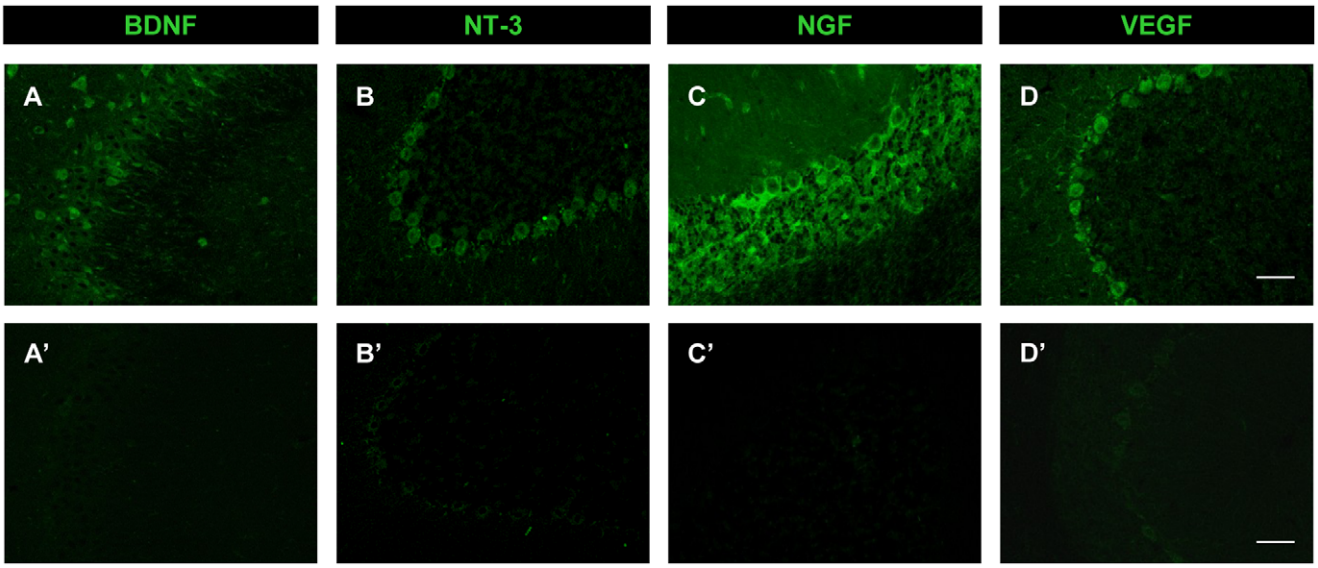

Figure 2. Antibody characterization. Confocal microscopy images of rat coronal sections through the hippocampus (A, A') and cerebellum (B, B', C, C') showing immunoreactivity to BDNF, NT-3, and NGF in positive controls (A, B and C, respectively) and in their respective blocking peptide-preadsorbed negative controls (A', B' and C'). D and D'. Confocal microscopy images of cerebellar coronal sections showing VEGF immunoreactivity in a positive control (D) and a negative control consisting of tissue pre-incubation with normal rabbit IgG instead of VEGF antibody (D'). Scale bars: 50 μm.
doi:10.1371/journal.pone.0054519.g002

made primary antibody, which also produced negative labeling in the cerebellum (Figure 2D') and in the other described regions.

VEGF Immunoreactivity is Increased in Lesioned Abducens Internuclear Neurons of Implanted Animals

As previously described, calretinin constitutes a good marker of the internuclear neurons located in the abducens nucleus [33]. Therefore, we used calretinin immunolabeling for the identification of this cell type. In all experimental groups (i.e., control, axotomized and implanted), the double immunofluorescence performed against calretinin and VEGF revealed that virtually all calretinin-positive abducens cells were also strongly immunoreactive for VEGF (Figure 3A). We further evaluated the intensity of the immunolabeling by quantifying the optical density within the neuronal soma of abducens internuclear neurons, as described in Materials and Methods. Thus, axotomy did not affect the intensity of VEGF immunoreaction, since injured neurons showed similar values of VEGF optical density in comparison with control cells (Figure 3A and 3B). Interestingly, abducens internuclear neurons from animals that received the NPC implants showed a significant increase in VEGF optical density, as compared with both control and axotomized cells (Figure 3B; $p<0.05$, ANOVA test; $n = 60–67$ neurons in each group obtained from 5 animals).

BDNF Immunoreactivity is Increased in Lesioned Neurons of Axotomized Animals but not of Implanted Animals

All calretinin-immunopositive neurons examined in the abducens nucleus also showed a strong immunoreactivity against BDNF, as observed in the three experimental groups (Figure 3A). However, the intensity of BDNF immunolabeling in abducens internuclear neurons changed eight weeks after MLF transection. Thus, BDNF optical density raised significantly in axotomized neurons in relation to control values (Figure 3C). In contrast, axotomized neurons from animals provided with NPC implants did not exhibit any change in BDNF optical density, as compared with the control group (Figure 3C; $n = 32–54$ neurons analyzed in each group from 4 animals).

Changes in VEGF and BDNF Immunoreactivity in the Abducens Nucleus are Selective for the Injured Cell Population

In order to test whether the effects of central axotomy and NPC implants on VEGF and BDNF expression were restricted to the injured neuronal population within the abducens nucleus (i.e., the abducens internuclear neurons) we also examined VEGF and BDNF immunoreactivity in the motoneurons of the same nucleus, whose axons were left intact. Abducens motoneurons were identified by their ChAT immunostaining (Figure 4A and C). Both VEGF and BDNF were expressed by virtually all abducens motoneurons analyzed in the three experimental groups ($n = 58–79$ motoneurons per group obtained from 3 animals) (Figure 4A–D), but their optical density values were not affected by either the MLF transection or the cell implantation (Figure 4E and 4F). Therefore, abducens motoneurons did not modify their VEGF or BDNF expression in response to the transected fascicle and NPC implants, so that the changes found in the immunoreactivity for these two neurotrophic molecules were specific to the population of injured abducens internuclear neurons.

Implanted Animals do not show Changes in NT-3 or NGF Immunoreactivity with Respect to Axotomized Animals

Abducens internuclear neurons showed a weak immunostaining against NT-3 (Figure 5A). The analysis of optical density after NT-3 immunolabeling revealed a significant increase of this parameter in the cell body of abducens internuclear neurons as a result of their axotomy (Figure 5B). Abducens internuclear neurons axotomized but provided with the NPC implants also showed a significant increase in NT-3 optical density as compared with control, which was similar to that exhibited by the axotomized group (Figure 5B). The number of calretinin-immunopositive

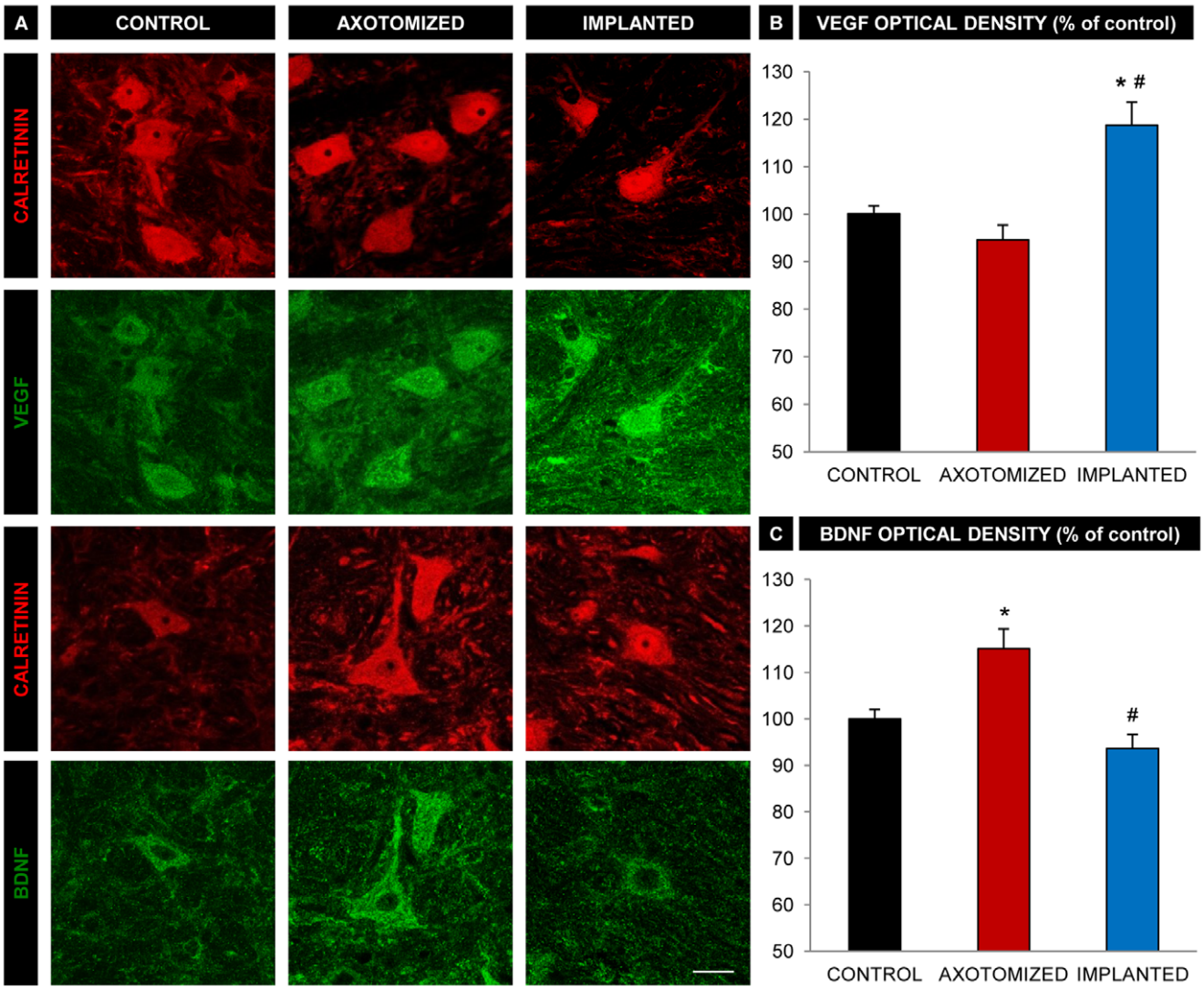

Figure 3. VEGF and BDNF immunoreactivity in abducens interneurons. A. Confocal microscopy images of abducens internuclear neurons (immunopositive for calretinin, in red) showing double immunoreactivity against either VEGF (in green, second row of images) or BDNF (in green, fourth row). Examples of neurons from the different experimental conditions are shown: non lesioned neurons (CONTROL column), lesioned neurons from the axotomized group (AXOTOMIZED column) and lesioned neurons from the implanted group (IMPLANTED column). Bar: 20 μm. B. Optical density quantification of VEGF immunoreactivity in unlesioned neurons (CONTROL), lesioned neurons from the axotomized group (AXOTOMIZED) and lesioned neurons from the implanted group (IMPLANTED). Values are expressed as percentages relative to control (unlesioned neurons). Bars represent the mean ± SEM of 60–67 neurons analyzed from five different animals in each group. * and # indicate significant differences with respect to the control and the axotomized group, respectively (ANOVA test followed by Dunn's method for multiple pairwise comparisons, $p<0.05$). C. Same as B, but for BDNF immunoreactivity. Bars represent the mean ± SEM of 32–54 neurons analyzed from four different animals in each group. * and # indicate significant differences with respect to the control and the axotomized group, respectively (ANOVA test followed by Dunn's method for multiple pairwise comparisons, $p<0.05$).
doi:10.1371/journal.pone.0054519.g003

neurons that appeared doubly labeled following the NT-3 immunofluorescence was similar in the three experimental groups and close to 100% (n = 25–38 neurons in each group obtained from 4 animals).

NGF immunoreactivity was mainly confined to the neuropil of the abducens nucleus, showing faintly-stained cell bodies (Figure 5A). Optical density quantification evidenced no significant change between groups in the intensity of NGF immunoreactivity, so that axotomized abducens internuclear neurons with or without the NPC implant showed values of NGF optical density that were similar to control (Figure 5C; n = 26–54 neurons per group obtained from 3 animals).

VEGF Expression by the Implanted Neural Progenitor Cells

We also aimed to explore whether implanted cells in the lesion site might constitute a retrograde source of neurotrophic factors for the axotomized abducens internuclear neurons, due to the close proximity between the proximal stump of sectioned axons and the implanted NPCs. For that, we performed VEGF, BDNF, NT-3 and NGF immunohistochemistry in brainstem parasagittal sections containing the lesion and NPC implantation site (Figure 1C–E). Implanted NPCs were identified by its GFP labeling. Approximately 25% of the GFP-positive NPCs examined appeared also labeled following VEGF immunoreactivity. Figure 6

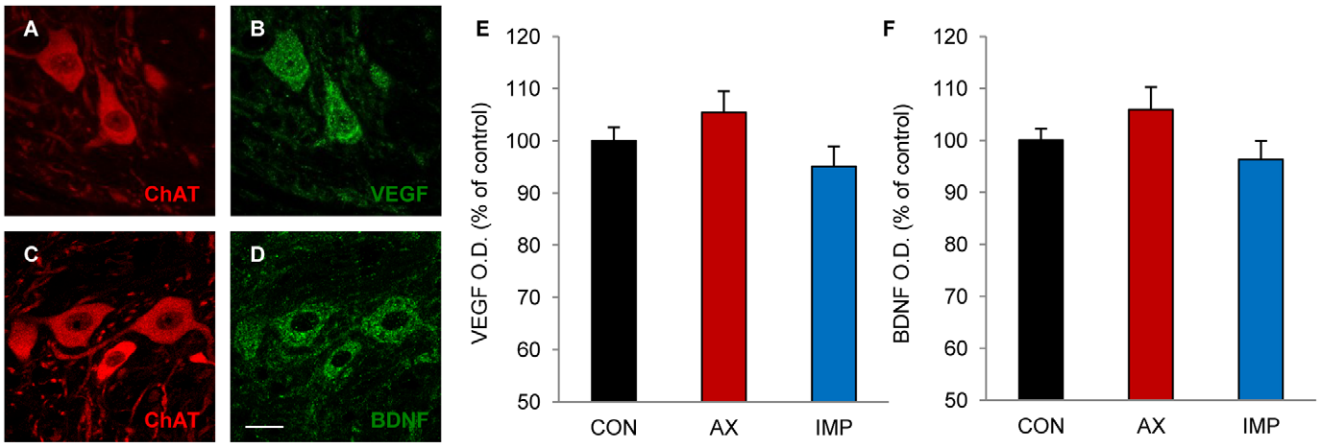

Figure 4. VEGF and BDNF immunoreactivity in abducens motoneurons. A to D. Confocal microscopy images of control abducens motoneurons showing double immunolabeling for ChAT (A, in red) and VEGF (B, in green), or for ChAT (C, in red) and BDNF (D, in green). Scale bar: 20 µm. E and F. Optical density (O.D.) quantification of VEGF immunoreactivity (E) and BDNF immunoreactivity (F) in abducens motoneurons from either the unlesioned side (CON), the lesioned side of the axotomized group (AX) or the lesioned side of the implanted group (IMP). Values represent percentages with respect to control (motoneurons from the unlesioned side). Bars show the mean ± SEM of 58–79 motoneurons analyzed from three different animals in each group. No significant differences were obtained between groups (ANOVA test followed by Dunn's method for multiple pairwise comparisons).
doi:10.1371/journal.pone.0054519.g004

illustrates an example of a NPC implanted at the lesion site which showed double labeling for both GFP and VEGF immunofluorescence. In contrast, none of the analyzed GFP-positive cells in the implant was found to be immunopositive for BDNF, NT-3 or NGF. Therefore, among all neurotrophic factors examined, VEGF was the only that could be delivered retrogradely from implanted cells to axotomized neurons.

Discussion

In this study, we have demonstrated that VEGF and BDNF expression in axotomized neurons can be modulated differentially by NPCs implanted in the site of injury. In addition, NPCs derived from the SVZ are able to express VEGF after implantation in the damaged brain. Based on the recently-demonstrated and relevant functions of VEGF in neuroprotection and synaptic modulation, we propose that this neurotrophic factor could play an important role in the benefitial effects of NPC implants on axotomized abducens internuclear neurons.

Transection of the MLF leaves abducens internuclear neurons disconnected from their natural target in the oculomotor nucleus. The axotomized neurons exhibit a profound removal of inhibitory and excitatory synapses and a reduction in eye position and velocity sensitivities [2,11]. In a previous work, we have shown that NPCs implanted in the cat after transection of the MLF induce a noticeable recovery in synaptic coverage and firing properties altered by the axotomy [19]. As described in other lesion models, NPCs might induce changes of protein expression in lesioned cells which could be determinant in the mechanism of NPC-induced recovery [21,22,23]. Therefore, we questioned whether NPC implants were able to modify neurotrophic factor expression in axotomized abducens internuclear neurons by means of immunohistochemical tools. First, we had to establish reliable immunohistochemical protocols with specific antibodies raised against VEGF, BDNF, NT-3 and NGF. Positive controls revealed immunolabeling in brain regions previously described to be immunopositive for the mentioned factors such as hippocampus, cerebral cortex or cerebellum [30,39,40,41,42,43]. Negative controls were performed by preadsorption of the antibody with the blocking peptide (for BDNF, NT-3 or NGF) or with normal IgG in substitution of the antibody (for VEGF). It is noteworthy that we never obtained specific labeling in these cases which indicated that antibodies used for this study were reliable and specific.

In the control situation, we observed that all analyzed abducens internuclear neurons displayed an intense immunoreactivity for VEGF and BDNF, whereas NT-3 and NGF revealed a faint staining. However, this was not the case for other brainstem neurons which showed an intense immunoreactivity for NT-3 and NGF (data not illustrated). Therefore, the intense labeling found in abducens internuclear neurons specifically after VEGF and BDNF immunoreactivity suggests that these two neurotrophic factors likely act as important molecules for the functional maintenance of this neuronal population, probably through autocrine or paracrine pathways, although the retrograde and/or anterograde routes can not be discarded.

After axotomy, abducens internuclear neurons did not modify their immunoreactivity to VEGF. However, VEGF content was significantly increased in these neurons when NPCs were implanted after axotomy. Two possible explanations may account for this finding: i) VEGF might have been retrogradely transported by the sectioned axons and accumulated in the soma, and ii) damaged neurons might have increased their VEGF expression in implanted animals. Since some of the implanted cells were VEGF-immunoreactive and abducens internuclear neurons express the receptor for VEGF, Flk-1 (unpublished data), the first possibility is feasible. With regard to the second possibility, it is well established that the new microenvironment created by the cross-talk between implanted and host tissue cells can induce changes in the neuronal expression of certain molecules [21,22,23,44]. Therefore, it is also possible that an increase in VEGF expression was induced in axotomized cells as a result of molecular interactions derived from this new microenvironment. Independently from the source, damaged neurons of implanted animals might benefit from the VEGF increased content. Indeed, recent evidence relates increased VEGF expression with neuroprotective actions. For instance, injured neurons after insults such as ischemia or brain seizures increase their VEGF expression and probably this might operate as an endogenous protective mechanism that reduces

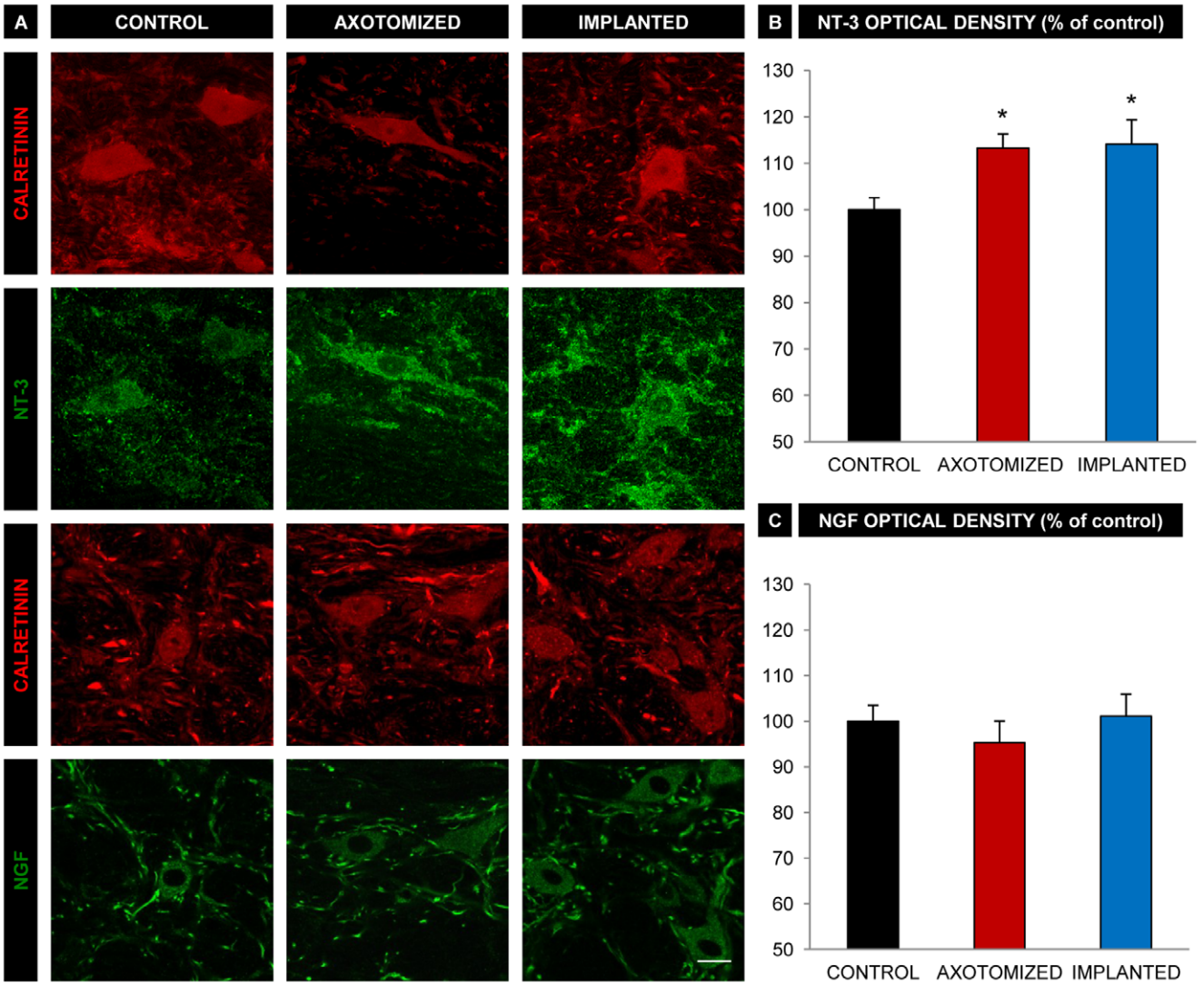

Figure 5. NT-3 and NGF immunoreactivity in abducens interneurons. A. Confocal images of abducens interneurons (immunopositive for calretinin, in red) showing double immunoreactivity against either NT-3 (in green, second row of images) or NGF (in green, fourth row). Examples of neurons from the different experimental conditions are shown: non lesioned neurons (CONTROL column), lesioned neurons from the axotomized group (AXOTOMIZED column) and lesioned neurons from the implanted group (IMPLANTED column). Scale bar: 20 μm B. Optical density quantification of NT-3 immunoreactivity in unlesioned neurons (CONTROL), lesioned neurons from the axotomized group (AXOTOMIZED) and lesioned neurons from the implanted group (IMPLANTED). Values are expressed as percentages with respect to control (unlesioned neurons). Bars represent the mean ± SEM of 25–38 neurons analyzed from four different animals in each group. *, $p<0.05$ compared to the control group, no significant differences were obtained between the axotomized and the implanted groups (ANOVA test followed by Dunn's method for multiple pairwise comparisons, $p<0.05$). C. Same as B, but for NGF immunoreactivity. Bars represent the mean ± SEM of 26–54 neurons analyzed from three different animals in each group. Note that there were no significant differences between groups (ANOVA test followed by Dunn's method for multiple pairwise comparisons, $p<0.05$).
doi:10.1371/journal.pone.0054519.g005

neuronal excitability [27,29]. Also, overexpression of VEGF is known to delay motor neuron degeneration in animal models of amyotrophic lateral sclerosis [28,45]. In the cat, NPC implants are able to restore most of the axotomy-induced alterations in firing properties and synaptic inputs of abducens internuclear neurons [19]. We propose that VEGF could be involved in the neuroprotective actions exerted by NPC implants in axotomized animals although further experiments are needed in order to elucidate this issue.

Abducens internuclear neurons of the axotomized group exhibited a significant increase in BDNF and NT-3 content eight weeks after MLF transection. We have previously demonstrated that abducens internuclear neurons express the trk receptors for BDNF and NT-3 (trkB and trkC, respectively) [15]. Therefore, by increasing BDNF and NT-3 expression, axotomized neurons might compensate for the lack of target-derived trophic support via autocrine or paracrine pathways [7,8,46]. However, in the implanted group, BDNF content of abducens internuclear neurons was not increased after axotomy and remained in values similar to healthy neurons. Probably, other endogenously-released molecules in the new microenvironment generated by the NPC implant might replace BDNF-dependent neurotrophic actions, and consequently this neurotrophin might be down-regulated as compared to the axotomy situation. This was not the case for NT-3, since this

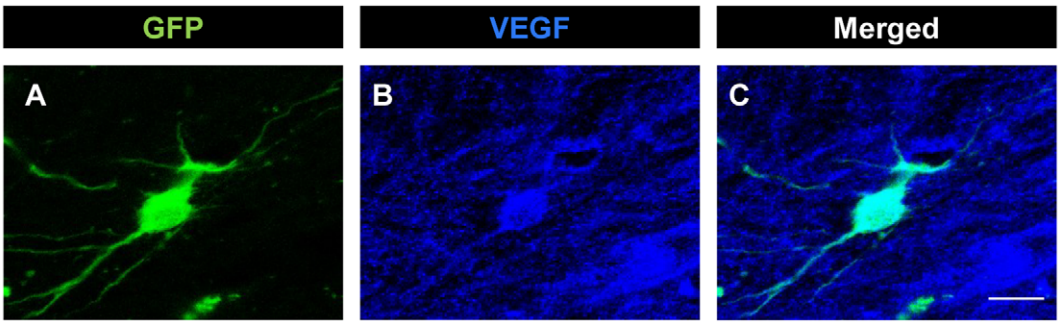

Figure 6. VEGF immunoreactivity in neural progenitor implanted cells. Confocal microscopy images of an implanted cell at the lesion site identified by its GFP expression (A, in green), which was also immunopositive for VEGF (B, in blue). C shows the merged image. Scale bar: 10 μm.
doi:10.1371/journal.pone.0054519.g006

neurotrophin increased significantly in both the axotomized and implanted groups and, therefore, neither the NPCs nor other cells from the host tissue that interacted with the NPCs could modify the axotomy-induced increase in NT-3 content. Since NGF immunoreactivity in abducens internuclear neurons was low and, in addition, was not affected by either the axotomy or the NPC implants, it seems that this neurotrophin is much less relevant in control as well as after lesion and implant.

A noticeably finding of the present study was that the motoneurons of the abducens nucleus, which lie intermingled with the internuclear neurons, did not show any change in the intensity of their immunostaining for either VEGF or BDNF. Since the same methodological protocol was used for both cell types, these data clearly validate the modifications found in the population of abducens internuclear neurons after NPC implants and, moreover, demonstrate that changes in neurotrophic factors were exclusive for those neurons that were axotomized by the lesion procedure.

As stated before, implanted cells might constitute a new source of trophic factors for axotomized cells. In fact, NPCs from the SVZ express VEGF in the neurogenic niche [24] and also when they are cultured in the form of neurospheres [47]. Fagerlund et al. [18] have recently reported that NPCs derived from the SVZ and transplanted in the lesioned hypoglossal nucleus express VEGF and promote motor neuron survival. In line with those findings, we pursued to investigate in our CNS lesion model whether SVZ neurosphere-derived cells were able to express VEGF or other neurotrophic factors eight weeks after implantation in the host lesioned tissue. Our results showed that none of the analyzed implanted cells were immunoreactive for BDNF, NT-3 or NGF, but a moderate percentage (approximately 25%) was immunopositive for VEGF, which indicated that implanted NPCs could release VEGF in the proximity of the proximal stumps of severed axons.

In summary, this study demonstrates that NPCs implanted in the injured brain express VEGF eight weeks after implantation in the host lesioned tissue and are able to modulate VEGF and BDNF expression in lesioned neurons. We propose that the increased VEGF expression promoted by NPCs in injured neurons might be involved in the restorative effects of NPC implants.

Supporting Information

Figure S1 Characterization of neurosphere cultures. A-B. Phase-contrast microscopy images of floating neurospheres (A) and dissociated neurosphere cells grown as a monolayer on a poly-lysine substrate (B). C, E, G. Fluorescence microscopy images of neurospheres immunostained with antibodies against nestin (C, red), βIII-tubulin (E, arrowhead, red), GFAP (E, arrow, green) and NG-2 (G, green) and counterstained with DAPI (blue). D, F, H. Fluorescence microscopy images of adhered cells immunostained with antibodies against nestin (D, red), βIII-tubulin (F, arrowhead, red), GFAP (F, arrow, green) and NG-2 (H, green) and counterstained with DAPI (blue). Scale bars: 50 μm in A, B and D; 25 μm in C and F; 15 μm in E, G and H.
(TIF)

Supporting Information S1 Characterization of neurosphere cultures.
(DOCX)

Acknowledgments

Some experiments were performed in the Biology and Microscopy Central Services of the Universidad de Sevilla (CITIUS). We wish to thank Dr. Juan Luis Ribas for his help with the confocal microscope and Dr. David Macías for kindly providing the lentivirus used in this study.

Author Contributions

Conceived and designed the experiments: ERM RRC AMP. Performed the experiments: RT ERM AMP. Analyzed the data: RT ERM RRC. Wrote the paper: ERM RRC AMP.

References

1. Titmus MJ, Faber DS (1990) Axotomy-induced alterations in the electrophysiological characteristics of neurons. Prog Neurobiol 35: 1–51.
2. Pastor AM, Delgado-García JM, Martínez-Guijarro FJ, López-García C, de la Cruz RR (2000) Response of abducens internuclear neurons to axotomy in the adult cat. J Comp Neurol 427: 370–390.
3. Giehl KM, Tetzlaff W (1996) BDNF and NT-3, but not NGF, prevent axotomy-induced death of rat corticospinal neurons in vivo. Eur J Neurosci 8: 1167–1175.
4. Kobayashi NR, Fan DP, Giehl KM, Bedard AM, Wiegand SJ, et al. (1997) BDNF and NT-4/5 prevent atrophy of rat rubrospinal neurons after cervical axotomy, stimulate GAP-43 and Talpha1-tubulin mRNA expression, and promote axonal regeneration. J Neurosci 17: 9583–9595.
5. Davis-López de Carrizosa MA, Morado-Díaz CJ, Tena JJ, Benítez-Temiño B, Pecero ML, et al. (2009) Complementary actions of BDNF and neurotrophin-3 on the firing patterns and synaptic composition of motoneurons. J Neurosci 29: 575–587.
6. Davis-López de Carrizosa MA, Morado-Díaz CJ, Morcuende S, de la Cruz RR, Pastor AM (2010) Nerve growth factor regulates the firing patterns and synaptic composition of motoneurons. J Neurosci 30: 8308–8319.
7. Venero JL, Vizuete ML, Revuelta M, Vargas C, Cano J, et al. (2000) Upregulation of BDNF mRNA and trkB mRNA in the nigrostriatal system and in the lesion site following unilateral transection of the medial forebrain bundle. Exp Neurol 161: 38–48.

8. Lee P, Zhuo H, Helke CJ (2001) Axotomy alters neurotrophin and neurotrophin receptor mRNAs in the vagus nerve and nodose ganglion of the rat. Brain Res Mol Brain Res 87: 31–41.
9. Morcuende S, Matarredona ER, Benítez-Temiño B, Muñoz-Hernández R, Pastor AM, et al. (2011) Differential regulation of the expression of neurotrophin receptors in rat extraocular motoneurons after lesion. J Comp Neurol 519: 2335–2352.
10. Giehl KM (2001) Trophic dependencies of rodent corticospinal neurons. Rev Neurosci 12: 79–94.
11. de la Cruz RR, Delgado-García JM, Pastor AM (2000) Discharge characteristics of axotomized abducens internuclear neurons in the adult cat. J Comp Neurol 427: 391–404.
12. Büttner-Ennever JA (2006) Neuroanatomy of the oculomotor system. In: Elsevier, Amsterdam, editors. Progress in Brain Research, vol 151.
13. Benítez-Temiño B, de la Cruz RR, Pastor AM (2002) Firing properties of axotomized central nervous system neurons recover after graft innervation. J Comp Neurol 444: 324–344.
14. Benítez-Temiño B, de la Cruz RR, Pastor AM (2003) Grafting of a new target prevents synapse loss in abducens internuclear neurons induced by axotomy. Neuroscience 118: 611–626.
15. Benítez-Temiño B, Morcuende S, Mentis GZ, de la Cruz RR, Pastor AM (2004) Expression of Trk receptors in the oculomotor system of the adult cat. J Comp Neurol 473: 538–552.
16. Lu P, Jones LL, Snyder EY, Tuszynski MH (2003) Neural stem cells constitutively secrete neurotrophic factors and promote extensive host axonal growth after spinal cord injury. Exp Neurol 181: 115–129.
17. Karimi-Abdolrezaee S, Eftekharpour E, Wang J, Morshead CM, Fehlings MG (2006) Delayed transplantation of adult neural precursor cells promotes remyelination and functional neurological recovery after spinal cord injury. J Neurosci 26: 3377–3389.
18. Fagerlund M, Estrada CP, Jaff N, Svensson M, Brundin L (2012) Neural stem/progenitor cells transplanted to the hypoglossal nucleus integrates with the host CNS in adult rats and promotes motor neuron survival. Cell Transplant 21: 739–747.
19. Morado-Díaz CJ, Matarredona ER, Davis-López de Carrizosa MA, de la Cruz RR, Pastor AM (2011) Neural progenitor cell implants in the lesioned medial longitudinal fascicle of adult cats regulate synaptic composition of abducens internuclear neurons. Abstr Soc Neurosci: 438.17.
20. Lladó J, Haenggeli C, Maragakis NJ, Snyder EY, Rothstein JD (2004) Neural stem cells protect against glutamate-induced excitotoxicity and promote survival of injured motor neurons through the secretion of neurotrophic factors. Mol Cell Neurosci 27: 322–331.
21. Capone C, Frigerio S, Fumagalli S, Gelati M, Principato M-C, et al. (2007) Neurosphere-derived cells exert a neuroprotective action by changing the ischemic microenvironment. PLoS ONE 2(4), e373. doi:10.1371/journal.-pone0000373.
22. Imitola J, In Park K, Teng YD, Nisim S, Lachyankar M, et al. (2004) Stem cells: cross-talk and developmental programs. Phil Trans R Soc Lond 359: 823–837.
23. Madhavan L, Ourednik V, Ourednik J (2008) Neural stem/progenitor cells initiate the formation of cellular networks that provide neuroprotection by growth factor-modulated antioxidant expression. Stem Cells 26: 254–265.
24. Tonchev AB, Yamashima T, Guo J, Chaldakov GN, Takakura N (2007) Expression of angiogenic and neurotrophic factors in the progenitor cell niche of adult monkey subventricular zone. Neuroscience 144: 1425–1435.
25. Sondell M, Sundler F, Kanje M (2000) Vascular endothelial growth factor is a neurotrophic factor which stimulates axonal outgrowth through the flk-1 receptor. Eur J Neurosci 12: 4243–4254.
26. Sun Y, Jin K, Xie L, Childs J, Mao XO, et al. (2003) VEGF-induced neuroprotection, neurogenesis, and angiogenesis after focal cerebral ischemia. J Clin Invest 111: 1843–1851.
27. Nicoletti J, Sachin S, McCloskey DP, Goodman JH, Scharfmann HE, et al. (2008) Vascular endothelial growth factor (VEGF) is upregulated after status epilepticus and protects against seizure-induced neuronal loss in hippocampus. Neuroscience 151: 232–41.
28. Azzouz M, Ralph GS, Storkebaum E, Walmsley LE, Mitrophanous KA, et al. (2004) VEGF delivery with retrogradely transported lentivector prolongs survival in a mouse ALS model. Nature 429: 413–417.
29. McCloskey DP, Croll SD, Scharfman HE (2005) Depression of synaptic transmission by vascular endothelial growth factor in adult rat hippocampus and evidence for increased efficacy after chronic seizures. J Neurosci 25: 8889–8897.
30. McCloskey DP, Hintz TM, Scharfman HE (2008) Modulation of vascular endothelial growth factor (VEGF) expression in motor neurons and its electrophysiological effects. Brain Res Bull 76: 36–44.
31. Torroglosa A, Murillo-Carretero M, Romero-Grimaldi C, Matarredona ER, Campos-Caro A, et al. (2007) Nitric oxide decreases subventricular zone precursor proliferation by inhibition of epidermal growth factor receptor and PI3-K/AKT pathway. Stem Cells 25: 88–97.
32. Paxinos G, Watson C (1997) The Rat Brain in Stereotaxic Coordinates. Academic Press. New York.
33. de la Cruz RR, Pastor AM, Martínez-Guijarro FJ, López-García C, Delgado-García JM (1998) Localization of parvalbumin, calretinin and calbindin D-28k in identified extraocular motoneurons and internuclear neurons of the cat. J Comp Neurol 390: 377–391.
34. Rieux C, Carney R, Lupi D, Dkhissi-Benyahya O, Jansen K, et al. (2002) Analysis of immunohistochemical label of Fos protein in the suprachiasmatic nucleus: comparison of different methods of quantification. J Biol Rhythms 17: 121–136.
35. Duprey-Díaz MV, Blagburn JM, Blanco RE (2003) Neurotrophin-3 and TrkC in the frog visual system: changes after axotomy. Brain Res 982: 54–63.
36. Gulino R, Lombardo SA, Casabona A, Leanza G, Perciavelle V (2004) Levels of brain-derived neurotrophic factor and neurotrophin-4 in lumbar motoneurons after low-thoracic spinal cord hemisection. Brain Res 2004: 174–181.
37. Qin DX, Zou Xl, Luo W, Zhang W, Zhang HT, et al. (2006) Expression of some neurotrophins in the spinal motoneurons after cord hemisection in adult rats. Neurosci Lett 410: 222–227.
38. Li X-L, Zhang W, Zhou X, Wang X-Y, Zhang H-T, et al. (2007) Temporal changes in the expression of some neurotrophins in spinal cord transacted adult rats. Neuropeptides 41: 135–143.
39. Conner JM, Lauterborn JC, Yan Q, Gall CM, Varon S (1997) Distribution of brain-derived neurotrophic factor (BDNF) protein and mRNA in the normal adult rat CNS: evidence for anterograde axonal transport. J Neurosci 17: 2295–2313.
40. Dugich-Djordjevic MM, Peterson C, Isono F, Obsawa F, Widmer HR, et al. (1995) Immunohistochemical visualization of brain-derived neurotrophic factor in the rat brain. Eur J Neurosci 7: 1831–1839.
41. Lambrechts D, Carmeliet P (2006) VEGF at the neurovascular interface: therapeutic implications for motor neuron disease. Biochim Biophys Acta 1762: 1109–1121.
42. Zhang H, Li L, Zou X, Song X, Hu Y, et al. (2007) Immunohistochemical distribution of NGF, BDNF, NT-3 and NT-4 in adult rhesus monkey brains. J Histochem Cytochem 55: 1–19.
43. Zhou XF, Rush RA (1994) Localization of neurotrophin-3 like immunoreactivity in the rat central nervous system. Brain Res 643: 162–172.
44. Pluchino S, Cusimano M, Bacigaluppi M, Martino G (2010) Remodelling the injured CNS through the establishment of atypical ectopic perivascular neural stem cell niches. Arch Ital Biol 148: 173–183.
45. Wang Y, Jin K, Mao XO, Xie L, Banwait S et al. (2007) Vascular endothelial growth factor overexpression delays neurodegeneration and prolongs survival in amyotrophic lateral sclerosis mice. J Neurosci 27: 304–307.
46. Tonra JR, Curtis R, Wong V, Cliffer KD, Park JS, et al. (1998) Axotomy upregulates the anterograde transport and expression of brain-derived neurotrophic factor by sensory neurons. J Neurosci 18: 4374–83.
47. Maurer MH, Tripps WK, Feldmann RE Jr, Kuschinsky W (2003) Expression of vascular endothelial growth factor and its receptors in rat neural stem cells. Neurosci Lett 344: 165–8.

ARTÍCULO 2

Implanted Neural Progenitor Cells Regulate Glial Reaction to Brain Injury and Establish Gap Junctions with Host Glial Cells

RESEARCH ARTICLE

Implanted Neural Progenitor Cells Regulate Glial Reaction to Brain Injury and Establish Gap Junctions with Host Glial Cells

Rocío Talaverón, Esperanza R. Matarredona, Rosa R. de la Cruz, David Macías, Victoria Gálvez, and Angel M. Pastor

Transplantation of neural stem/progenitor cells (NPCs) in the lesioned brain is able to restore morphological and physiological alterations induced by different injuries. The local microenvironment created at the site of grafting and the communication between grafted and host cells are crucial in the beneficial effects attributed to the NPC implants. We have previously described that NPC transplantation in an animal model of central axotomy restores firing properties and synaptic coverage of lesioned neurons and modulates their trophic factor content. In this study, we aim to explore anatomical relationships between implanted NPCs and host glia that might account for the implant-induced neuroprotective effects. Postnatal rat subventricular zone NPCs were isolated and grafted in adult rats after transection of the medial longitudinal fascicle. Brains were removed and analyzed eight weeks later. Immunohistochemistry for different glial markers revealed that NPC-grafted animals displayed significantly greater microglial activation than animals that received only vehicle injections. Implanted NPCs were located in close apposition to activated microglia and reactive astrocytes. The gap junction protein connexin43 was present in NPCs and glial cells at the lesion site and was often found interposed within adjacent implanted and glial cells. Gap junctions were identified between implanted NPCs and host astrocytes and less frequently between NPCs and microglia. Our results show that implanted NPCs modulate the glial reaction to lesion and establish the possibility of communication through gap junctions between grafted and host glial cells which might be involved in the restorative effects of NPC implants.

GLIA 2014;00:000–000

Key words: axotomy, subventricular zone, microglia, astrocytes, connexin43

Introduction

Neural stem/progenitor cells (NPCs) are a heterogeneous population of self-renewing and multipotent cells in the developing mammalian nervous system as well as in the subventricular zone (SVZ) of the lateral ventricles and the hippocampal dentate gyrus of the adult brain (Alvarez-Buylla et al., 2002; Anderson, 2001; Gage, 2000). NPCs can give rise to the three major lineages of the nervous system: neurons, astrocytes and oligodendrocytes and can be expanded *in vitro* from fetal, postnatal or adult brains (Carpenter et al., 1999; Gage, 2000; Reynolds and Weiss, 1992; Svendsen et al., 1996). In recent years, the use of NPCs for transplantation purposes has been tested in different types of nervous system disorders such as Parkinson's disease, Huntington's disease, multiple sclerosis, spinal cord injury or stroke, with generally reported beneficial effects (Cummings et al., 2005; Kelly et al., 2004; McBride et al., 2004; Pluchino et al., 2003, 2005; Richardson et al., 2005; Ziv et al., 2006). The local microenvironment that surrounds implanted NPCs in the injured nervous system has been described to influence NPC survival, integration, migration and differentiation (Englund et al., 2002; Jeong et al., 2003; Pluchino et al., 2003, 2005; Pluchino and Cossetti, 2013; Yang et al., 2002) and, in turn, NPC-derived signaling factors also influence this local environment and can be partially responsible for the beneficial effects attributed to NPC implants (Mosher et al., 2012;

View this article online at wileyonlinelibrary.com. DOI: 10.1002/glia.22630

Published online Month 00, 2013 in Wiley Online Library (wileyonlinelibrary.com). Received Oct 14, 2013, Accepted for publication Dec 23, 2013.

Address correspondence to Angel M. Pastor, Departamento de Fisiología, Facultad de Biología, Universidad de Sevilla, Avenida Reina Mercedes, 6, Sevilla 41012, Spain. E-mail: ampastor@us.es

From the Departamento de Fisiología, Facultad de Biología, Universidad de Sevilla, Sevilla, Spain.

Rocío Talaverón and Esperanza R. Matarredona contributed equally to this report.

Additional Supporting Information may be found in the online version of this article.

Talaverón et al., 2013). How signals from the endogenous micro-environment affect implanted NPCs and vice versa is a crucial question to understand the mechanisms underlying the benefits of transplanted cell-based therapies.

In line with this, Jäderstad et al. (2010) have recently described that communication via gap junctions between implanted NPCs and host neurons is an essential step in their integration into the host neural circuitry and in the mechanisms of their protective effects. Indeed, suppression of the gap-junctional intercellular communication is associated with significant decreases in the host rescue effects attributed to NPC engraftment (Jäderstad et al., 2010). Gap junctions allow the exchange of ions, second messengers and low weight molecules between connected cells, therefore providing a mechanism for the coordination of metabolic and electrical activities (Bruzzone et al., 1996; Kumar et al., 1996). A gap junction channel is formed by two joined hemichannels, each comprising six monomers of connexins, a family of proteins with more than 20 members (reviewed in Söhl and Willecke, 2003). Among all connexin isoforms, connexin43 (Cx43) is the predominant isoform within the CNS. Cx43 has an important role in the neurogenic process of NPC proliferation, differentiation and migration during development (Cheng et al., 2004; Duval et al., 2002; Elias et al., 2007; Marins et al., 2009; Santiago et al., 2010). In the postnatal and adult brain, Cx43 expression becomes much more restricted to astrocytes (Rash et al., 2001), but its expression remains in ependymal and endothelial cells, NPCs and migratory neuroblasts of the SVZ (Contreras et al., 2004; Lacar et al., 2011; Miragall et al., 1997; Nagy and Rash, 2000). Cx43 protein expression significantly changes in astrocytes following various models of CNS injury (Chew et al., 2010; Esen et al., 2007; Lee et al., 2005; Nakase et al., 2006). Interestingly, microglial cells, which do not express Cx43 under resting conditions, become immunoreactive to this connexin isoform after brain stab-wound injury (Eugenin et al., 2001) or in response to inflammatory stimuli such as cytokines or bacterial pathogens (Eugenin et al., 2001; Garg et al., 2005). Therefore, communication via gap junctions in glial cells may be important for tissue remodeling in a diseased state.

In previous reports, we have shown that implanted NPCs from the postnatal SVZ prevent the alterations in firing properties and synaptic coverage induced after the transection of the medial longitudinal fascicle (MLF) in the axotomized abducens internuclear neurons (Morado-Díaz et al., 2011), and also modulate their neurotrophic factor content (Talaverón et al., 2013). Now we have focused on the analysis of possible interactions between implanted NPCs and host glial cells that might be relevant not only for the integration of implanted cells but also for the prevention of lesion-induced alterations. Therefore, we have explored the glial reaction to lesion and NPC implantation, as well as the possibility of gap junctional communication between implanted NPCs and activated host astrocytes and microglia, as a likely important pathway mediating the graft-host signaling finally leading to neuronal improvement.

Materials and Methods

Experiments were performed in adult and 7-day postnatal (P7) Wistar rats in accordance with the guidelines of the European Union (2010/63/EU) and Spanish law (R.D. 53/2013 BOE 34/11370-420, 2013) for the use and care of laboratory animals. Surgical procedures used in this study were approved by the ethics committee of Universidad de Sevilla.

Neural Progenitor Cell Culture and Transduction

Neural progenitor cells were isolated from the SVZ of P7 rats (Fig. 1A) and were expanded in the form of neurospheres as described before (Talaverón et al., 2013; Torroglosa et al., 2007) (Fig. 1B).

Neurospheres were transduced with a lentiviral vector containing a reporter gene encoding for the green fluorescent protein (GFP) under the control of the cytomegalovirus promoter (Macías et al., 2009) with a titer of 3 x 10^6 IFU/mL and a multiplicity of infection of 3. Neurosphere-derived cells were incubated for 8 h with virus-added medium in T25 flasks containing 250,000 cells. After 72 h, cells from neurospheres expressed GFP (Fig. 1C). Neither viability nor multipoteniality of neurosphere-derived cells were affected by the viral transduction (Talaverón et al., 2013).

For immunocytochemical purposes, neurospheres were left to settle for 4 h on coverslips pretreated with poly-ornithine (Sigma Aldrich, St. Louis, MO) and then fixed with paraformaldehyde (4% in 0.1 M phosphate buffer, for 10 min).

CNS Lesion: Transection of the Medial Longitudinal Fascicle

Under general anesthesia (4% chloral hydrate, 1 mL/100 g, i.p.), adult rats were placed on a stereotaxic frame and a window trephined in the occipital bone. A unilateral transection of the right MLF was performed with a 750-μm width microblade aimed with a 35-degree anterior angle at the following stereotaxic coordinates: 3.5 mm caudal to lambda, 0 mm lateral and 7.5 mm depth (Paxinos and Watson, 1997) (Fig. 1D). The MLF contains, among others, axons of abducens internuclear neurons that project to the contralateral oculomotor nucleus and its disruption causes severe morphophysiological alterations within this neuronal population (de la Cruz et al., 2000; Pastor et al., 2000).

Neural Progenitor Cell Implantation

Immediately after lesion, a suspension of 50,000 viable GFP-expressing neurosphere-derived cells was prepared in DMEM/F-12 (Invitrogen, Camarillo, CA) and 1 μL of the cell suspension was injected at the same coordinates as the lesion with a Hamilton microsyringe coupled to a glass capillary (Fig. 1D). This

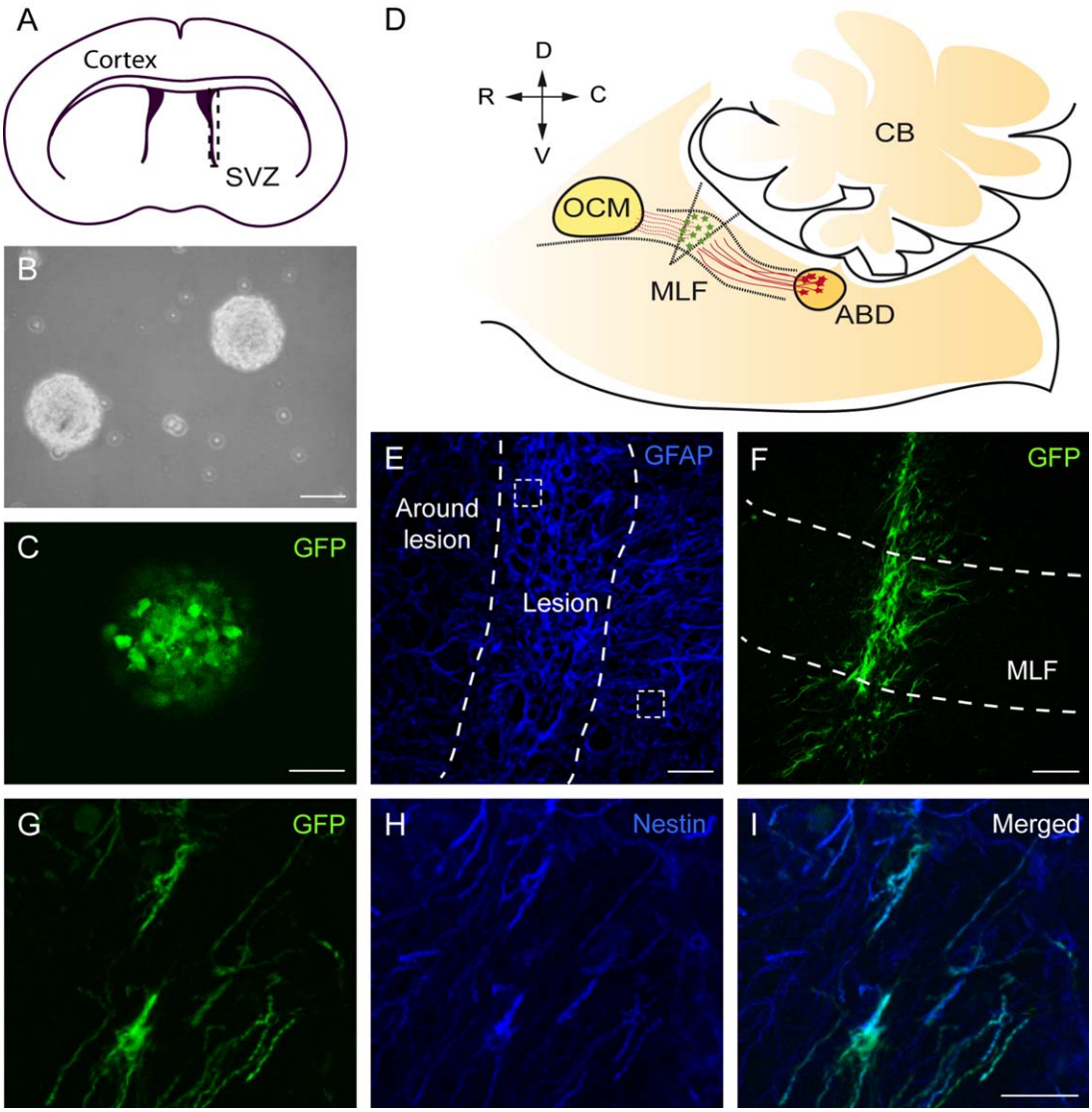

FIGURE 1: Neural progenitor cell culture, axotomy, cell implant and glial quantification. (A): Schematic drawing of a coronal slice obtained from a 7-day postnatal rat brain. Slices were cut beginning at the rostral opening of the third ventricle and extending 1.5-2.5 mm caudally. The subventricular zones (SVZ) adjacent to the lateral ventricles were dissected out (delimited between dashes) and neural progenitor cells contained in this region were cultured in the form of neurospheres. **(B)** and **(C):** Appearance of neurospheres in a phase contrast microscopy image (B) and in a confocal microscopy image showing GFP expression after viral transduction (C). Scale bar = 50 μm. **(D):** Schematic drawing of a rat brainstem parasagittal section showing the location of the medial longitudinal fascicle (MLF) transection and cell implant. Internuclear neurons of the abducens nucleus (ABD) are represented in red and implanted neural progenitor cells in green. Axons of abducens internuclear neurons (red lines) course through the MLF towards the contralateral oculomotor nucleus (OCM). The distal stumps of disrupted axons are represented in red dashed lines. **(E):** Confocal microscopy image from an axotomized rat brainstem section after GFAP immunohistochemistry (in blue). Lesion limits are represented between dashed lines and comprise approximately 75 μm bilaterally from the core of lesion. Examples of square boxes used to quantify optical density values of glial immunoreactivity in the lesion or around the lesion are shown. Scale bar = 50 μm. **(F):** Confocal microscopy image of a brainstem parasagittal section showing implanted cells identified by their GFP expression (in green) at the site of axotomy. Dorso-ventral limits of the MLF are shown in dashed lines. Scale bar = 100 μm. **(G-I):** Confocal microscopy images of a brainstem parasagittal section showing implanted cells identified by their GFP expression (in green, G) and after immunohistochemistry for nestin (in blue, H). I is the merged image of G and H. GFP- positive cell processes were immunoreactive for nestin. Scale bar = 25 μm. Dorso-ventral and rostro-caudal orientation of images D to I are the same as in D. Other abbreviations: C, caudal; CB, cerebellum; D, dorsal; GFAP, glial fibrillary acidic protein; GFP, green fluorescent protein; R, rostral; V, ventral.

experimental group will be referred to as implanted. Another group of animals, the so-called axotomized, received only vehicle injection (1 μL of DMEM/F-12) after the axotomy.

Eight weeks after lesion, animals were perfused transcardially under deep anesthesia (sodium pentobarbital, 50 mg/kg, i.p.) with 100 mL of physiological saline followed by 250 mL of 4%

paraformaldehyde in 0.1 M phosphate buffer, pH 7.4. Brainstems were removed and cryoprotected by immersion in a solution of 30% sucrose in sodium phosphate-buffered saline (PBS) until they sank. Then, 40-μm thick parasagittal sections were obtained with a cryostat to be processed for different immunostainings.

Immunohistochemistry for the Detection of Glial Cells and Connexin43

Parasagittal brainstem sections from axotomized and implanted animals were divided in adjacent series to be processed for the immunoidentification of astrocytes, oligodendrocyte precursors or activated microglia with antibodies raised against glial fibrillary acidic protein (GFAP), NG2 chondroitin sulfate proteoglycan (NG2), and MHC class II RT1B clone OX-6 (OX-6), respectively. After washing in PBS, sections were incubated with 1% sodium borohydride for 10 min for antigen retrieval. Sections were rinsed again in PBS and incubated for 1 h in a blocking solution consisting of 5% normal donkey serum in PBS with 0.1% Triton X-100 (PBS-T). Then, sections were incubated overnight at room temperature with one of the following primary antibodies: rabbit anti-GFAP (1:500; DAKO, Glostrup, Denmark, catalogue number Z0334), rabbit anti-NG2 (1:400; Millipore, Billerica, MA, catalogue number AB5320), mouse anti-MHC class II RT1B (Clone OX-6; 1:50; Serotec, Oxford, UK, catalogue number MCA46R) or goat anti-nestin (1:50; Santa Cruz Biotechnology, Dallas, TX, catalogue number sc-21249), prepared in blocking solution. After repetitive washings, sections were incubated for 2 h with the corresponding secondary antibody in PBS-T (anti-rabbit, anti-mouse or anti-goat IgG coupled to Cy3 or Cy5, 1:100; Jackson ImmunoResearch, West Grove, PA). Finally, sections were washed, mounted on slides and coverslipped with a 0.1 M solution of propyl gallate prepared in glycerol:PBS (9:1).

In some series of sections, immunohistochemistry for the detection of Cx43 (mouse anti-Cx43, 1:50, BD Biosciences, catalogue number 610062 or rabbit anti-Cx43, 1:200, Invitrogen, catalogue number 71-0700) was performed subsequently following the same described procedure but with the use of a biotinylated secondary antibody (biotinylated anti-mouse or anti-rabbit IgG, 1:500; Jackson ImmunoResearch) followed by 45-min incubation with DyLight 649 Streptavidin in PBS (1:800; Jackson ImmunoResearch).

Every immunohistochemical experiment was always performed simultaneously with sections from both axotomized and implanted animal groups.

Double immunocytochemistry for the simultaneous detection of nestin and Cx43 was performed in coverlisps with attached neurospheres. Coverslips were incubated for 30 min in blocking solution containing 2.5% bovine serum albumin (BSA) in PBS and then overnight with the primary antibodies (goat anti-nestin from Santa Cruz Biotechnology at 1:50 and mouse anti-Cx43 from BD Biosciences at 1:50) and 1.5 h with the secondary antibodies (anti-goat and anti-mouse IgGs labeled with FITC and Cy5, respectively), all prepared in blocking solution. After repetitive washings, cells were counterstained with 4′-6′-diamidino-2-phenylindole (DAPI, 0.1 μg/mL) for 10 min. Finally, coverslips were mounted on slides with the mounting medium described before. Negative controls carried out by omission of the primary antibodies resulted in absence of staining in all cases.

Confocal Microscopy and Image Analysis

Images were captured with a confocal laser scanning microscope (Leica TCS SP2) using the 20×, 40×, and 63× objectives. Different focal planes separated 2 μm in the *z*-axis were scanned by exciting GFP, Cy3, and Cy5 fluorophores with excitation wavelengths of 488, 561, and 633 nm, respectively.

Quantification of GFAP-, NG2-, or OX-6-immunoreactivity was performed with Image J (NIH, Bethesda, MD) on 8-bit images captured with the 40× objective. Eight nonoverlapping square boxes of 30.4 μm (80 pixels) per side were randomly selected in the lesion site in the channel corresponding to the glial immunoreactivity image (Fig. 1E). Mean gray values (as an index of optical density, in counts per pixel) were obtained for every box and the average was calculated after background level substraction. The same procedure was performed in the same image in the region directly surrounding the lesion (a minimum lateral distance of 75 μm from the core of the lesion). Therefore, for every image, two optical density values were obtained, one in the lesion and other surrounding the lesion.

For the analysis of Cx43 expression by NPCs and glial cells, images (8-bit) were captured at different focal planes (0.5-1 μm along the z axis) with a Zeiss LSM DUO confocal microscope. GFP, Cy3 and DyLight649 fluorophores were excited with 488-nm argon, DPSS 561 nm and HeNe 633 nm lasers, respectively. For three-dimensional reconstructions, confocal Z-stacks were captured at 63× in 0.4 or 1 μm intervals and images rendered with the ZEN 2009 Light Edition software.

Fixation and Tissue Preparation for Electron Microscopy

Six implanted animals were prepared for electron microscopy processing. After a brief saline perfusion animals were fixed with 300 mL of 4% paraformaldehyde and 0.3% glutaraldehyde in phosphate buffer (PB) 0.1 M. Brains were cut in 50-μm thick parasagittal sections on a vibratome (Leica VT 1000 S). Sections were cryoprotected for 1 h by immersion in 25% sucrose and 10% glycerol in 0.05 M PB and then frozen and thawed three times on liquid nitrogen for membrane permeabilization. Finally, they were treated with 1% sodium borohydride in PB during 20 min and extensively rinsed in PB.

Double Pre-Embedding Immunohistochemistry

To analyse the anatomical relationships between implanted cells and host microglia, pre-embedding immunogold-silver detection of GFP (expressed by implanted cells) was combined with pre-embedding immunohistochemistry for the microglial marker Iba1 (ionized calcium binding adaptor molecule 1) using the avidin-biotin-peroxidase (ABC) method. In this procedure, sections were sequentially incubated in: (i) blocking solution, containing 0.2 M glycine, 0.2 M lysine, 0.2% BSA, and 10% normal goat serum (NGS) in PB, for 60 min; (ii) monoclonal mouse anti-GFP antibody (1:2,000; Millipore, catalogue number MAB3580) together with rabbit anti-Iba1 (1:1,000; Wako, Osaka, Japan, catalogue number 019–19741) diluted in 0.8% BSA and 5% NGS (incubation solution) for 48 h at 4°C; (iii) 1 nm colloidal gold-labeled goat anti-mouse IgG (Aurion, Wageningen, The Netherlands) diluted 1:100 together with biotinylated goat anti-rabbit IgG diluted 1:200 (Jackson

ImmunoResearch) prepared in incubation solution for 2 h at 20°C followed by 24 h at 4°C; (iv) 2% glutaraldehyde in PB for 10 min to fix gold particles. After each step, sections were rinsed (3 x 10 min) in PB. Gold particles were enlarged using silver enhancer (R-Gent SE-LM; Aurion) for 18 min at 20°C. The reaction was stopped in 0.03 M sodium thiosulphate (Aurion) for 10 min. Finally, sections were incubated in ABC (1:200; Vector Laboratories, Burlingame, CA) for 2 h at 20°C. The peroxidase reaction was developed using 0.05% 3,3'-diaminobenzidine tetrahydrochloride (DAB) (Sigma Aldrich) and 0.0075% hydrogen peroxide in PB for 5 min at 20°C. Afterwards, sections were washed and then postfixed with 1% osmium tetroxide in PB for 60 min at 20°C, stained in block with uranyl acetate for 45 min at 20°C, dehydrated through increasing graded ethanol series and flat-embedded in Durcupan resin (ACM; Fluka, Buchs, Switzerland).

In other sections, pre-embedding immunohistochemistry of GFP using the ABC method was combined with pre-embedding immunogold-silver detection of Cx43. Sections were incubated with rabbit anti-Cx43 (1:200; Invitrogen) and mouse anti-GFP (1:2000; Millipore) antibodies followed by 1 nm colloidal gold-labeled goat anti-rabbit IgG (1:100; Aurion; 1:100) and biotinylated goat anti-mouse IgG (1:500; Jackson ImmunoResearch). All steps were performed as described before.

Finally, ultrathin sections 60 nm thick were cut with an ultramicrotome (Leica EM UC7), collected on single-slot Formvar-coated nickel grids, counterstained with uranyl acetate and lead citrate and examined on a Philips CM-10 transmission electron microscope. Images were digitally captured using a VELETA side-mounted camera (Olympus).

Postembedding Immunohistochemistry of Glial Fibrillary Acidic Protein

Postembedding GFAP immunostaining was performed on ultrathin sections with an anti-GFAP antibody (rabbit, 1:500; DAKO) and a 5 nm colloidal gold-labeled goat anti-rabbit IgG (1:15; Sigma Aldrich) following an already reported procedure (Pastor et al., 2000). A silver enhancer method was applied to enlarge the size of the gold particles previous to counterstaining with lead citrate and uranyl acetate (Danscher and Zimmer, 1978).

Statistics

The optical density values of GFAP, NG2, and OX-6 immunofluorescence were compared between experimental groups (axotomized *vs*. implanted) and between locations (lesion *vs*. around lesion). The statistical analysis was carried out in Sigma Plot 11 (Systat Software) by using the two-way ANOVA followed by *post hoc* multiple comparisons (Holm-Sidak's method) at a significant level of $P < 0.05$. All values are expressed as the mean ± standard error of the mean (SEM).

Results

Local Glial Cell Response to Axotomy and NPC Implants

The glial reaction to axotomy and NPC implants was analyzed 8 weeks after injury. Implanted NPCs were identified in the host tissue by their GFP expression. They appeared distributed in areas restricted to the lesion site, approximately 75 μm lateral from the core of lesion in the rostrocaudal axis, and covering the dorsoventral limits of the MLF (Fig. 1F). Most of the implanted NPCs presented cell processes of variable length (15–50 μm for short processes and up to 200 μm for longer processes) and were immunopositive for nestin, an intermediate filament protein expressed by neural stem cells (Fig. 1G–I).

Quantification of the glial cell response to injury was carried out by comparing the intensity of immunofluorescence corresponding to each glial marker (i.e., optical density) in the lesion site with respect to that found in the surrounding tissue, as described in Materials and methods, based on a previously described procedure (Whitman et al., 2009).

Axotomy induced a significant sixfold increase in GFAP optical density in the lesion site as compared to the area around lesion (Fig. 2A,C). A similar astrocytic response to injury was obtained in implanted animals (Fig. 2B,C). No significant differences were found in GFAP optical density values between axotomized and implanted groups, therefore, the presence of NPCs at the site of injury did not quantitatively modify the astroglial reaction to the fascicle transection.

NG2-immunopositive cells presented oval cell bodies with multiple branched thin processes (inset in Fig. 2D). Analysis of NG2 immunoreactivity revealed that 8 weeks after MLF transection, optical density values remained similar in the lesion site as compared to the surrounding area (Fig. 2D,F), and this was applicable to implanted animals (Fig. 2E,F). Similarly, comparisons between experimental groups (i.e., axotomized *vs*. implanted) revealed no significant differences of immunofluorescence intensity using the oligodendrocyte precursor marker NG2 (Fig. 2F).

With respect to microglia, two major types of OX-6-positive (MHC-II expressing) cell morphologies were observed: microglial cells with short thick processes and further activation states characterized by ameboid morphology (Fig. 2G,I). The lesion site displayed significantly higher optical density values of OX-6 immunoreactivity than the surrounding area both for axotomized and implanted animals (Fig. 2G–I). However, OX-6 optical density within the lesion resulted in approximately two times more prominent values in NPC implanted animals than in animals that received only vehicle injections ($P < 0.05$; Fig. 2G–I).

Implanted NPCs are Located in Close Proximity to Reactive Astrocytes and Activated Microglia

GFAP immunohistochemistry in the lesion site of implanted animals revealed a close apposition between astrocytic processes and implanted cells (Fig. 3A–D). Frequently, we observed astrocytic processes surrounding a large portion of the cell body of GFP-positive cells (see arrows in Fig. 3A,B).

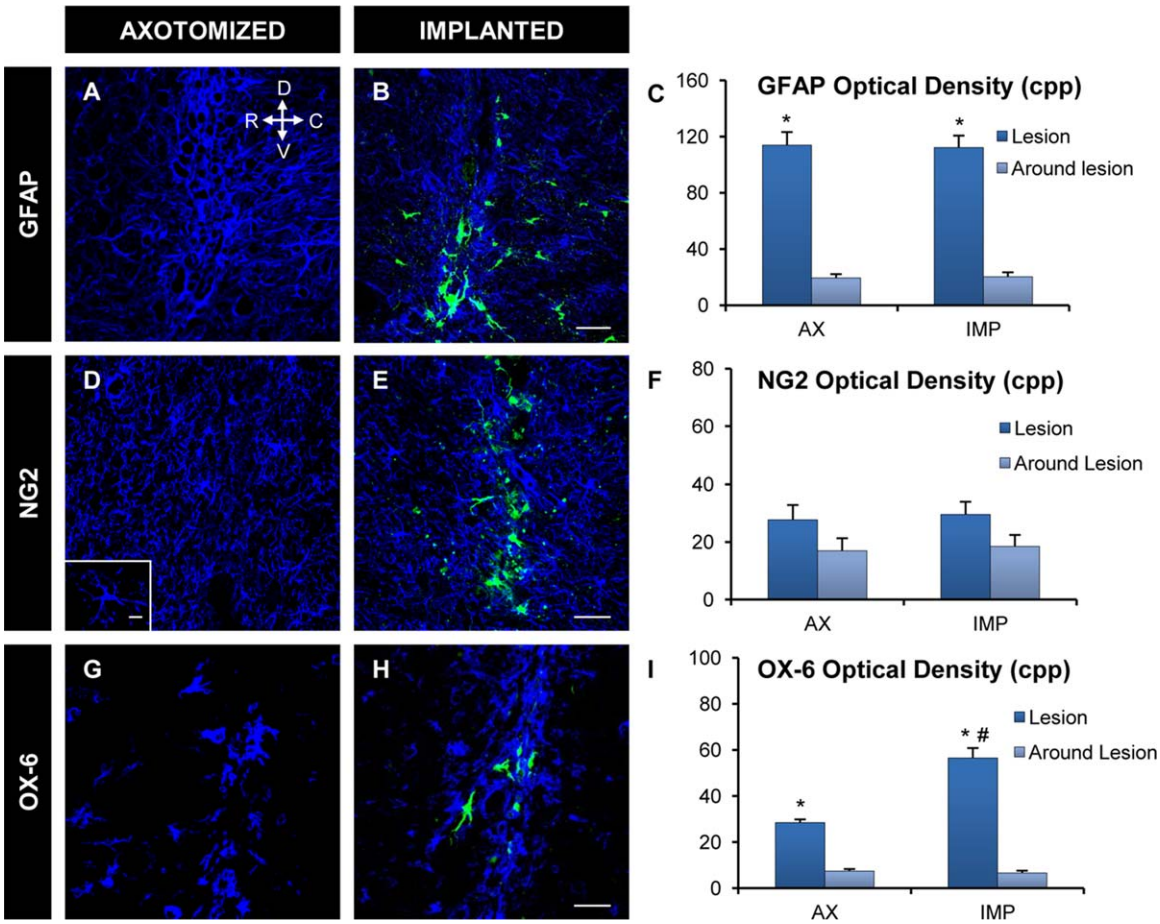

FIGURE 2: Glial reaction to axotomy and NPC implant. (A and B, D and E, G and H): Confocal microscopy images captured with the ×40 objective showing immunoreactivity to the astrocytic marker GFAP (A and B, in blue), the oligodendrocyte precursor marker NG2 (D and E, in blue) and the activated microglia marker OX-6 (G and H, in blue) in parasagittal sections containing the site of lesion from axotomized animals (A, D, G) and implanted animals (B, E, H). Implanted NPCs were identified in green by their GFP expression (B, E, and H; merged images of the glial marker and GFP channels). Inset in D represents a NG2-positive cell shown at higher magnification. Scale bars = 50 μm; 10 μm for the inset. C, caudal; D, dorsal; R, rostral; V, ventral. **(C):** Optical density values of GFAP immunoreactivity (in counts per pixel, cpp) in the lesion and around lesion from axotomized (AX) or implanted (IMP) animals. Bars represent the mean ± SEM of 8–10 sections analyzed from three different animals of each group. *$P < 0.05$, lesion compared to around lesion values. No significant differences between the axotomized and the implanted groups were found. **(F):** Optical density values of NG2 immunoreactivity (in counts per pixel, cpp) in the lesion and around lesion obtained from axotomized (AX) or implanted (IMP) animals. Bars represent the mean ± SEM of 8–9 sections analyzed from three different animals of each group. No significant differences were found between either lesion *versus* around lesion values in each group or axotomized *versus* implanted groups. **(I):** Optical density values of OX-6 immunoreactivity (in counts per pixel, cpp) in the lesion and around lesion from axotomized (AX) or implanted (IMP) animals. Bars represent the mean ± SEM of 28–31 sections analyzed from four different animals of each group. *$P < 0.05$, lesion compared to around lesion values; #$P < 0.05$, implanted compared to axotomized group. In C, F and I, the two-way ANOVA test was used followed by Holm-Sidak's method for multiple pairwise comparisons.

In addition, implanted NPCs were often located close to blood vessels together with astrocyte processes (Fig. 3C,D).

Some implanted NPCs developed long processes (up to 200 μm) directed mainly towards the caudal direction (Fig. 3E). Many of these cell processes were located in close proximity to activated microglial cells (Fig. 3E,G,H) and occasionally enwrapped them (Fig. 3E,F). In contrast, no evidence of close proximity between NG2-positive cells and NPCs was found.

Electron microscopy was performed to further confirm the interactions between implanted cells and host glia. Implanted NPCs were identified at the ultrastructural level by pre-embedding GFP immunostaining (Fig. 4A,B). They presented a branched morphology with elongations arising from the cell body. Numerous astrocytes were visualized in the lesion site after postembedding immunogold staining for GFAP. Gold particles were associated specifically with their typical intermediate filaments (Fig. 4C,D). Pre-embedding immunostaining for Iba1 allowed the ultrastructural identification of microglial cells (Fig. 4E,F). They were characterized by their small size, irregular nucleus and clumps of nuclear chromatin, especially close to the

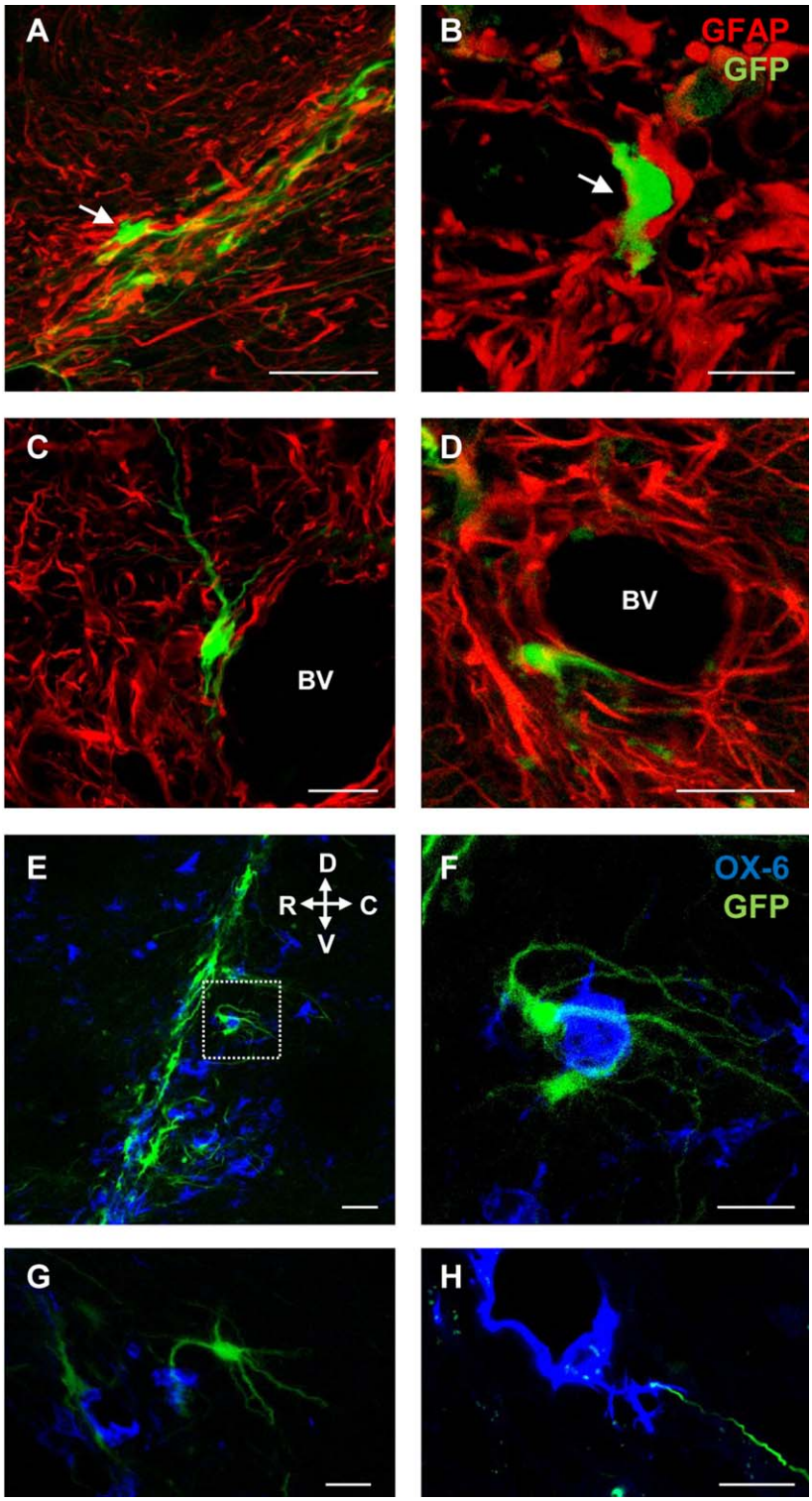

FIGURE 3: Close association between implanted NPCs and host glia. (A–D): Confocal microscopy images of parasagittal sections of the lesion site showing examples of the close proximity between implanted NPCs (GFP positive, in green) and reactive astrocytes (GFAP immunoreactive, in red). Arrows in A and B point to implanted cells surrounded by GFAP-positive processes. C and D are examples of implanted NPCs located nearby putative blood vessels (BV). Note that blood vessels appear surrounded by astrocytic processes. Scale bars = 50 μm in A and 25 μm in B to D. **(E–H):** Confocal microscopy images of parasagittal sections through the lesion site illustrating the close proximity between implanted NPCs (GFP-positive, in green) and activated microglia (OX-6 immunoreactive, in blue). F shows the framed region of E at higher magnification. Note NPC processes surrounding ameboid microglial cells. G and H illustrate processes of implanted cells adjacent to activated microglia. Scale bars = 50 μm in E and 25 μm in F to H.

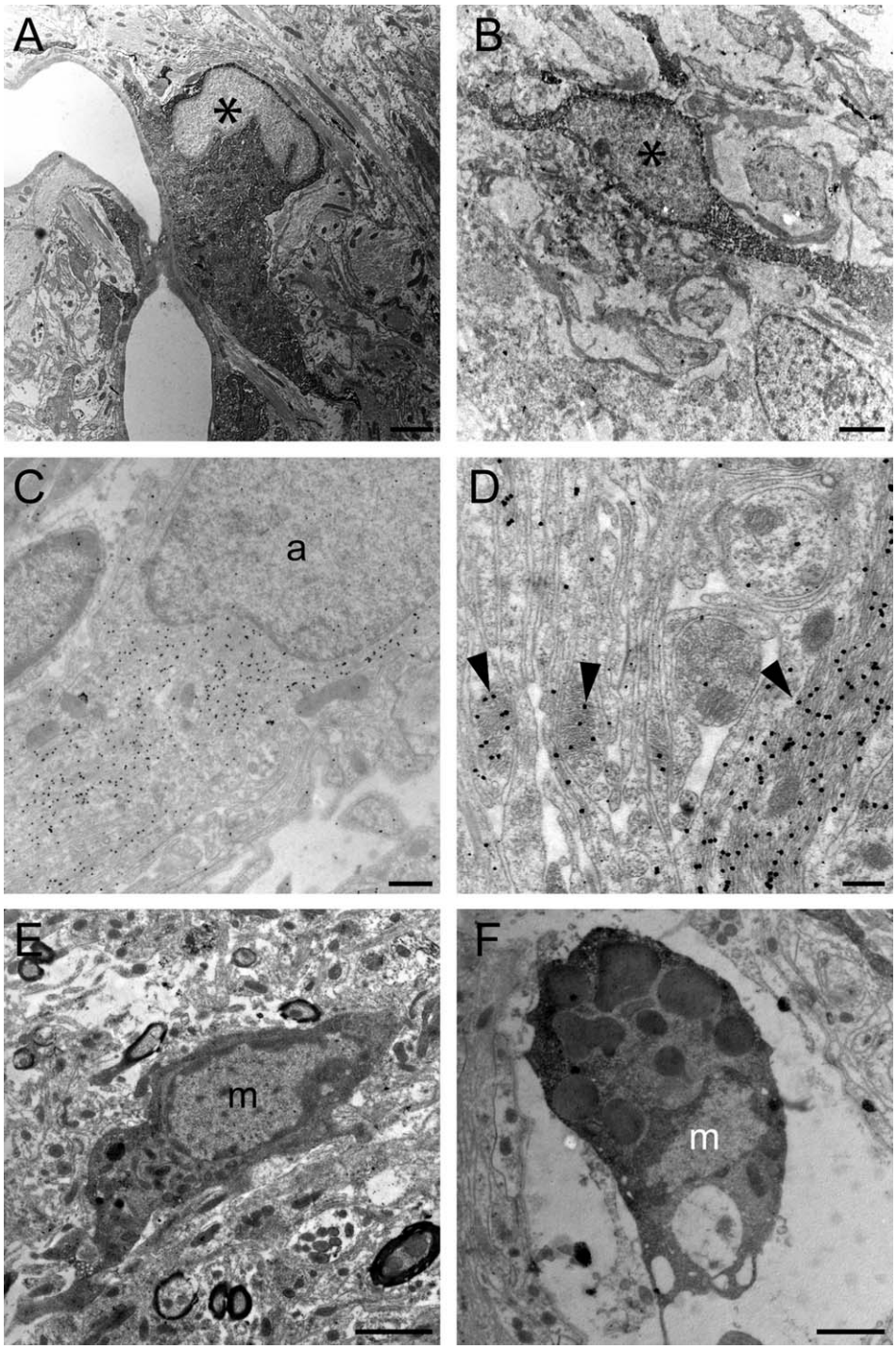

FIGURE 4: Ultrastructural and immunohistochemical identification of implanted NPCs and glial cells at the lesion site. **(A, B):** Examples of two NPCs identified by pre-embedding GFP immunohistochemistry using DAB, thereby conferring an electron-dense appearance to the cell (asterisks indicate the nucleus of the two NPCs). These cells presented a branched morphology (note the elongations arising from the implanted cell in B) and frequently appeared surrounded by a field of labeled processes (in A and B), that corresponded to either the observed cell or other neighboring implanted NPCs. The lesion site was characterized by a widened extracellular space (clearly notorious in B). Scale bars = 1 μm. **(C, D):** Electron microscopy images of astrocytes identified by post-embedding immunogold for GFAP. Note that gold particles are associated to filaments (arrowheads in D). The nucleus of the astrocyte in C is indicated as a. Scale bars = C, 0.125 μm; D, 0.5 μm. **(E, F):** Examples of two different types of microglial cells found at the lesion site according to their ultrastructural characteristics. Both types of microglia cells were identified by pre-embedding Iba-1 immunohistochemistry (DAB labeling). Note that the microglia in F is characterized by the presence of phagocytic vacuoles filling a large portion of its cytoplasm (ameboid type), whereas the microglia cell in E lacked such vacuoles. The nucleus of the microglia (m) typically contained clumped chromatin, specially surrounding the nuclear membrane. Scale bars = 2 μm.

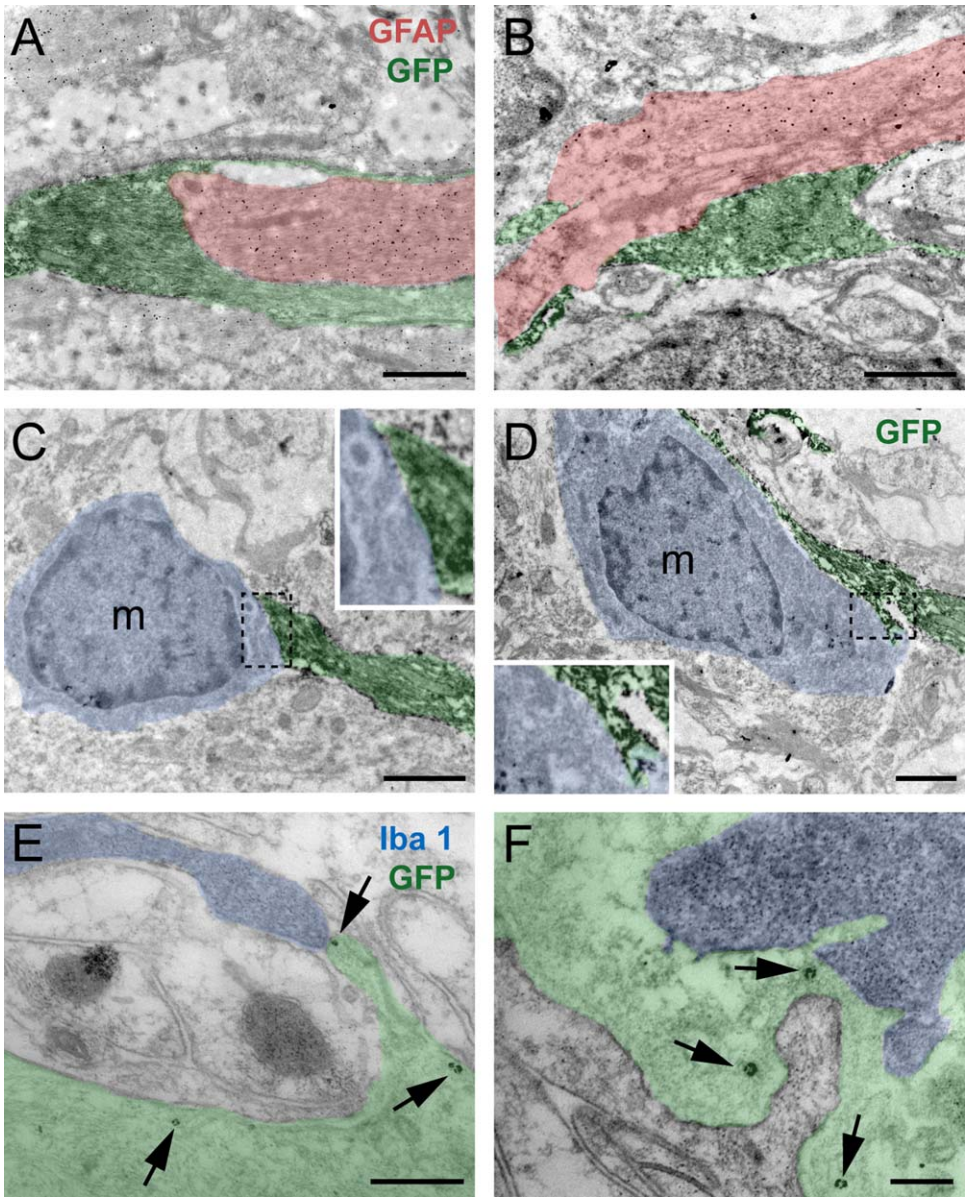

FIGURE 5: Direct appositions between implanted NPCs and glial cells at the lesion site. (A, B): Electron microscopy images of NPC processes identified by pre-embedding GFP immunohistochemistry with DAB (pseudo-colored in green) in direct contact to astrocytic prolongations labeled by GFAP immunogold (pseudo-colored in pink). Note the NPC process in A partly enwrapping an astrocytic element. Scale bars = A, 2 μm; B, 1.5 μm. **(C, D):** Direct contacts between the cell membranes of implanted NPCs (GFP-identified in pre-embedding with DAB; pseudo-colored in green) and likely microglial cells according to their ultrastructural features (pseudo-colored in blue; m indicates the microglial nuclei). Insets show higher magnification images of the framed regions in C and D to better illustrate the cell-to-cell contact. In some cases (D) an extensive area of the microglial plasma membrane appeared covered by NPC elements. Scale bars = 2 μm. **(E, F):** Examples of direct membrane appositions between identified NPC processes (labeled with GFP immunogold in pre-embedding; arrows point to some gold particles; pseudo-colored in green) and microglial elements (labeled with pre-embedding Iba1 immunocytochemistry using DAB; pseudo-colored in blue). Scale bars = 0.2 μm.

nuclear envelope (Fig. 4E,F; m). As previously observed at the confocal level, some microglial cells displayed ameboid appearance and contained phagocytic vesicles (Fig. 4F), whereas others lacked this phagocytic aspect (Fig. 4E).

At the ultrastructural level, we frequently observed direct appositions between GFP-immunostained NPC processes and GFAP-identified astrocytic profiles (Fig. 5A,B). Direct contacts between labeled NPC processes and putative microglia were also detected (Fig. 5C,D; see also insets). In addition, it was also possible to observe direct appositions between NPCs and microglial cells, both identified, by combining GFP pre-embedding immunogold to identify the NPCs with Iba1 pre-embedding immunocytochemistry using DAB for the microglial identification (Fig. 5E,F).

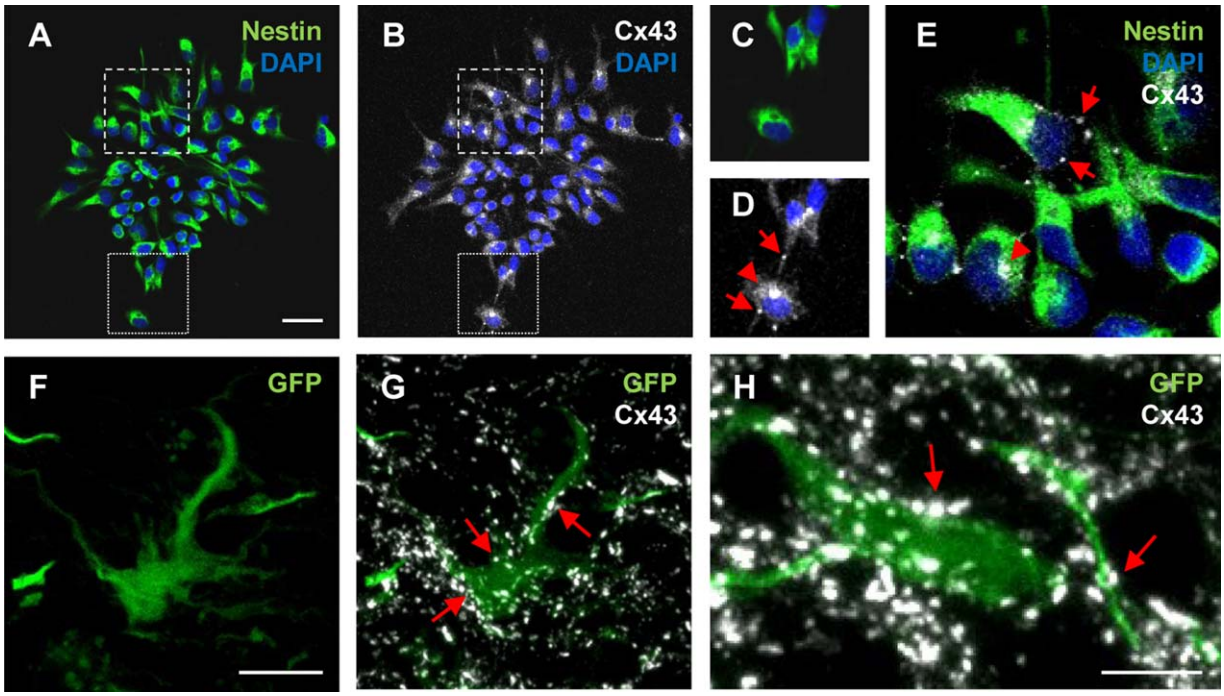

FIGURE 6: Cx43 expression in NPCs *in vitro* and after implantation. (A and B): Confocal microscopy images of a SVZ-derived neurosphere after double immunostaining for nestin (A, in green) and Cx43 (B, in white). Cell nuclei were identified by staining with DAPI (A and B, in blue). Scale bar = 25 μm. (C and D): Higher magnification images of the dotted frames of A and B, respectively. In D (also applies to E), red arrows point to Cx43-immunoreactive clusters showing a punctate appearance, whereas red arrowheads indicate other regions of the cell where Cx43-immunoreactive dots were evenly distributed. (E): Higher magnification image of the dashed frames in A and B showing the merged picture of the three channels corresponding to DAPI (blue) and immunoreactivity to nestin (green) and Cx43 (white). (F and G): Confocal microscopy images of an implanted cell identified by its GFP expression (F, green) showing Cx43 immunoreactivity (G, white) in the soma and in cell processes (examples in red arrows). Scale bar = 10 μm. (H): Higher magnification image showing the pattern of Cx43 immunoreactivity (in white) over a GFP-positive implanted cell (in green). The arrows point to some examples of Cx43-immunoreactive clusters characterized by their dotted aspect. Scale bar = 5 μm.

Gap Junction Protein Cx43 is Expressed by NPCs In Vitro and After Implantation in the Lesioned Tissue

The close apposition between the plasma membranes of implanted NPCs and host astrocytes and microglia led us to investigate the expression of the gap junction protein Cx43 in these cells to check for the possibility of gap junctions between them.

First, we wanted to elucidate whether Cx43 was already present in neurosphere-derived cells before their implantation. Double immunocytochemistry experiments for nestin and Cx43 revealed that most cells in each neurosphere were immunoreactive to nestin (98.9 ± 0.6%, Fig. 6A) and also to Cx43 (93.8 ± 1.7%; Fig. 6B, $n = 892$ cells from three different cultures). Indeed, most of the nestin-positive cells also presented Cx43 immunoreactivity (94.9 ± 0.4%; Fig. 6C–E).

In a further step, we determined whether Cx43 was also present in NPCs implanted at the lesioned MLF. Thus, 8 weeks after NPC implantation, Cx43 expression persisted in most of the GFP-positive implanted cells (77.12% of 153 analyzed cells). An example of an implanted GFP-identifed NPC is shown in Fig. 6F, which also revealed an intense labeling of Cx43-immunoreactive dots (Fig. 6G). Cx43 immunoreactivity in implanted cells was characterized by the presence of numerous labeled dots conferring a punctate appearance to this staining (Fig. 6G,H; arrows). Cx43-immunoreactive clusters were located over both the cell body and processes of implanted cells (Fig. 6G,H).

Identification of Cx43-Positive Profiles Located Between Implanted NPCs and Host Glial Cells

Reactive astrocytes at the lesion site also expressed Cx43 (Fig. 7A). Interestingly, Cx43-immunopositive clusters were often located at the intersection between NPCs and astrocytes. Some examples of Cx43-immunoreactive dots located between a GFAP-positive (astrocytic) and a GFP-positive (NPC) element are illustrated in Fig. 7B–E (circles).

Activated microglial cells (immunopositive for OX-6) located close to implanted NPCs also showed Cx43 immunoreactivity (Fig. 7F–H). Although less abundant than in astrocytes, interposition of Cx43-positive profiles between NPCs and microglial processes were also found. Some examples of these triads (microglia-connexin-implanted cell) identified by their respective markers (OX-6/Cx43/GFP) are outlined in the circles of Fig. 7I,J, and illustrated at a higher

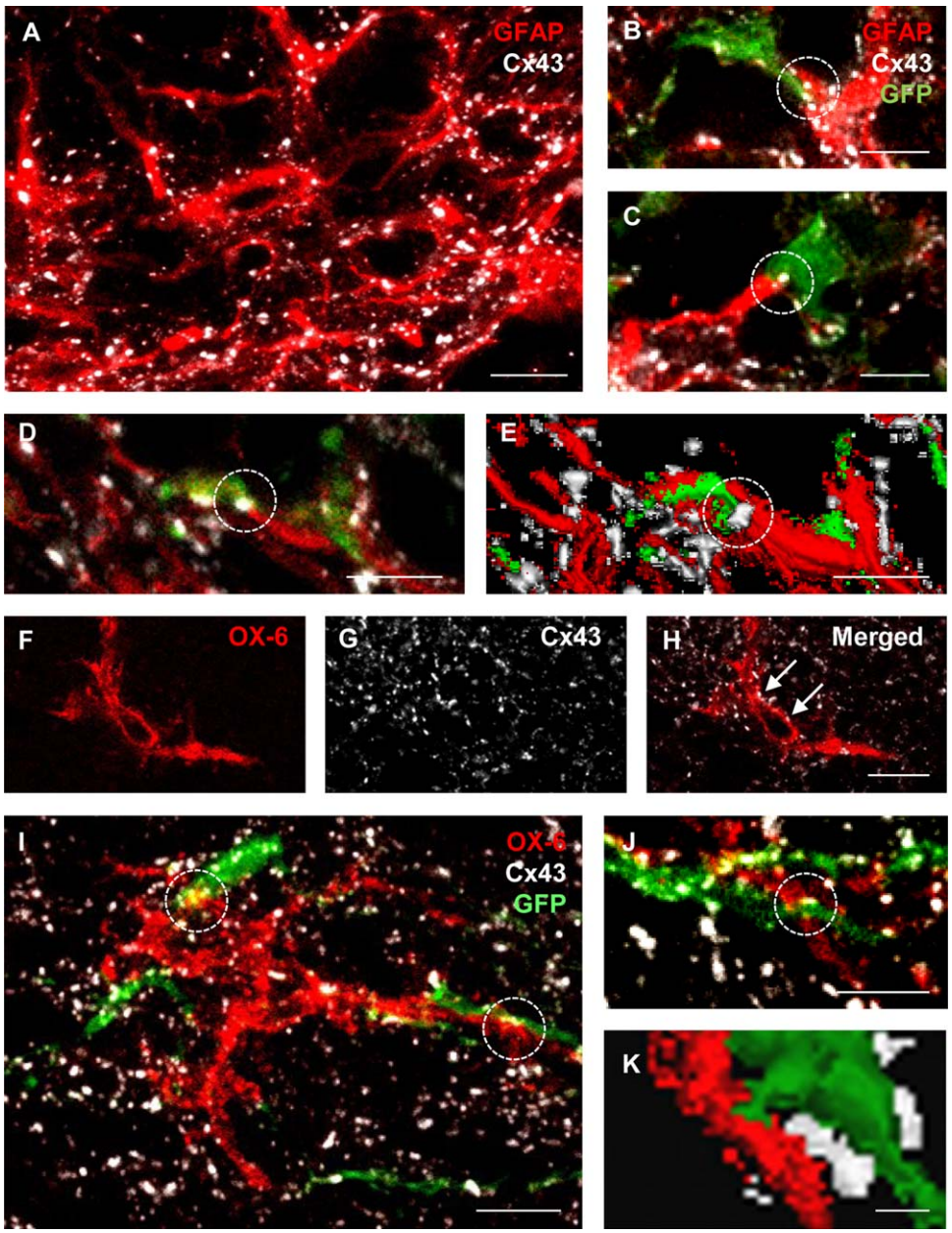

FIGURE 7: Cx43 expression in reactive astrocytes and activated microglia at the lesion site. (A): Confocal microscopy image showing Cx43-immunoreactive clusters (in white) on reactive astrocytes (GFAP-immunopositive, in red). Scale bar = 10 μm. (B–D): Confocal microscopy images of brainstem sections from implanted animals at the lesion site after double immunofluorescence for GFAP (in red) and Cx43 (in white) showing examples (delimited by dashed circles) of Cx43 location between implanted cells (GFP expression, in green) and astrocytic processes. Scale bars = 5 μm. (E): 3D reconstruction of one Z-stack formed by 5 confocal planes of 1 μm thickness, one of which is shown in D. Note Cx43-immunopositive clusters located between the process of one NPC and an astrocyte (dashed circle), suggesting the presence of gap junctions between these two cell types. Scale bar = 5 μm. (F–H): Confocal microscopy images of an activated microglial cell through the lesioned MLF (F, immunopositive for OX-6, in red) showing Cx43 expression (G, in white). Arrows in the merged image (H) point to some Cx43-immunoreactive dots over the microglial cell. Scale bar = 10 μm. (I and J): Confocal microscopy images obtained at the lesion site showing an OX-6-immunopositive microglial cell (in red), NPC processes (GFP-positive, in green) and Cx43-immunoreactive clusters (in white). Dashed circles delimite regions where Cx43-immunoreactive profiles appeared located between a microglial cell and a NPC process. Scale bars = 5 μm. (K): Three-dimensional reconstruction of one Z-stack made from six confocal planes of 1 μm thickness, captured from a brainstem section at the lesion site showing the tripartite configuration formed by a Cx43-immunoreactivity profile (white) located between a GFP-positive implanted NPC process (green) and an activated microglial process (OX-6-positive, red), suggestive of gap junctions formed between implanted cells and host microglia. Scale bar = 1 μm.

magnification in a rendered image in Fig. 7K. These findings indicate the possibility of communication between grafted NPCs and host astrocytes and microglia via gap junctions.

Ultrastructural Evidence of Gap Junctions in Implanted NPCs, Astrocytes, and Microglia at the Lesion Site

The combination of electron microscopy with immunohistochemistry against Cx43 by pre-embedding immunogold allowed us the ultrastructural demonstration of the presence of this connexin in gap junctions between cells at the lesion site (Fig. 8A). Thus, as previously described (Peters et al., 1991), the two adjacent membranes lie parallel to each other and converge to a nearly complete obliteration of the extracellular space (Fig. 8B).

Diverse combination of pre-embedding immunohistochemical protocols using DAB and gold particles for the visualization of different markers demonstrated the presence of gap junctions in GFP-identified implanted NPCs. Therefore, we found NPCs linked to other cellular elements through gap junctions (Fig. 8C; NPC labeled by GFP immunogold), which in some cases could be recognized as either other NPC profiles (Fig. 8D; both NPC processes identified by GFP immunogold) or presumptive astrocytes (Fig. 8E; NPC and gap junction labeled by GFP immunocytochemistry with DAB and Cx43 immunogold, respectively). Occasionally, gap junctions were also found between NPC and microglial processes (identified by GFP immunogold and Iba1 immunolabeling with DAB, respectively, Fig. 8I). Astrocytes joined together by gap junctions with Cx43 were also commonly observed (Fig. 8F; Cx43 immunogold). An interesting finding was that microglia cells also presented gap junctions, not only linked to NPCs (Fig. 8I), but also to other unidentified profiles (Fig. 8G,H).

Discussion

In this study we demonstrate that microglial activation after CNS injury can be regulated by implanted NPCs. In addition, we show evidence of Cx43 expression and the presence of gap junctions in implanted NPCs, reactive microglia and astrocytes at the lesion site, providing anatomical bases for gap junctional coupling between implanted NPCs and host glia.

It is well known that axon injury rapidly activates astroglial and microglial cells at the lesion site. Reactive astrocytes up-regulate GFAP and microglial cells proliferate, express inflammatory and immune mediators and acquire phagocytic activity upon activation (Aldskogius and Kozlova, 1998). The glial reaction to the transection of the MLF has been previously characterized (Pastor et al., 2000) and, as in other models of axotomy, a remarkable astrocytic and microglial activation is produced around the lesion. We now describe that the glial reaction to MLF transection was modified in animals receiving NPC implants. Thus, whereas GFAP immunoreactivity in the lesion site was similar in axotomized and NPC-implanted animals, OX-6 immunoreactivity in NPC-grafted animals significantly increased by twofold with respect to only injured animals. Therefore, the presence of NPCs in the host tissue induced an alteration in the microglial response to the lesion. Mosher et al. (2012) described that 24 h after NPC transplants in rat striatum, the microglial cell number was significantly increased in the site of grafting compared to animals that received only vehicle injections. In their study, all type of microglial cells (resting and activated) were identified by immunohistochemistry for the general microglial marker Iba1, although they also described an increased number of microglia with activated morphology in NPC-grafted animals compared to vehicle-injected ones. We have analyzed only the activated microglial population (immunoreactive to OX-6) at a much longer time period (two months), and still a considerable difference in microglial activation was quantified between implanted and axotomized animals. Therefore, we demonstrate that NPCs can up-regulate microglial activation *in vivo* after a mechanical brain lesion and this effect is maintained over time.

In line with this, our confocal analysis revealed a close association between grafted NPCs and activated microglial cells in the lesion environment. NPC processes were often located in intimate apposition to microglia and occasionally enwrapped a large extent of the microglial cell. This anatomical relationship probably indicates that both cell types can interact either directly, via gap junctions, or paracrinally, through the release of diffusible factors. For instance, Mosher et al. (2012) demonstrated a NPC-secreted factor involved in the regulation of host microglia, the vascular endothelial growth factor (VEGF). Interestingly, we have previously reported that postnatal SVZ-derived NPCs are immunoreactive to VEGF eight weeks after implantation (Talaverón et al., 2013), suggesting the possibility that this factor could also participate in the microglial response to NPC implants in our lesion model. Other authors have also described the importance of the interaction of implanted NPCs with microglia for the functional recovery from spinal cord injury induced by NPC grafting (Pluchino et al., 2005; Ziv et al., 2006). As it happened with microglia, a close proximity was also observed between host astrocytes and implanted NPCs, which also provides an anatomical basis for possible direct and/or paracrine communications between these two types of cells after injury.

Direct appositions between grafted NPCs and recipient astroglial and microglial cells were also confirmed at the ultrastructural level, so we next questioned the possibility of gap junctional communication among these cells. As an initial step, we evaluated whether the gap junction protein Cx43 was expressed by NPCs, before and after implantation, and also by glial cells surrounding the lesion. Before implantation,

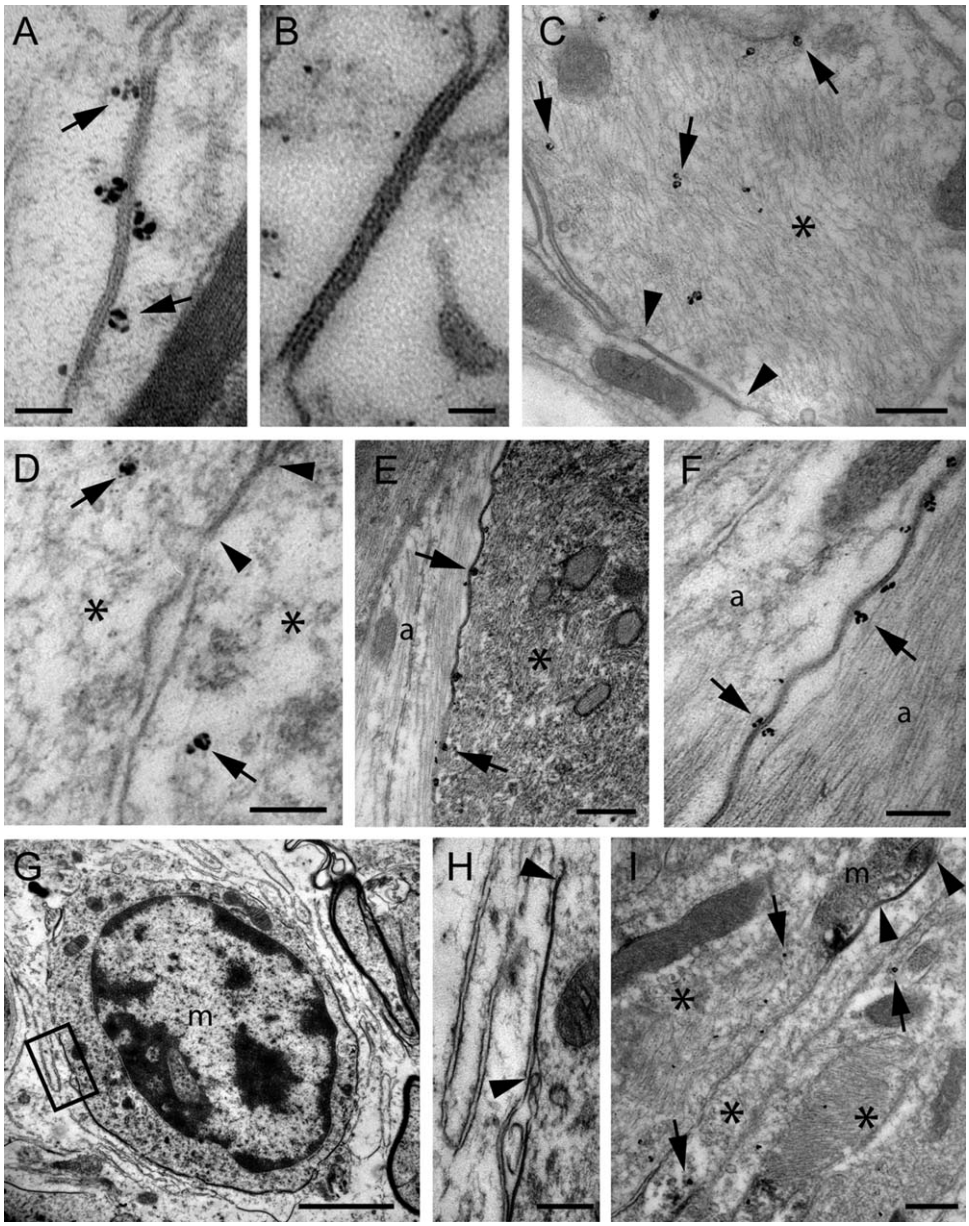

FIGURE 8: Electron microscopy images of gap junctions in implanted NPCs, astrocytes, or microglial cells at the lesion site. (A): Identification of gap junctions by Cx43 immunogold in pre-embbeding. Note the gold particles (arrows) attached to the cell membranes at both sides of the junction. Scale bar = 0.1 μm. (B): Higher magnification of a gap junction showing the intimate apposition of the two cell membranes characteristic of this type of coupling, as well as the detachment of both membranes, and consequent widening of the extracellular space, at the edges of the junctional zone. Scale bar = 0.05 μm. (C): Example of a NPC process (asterisk) identified by pre-embedding immunogold against GFP (arrows point to some gold particles) linked to other cellular element by a gap junction (delimited between arrowheads). Scale bar = 1 μm. (D): Two different NPC elements (asterisks) identified by pre-embedding GFP immunogold (arrows point to gold particles) joined together by a gap junction (between arrowheads). Scale bar = 0.4 μm. (E): Electron microscopy image of an identified gap junction labeled by pre-embedding Cx43 immunogold in pre-embedding formed between a NPC (asterisk; identified by pre-embedding GFP immunocytochemistry with DAB) and a likely astrocyte (a). The gold particles (some of them indicated by arrows) denote the presence of the gap junction. Scale bar = 0.5 μm. (F): Pre-embedding Cx43 immunogold identification of a gap junction linking two presumptive astrocytes (a) as suggested by their typical filaments. Note the presence of gold particles (arrows), tagging the Cx43, at both sides of the junction. Scale bar = 0.2 μm. (G, H): Electron microscopy images of a putative microglial cell (m), suggested by its ultrastructural characteristics, coupled to another cellular element by a gap junction (framed region). H shows at a higher magnification the marked region in G to illustrate the gap junction between this likely microglia and another unidentified cellular process. Arrowheads delimite the junctional zone. Scale bars = G, 2 μm; H, 0.2 μm. (I): Three NPC processes (asterisks) identified by pre-embedding GFP immunogold (arrows point to some gold particles) and an identified DAB-labeled microglial element (m; after Iba1 pre-embedding immunocytochemistry), all of them in close apposition. Note the presence of a gap junction between one of the NPC elements and the microglia; arrowheads indicate the limits of this junction. Scale bar = 0.8 μm.

the analysis of Cx43 expression in cells from SVZ neurospheres revealed that the vast majority of the cells within each neurosphere presented Cx43 immunoreactivity and were neural progenitor cells, as revealed by nestin immunolabeling. These results are in agreement with others (Duval et al., 2002) that showed a high degree of Cx43 expression in undifferentiated cells from mouse embryonic striatal ventricular zone neurospheres suggesting an active role of Cx43 and intercellular communication during proliferation and differentiation of NPCs. Next, we analyzed Cx43 expression by NPCs eight weeks after their implantation. Most of the GFP-positive implanted NPCs were immunoreactive to Cx43 and remained in a nestin-expressing undifferentiated state. Other authors have reported that when NPCs are implanted in inflammed brain, a crosstalk between transplanted NPCs and immune cells is established that preserves the NPCs in a non-differentiated state (Pluchino et al., 2005) and that, in this state, they exert neuroprotective actions by immunomodulatory mechanisms (Pluchino et al., 2005; Ziv et al., 2006). Thus, it is possible that the inflammatory response associated to injury probably preserves the NPCs in a Cx43-expressing undifferentiated state in which they are able to communicate with each other and/or with host cells by gap junctions.

Host astrocytes at the lesion site also expressed Cx43 and formed gap junctions. Interestingly, in many of the astrocytes located adjacent to NPCs, Cx43 immunoreactive profiles were identified in the interface between the GFP-positive NPC and the astrocyte, a result confirmed by electron microscopy. Therefore, these findings indicate that NPCs can communicate with host astrocytes through gap junctions. With respect to microglia, our data showed the presence of Cx43 protein in activated OX-6 expressing microglia. Eugenin et al. (2001) previously demonstrated that, under resting conditions *in vivo*, most microglia do not express Cx43 but they do so at brain stab wounds. In this work, we describe Cx43 expression in activated microglia after a central fascicle transection, and it is important to highlight that some of these Cx43-immunoreactive profiles appeared located closely adjacent to implanted NPCs. Furthermore, gap junctions were demonstrated by electron microscopy in microglial cells and, occasionally, between an implanted NPC and a microglial cell identified by Iba1 immunolabeling.

Our findings suggest that implanted NPCs could communicate with recipient astroglial and microglial cells through gap junctions at a long time period after lesion. To our knowledge, this is the first study that demonstrates gap junctions between implanted NPCs and host glia *in vivo*, in adult animals, and at a long time after injury. In 2010, Jäderstad et al. reported gap junctional coupling between implanted NPCs and host neurons and the importance of such communication for the survival and protective actions attributed to the cell implants. NPCs were grafted in mutant murine models that underwent Purkinje neuron degeneration and they demonstrated that early cell coupling by gap junctions between grafted NPCs and host Purkinje neurons was essential to rescue these cerebellar neurons from degeneration. In our study, however, the lesion model was different (central axotomy) and evaluation of the presence of gap junctions was undertaken at the ultraestructural level and two months after the damage. Therefore, we suggest that not only paracrine signals can be established between implanted NPCs and host glia, but also direct communication through gap junctions, in which coupled cells can share small molecules, ions or some metabolites with an essential role in the neutralization of pathological processes, in the prevention from cell death, or in the improvement of neuronal function.

Conclusions

In summary, we have revealed an intimate association between implanted NPCs and host glial cells at the injury site in a model of central lesion. In particular, we have shown the ability of NPCs to up-regulate microglial reaction to injury after their implantation in the brain of adult animals suffering a mechanical damage. Furthermore, we have demonstrated the presence of gap junctions in implanted NPCs and host astrocytes and microglia. Our findings establish the possibility that, not only diffusible factors, but also cell-to-cell direct coupling might play an important role in graft-host communication with benefits for NPC integration in the tissue as well as for their neuroprotective effects following lesion.

Acknowledgment

Grant sponsor: MEC-FEDER; Grant number: BFU2009-07121 and BFU2012–33975; Grant sponsor: Junta de Andalucía-FEDER; Grant number: CVI-6053.

Some experiments were performed in the Biology and Microscopy Central Services of the Universidad de Sevilla (CITIUS). The authors thank Dr. J.M. Blasco-Ibáñez from Universidad de Valencia for comments to the article.

References

Aldskogius A, Kozlova EN. 1998. Central neuron-glial and glial-glial interactions following axon injury. Prog Neurobiol 55:1–26.

Alvarez-Buylla A, Seri B, Doetsch F. 2002. Identification of neural stem cells in the adult vertebrate brain. Brain Res Bull 57:751–758.

Anderson DJ. 2001. Stem cells and pattern formation in the nervous system: The possible *versus* the actual. Neuron 30:19–35.

Bruzzone R, White TH, Paul DL. 1996. Connection with connexins: The molecular basis of direct intercellular signaling. Eur J Biochem 238:1–27.

Carpenter MK, Cui K, Hu ZY, Jackson J, Sherman S, Seiger A, Wahlberg LU. 1999. *In vitro* expansion of a multipotent population of human neural progenitor cells. Exp Neurol 158:265–278.

Cheng A, Tang J, Cai J, Zhu M, Zhang X, Rao M, Mattson MP. 2004. Gap junctional communication is required to maintain mouse cortical neural progenitor cells in a proliferative state. Dev Biol 272:203–216.

Chew SSL, Johnson CS, Gree CR, Danesh-Meyer HV. 2010. Role of connexin43 in central nervous system injury. Exp Neurol 225:250–261.

Contreras JE, Sanchez HA, Veliz LP, Bukauskas FF, Bennet MV, Sáez JC. 2004. Role of connexin-based gap junction channels and hemichannels in ischemia induced cell death in nervous system. Brain Res Rev 47:290–303.

Cummings BJ, Uchida N, Tamaki SJ, Salazar DL, Hooshmand CN, Summers R, Gage FH, Anderson AJ. 2005. Human neural stem cells differentiate and promote locomotor recovery in spinal cord-injured mice. Proc Natl Acad Sci USA 102:14069–14074.

Danscher G, Zimmer J. 1978. An improved Timm-sulphide method for light and electron microscopic localization of heavy metals in biological tissues. Histochemistry 55:27–40.

de la Cruz RR, Delgado-García JM, Pastor AM. 2000. Discharge characteristics of axotomized abducens internuclear neurons in the adult cat. J Comp Neurol 427:391–404.

Duval N, Gomès D, Calaora V, Calabrese A, Meda P, Bruzzone R. 2002. Cell coupling and Cx43 expression in embryonic mouse neural progenitor cells. J Cell Sci 16:3241–3251.

Elias LAB, Wang DD, Kriegstein AR. 2007. Gap junction adhesion is necessary for radial migration in the neocortex. Nature 448:901–907.

Englund U, Bjorklund A, Wictorin K, Lindvall O, Kokaia M. 2002. Grafted neural stem cells develop into functional pyramidal neurons and integrate into host cortical circuitry. Proc Natl Acad Sci USA 99:17089–17094.

Esen N, Shuffield D, Syed MM, Kielian T. 2007. Modulation of connexin expression and gap junction communication in astrocytes by the gram-positive bacterium *S. Aureus*. Glia 55:104–117.

Eugenin EA, Eckardt D, Theis M, Willecke K, Bennet MV, Sáez JC. 2001. Microglia at brain stab wounds express connexin43 and *in vitro* form functional gap junctions after treatment with interferon-γ and tumor necrosis factor-α. Proc Natl Acad Sci USA 7:4190–4195.

Gage FH. 2000. Mammalian neural stem cells. Science 287:1433–1438.

Garg S, Syed MM, Kielian T. 2005. *Staphylococcus aureus*-derived peptidoglycan induces Cx43 expression and functional gap junction intercellular communication in microglia. J Neurochem 95:475–483.

Jäderstad J, Jädersatd LM, Li J, Chintawar S, Salto C, Pandolfo M, Ourednik V, Teng YD, Sidman RL, Arenas E, Snyder EY, Herlenius E. 2010. Communication via gap junctions underlies early functional and beneficial interactions between grafted neural stem cells and the host. Proc Natl Acad Sci USA 11:5184–5189.

Jeong SW, Chu K, Jung KH, Kim SU, Kim M, Roh JK. 2003. Human neural stem cell transplantation promotes functional recovery in rats with experimental intracerebral hemorrhage. Stroke 34:2258–2263.

Kelly S, Bliss TM, Shah AK, Sun GH, Ma M, Foo WC, Masel J, Yenari MA, Weissman IL, Uchida N, Palmer T, Steinberg GK. 2004.Transplanted human fetal neural stem cells survive, migrate and differentiate in ischemic rat cerebral cortex. Proc Natl Acad Sci USA 101:11839–11844.

Kumar NM, Gilula NB. 1996. The gap junction communication channel. Cell 84:381–388.

Lacar B, Young SZ, Platel JC, Bordey A. 2011. Gap junction-mediated calcium waves define coomunication networks among murine postnatal neural progenitor cells. Eur J Neurosci 34:1895–1905.

Lee I-H, Lindqvist E, Kiehn O, Widenfalk J, Olson L. 2005. Glial and neuronal connexin expression patterns in the rat spinal cord during development and following injury. J Comp Neurol 489:1–10.

Macías D, Oya R, Saniger L, Martín F, Luque F. 2009. A lentiviral vector that activates latent human immunodeficiency virus-1 proviruses by the overexpression of tat and that kills the infected cells. Hum Gene Ther 20:1259–1268.

Marins M, Xavier ALR, Viana NB, Fortes FS, Fróes MM, Menezes JR. 2009. Gap junctions are involved in cell migration in the early postnatal subventricular zone. Dev Neurobiol 69:715–730.

McBride JL, Behrstock SP, Chen EY, Jakel RJ, Siegel I, Svendsen CN, Kordower JH. 2004. Human neural stem cell transplants improve motor function in a rat model of Huntington's disease. J Comp Neurol 475:211–219.

Miragall F, Albiez P, Bartels H, de Vries U, Dermietzel R. 1997. Expression of the gap junction protein connexin43 in the subependymal layer and the rostral migratory stream of the mouse: Evidence for an inverse correlation between intensity of connexin43 expression and cell proliferation activity. Cell Tissue Res 287:243–253.

Morado-Díaz CJ, Matarredona ER, Davis-López de Carrizosa MA, de la Cruz RR, Pastor AM. 2011. Neural progenitor cell implants in the lesioned medial longitudinal fascicle of adult cats regulate synaptic composition of abducens internuclear neurons. Soc Neurosci Meet Abstr 438:17.

Mosher KI, Andres RH, Fukuhara T, Bieri G, Hasegawa-Moriyama M, He Y, Guzman R, Wyss-Coray T. 2012. Neural progenitor cells regulate microglia functions and activity. Nat Neurosci 15:1485–1487.

Nagy JI, Rash JE. 2000. Connexins and gap junctions of astrocytes and oligodendrocytes in the CNS. Brain Res Rev 32:29–34.

Nakase T, Yoshida Y, Nagata K. 2006. Enhanced connexin43 immunoreactivity in penumbral areas in the human brain following ischemia. Glia 54:369–375.

Pastor AM, Delgado-García JM, Martínez-Guijarro FJ, López-García C, de la Cruz RR. 2000. Response of abducens internuclear neurons to axotomy in the adult cat. J Comp Neurol 427:370–390.

Paxinos G, Watson C. 1997. The rat brain in stereotaxic coordinates. New York: Academic Press.

Peters A, Palay SL, Webster HD. 1991. The Fine Structure of the Nervous System: Neurons and their Supporting Cells, 3rd ed. New York, NY: Oxford University Press.

Pluchino S, Quattrini A, Brambilla E, Gritti A, Salani G, Dina G, Galli R, DelCarro U, Amadio S, Bergami A, Furlan R, Comi G, Vescovi AL, Martino G. 2003. Injection of adult neurospheres induces recovery in a chronic model of multiple sclerosis. Nature 422:688–694.

Pluchino S, Zanotti L, Rossi B, Brambilla E, Ottoboni L, Salani G, Martinello M, Cattalini A, Bergami A, Furlan R, Comi G, Constantin G, Martino G. 2005. Neurosphere-derived multipotent precursors promote neuroprotection by an immunomodulatory mechanism. Nature 436:266–271.

Pluchino S, Cossetti C. 2013. How stem cells speak with host immune cells in inflammatory brain diseases. Glia 61:1379–1401.

Rash JE, Yasumura T, Davidson KGV, Furman CS, Dudek FE, Nagy JI. 2001. Identification of cells expressing Cx43, Cx30, Cx26, Cx32 and Cx36 in gap junctions of rat brain and spinal cord. Cell Commun Adhes 8:315–320.

Reynolds BA, Weiss S. 1992. Generation of neurons and astrocytes from isolated cells of the adult mammalian central nervous system. Science 255:1707–1710.

Richardson RM, Broaddus WC, Holloway KL, Fillmore HL. 2005. Grafts of adult subependymal zone neuronal progenitor cells rescue hemiparkinsonian behavioural decline. Brain Res 1032:11–22.

Santiago MF, Alcami P, Striedinger KM, Spray DC, Scemes E. 2010. The carboxyl-terminal domain of Connexin43 is a negative regulator of neuronal differentiation. J Biol Chem 285:11836–11845.

Söhl G, Willecke K. 2003. An update on connexin genes and their nomenclature in mouse and man. Cell Commun Adhes 10:173–180.

Svendsen CN, Clarke DJ, Rosser AE, Dunnet SB. 1996. Survival and differentiation of rat and human epidermal growth factor-responsive precursor cells following grafting into the lesioned adult central nervous system. Exp Neurol 137:376–388.

Talaverón R, Matarredona ER, de la Cruz RR, Pastor AM. 2013. Neural progenitor cell implants modulate vascular endotelial growth factor and brain-derived neurotrophic factor expression in rat axotomized neurons. PLoS One 8:e54519.

Torroglosa A, Murillo-Carretero M, Romero-Grimaldi C, Matarredona ER, Campos-Caro A, Estrada C. 2007. Nitric oxide decreases subventricular zone stem cell proliferation by inhibition of epidermal growth factor receptor and phosphoinositide-3-kinase/Akt pathway. Stem Cells 25:88–97.

Whitman MC, Fan L, Rela L, Rodriguez-Gil DJ, Greer CA. 2009. Blood vessels form a migratory scaffold in the rostral migratory stream. J Comp Neurol 516:94–104.

Yang M, Stull ND, Berk MA, Snyder EY, Iacovitti L. 2002. Neural stem cells spontaneously express dopaminergic traits after transplantation into the intact or 6-hydroxydopamine-lesioned rat. Exp Neurol 177:50–60.

Ziv Y, Avidan H, Pluchino S, Martino G, Schwartz M. 2006. Synergy between immune cells and adult neural stem/progenitor cells promotes functional recovery from spinal cord injury. Proc Natl Acad Sci USA 103: 13174–13179.

ARTÍCULO 3

Neural Progenitor Cells Isolated from the Subventricular Zone Present Hemichannel Activity and Form Functional Gap Junctions with Glial Cells. **2015. Frontiers Cellular Neuroscience**

frontiers in
CELLULAR NEUROSCIENCE
IMPACT 4.2 FACTOR

Neural progenitor cells isolated from the subventricular zone present hemichannel activity and form functional gap junctions with glial cells

Rocío Talaverón, Paola Fernández, Rosalba Escamilla, Angel M. Pastor, Esperanza R. Matarredona and Juan Carlos Sáez

Journal Name:	Frontiers in Cellular Neuroscience
ISSN:	1662-5102
Article type:	Original Research Article
First received on:	25 May 2015
Frontiers website link:	www.frontiersin.org

Neural progenitor cells isolated from the subventricular zone present hemichannel activity and form functional gap junctions with glial cells

Rocío Talaverón[1], Paola Fernández[2], Rosalba Escamilla[2], Angel M. Pastor[1], Esperanza R. Matarredona[1,*], Juan C. Sáez[2,*]

[1]Departamento de Fisiología, Facultad de Biología, Universidad de Sevilla, Sevilla, Spain

[2]Departamento de Fisiología, Pontificia Universidad Católica de Chile, Santiago de Chile, Chile and Instituto Milenio, Centro Interdisciplinario de Neurociencias de Valparaíso, Chile.

*Correspondence:

Dr. E.R. Matarredona
Departamento de Fisiología
Facultad de Biología
Universidad de Sevilla
Avda. Reina Mercedes s/n
41012 Seville, Spain.
matarredona@us.es

Dr. J.C. Sáez
Departamento de Fisiología
Facultad de Ciencias Biológicas
Alameda 340
Pontificia Universidad Católica de Chile
Santiago de Chile, Chile.
jsaez@bio.puc.cl

Running title: Dye coupling NPCs-glia

Key words: subventricular zone, microglia, astrocytes, gap junctions, hemichannels, dye coupling, dye uptake

Number of words: 6874

Number of figures: 6

ABSTRACT

The postnatal subventricular zone lining the walls of the lateral ventricles contains neural progenitor cells (NPCs) that generate new olfactory bulb interneurons. Communication via gap junctions between cells in the subventricular zone is involved in NPC proliferation and in neuroblast migration towards the olfactory bulb. Subventricular zone NPCs can be expanded *in vitro* in the form of neurospheres that can be used for transplantation purposes after brain injury. We have previously reported that neurosphere-derived NPCs form heterocellular gap junctions with host glial cells when they are implanted after mechanical injury. To analyze functionality of NPC-glial cell gap junctions we performed dye coupling experiments in co-cultures of subventricular zone NPCs with astrocytes or microglia. Neurosphere-derived cells expressed mRNA for at least the hemichannel/gap junction channel proteins connexin 26 (Cx26), Cx43, Cx45 and pannexin 1. Dye coupling experiments revealed that gap junctional communication occurred among neurosphere cells (incidence of coupling: 100%). Moreover, hemichannel activity was also detected in neurosphere cells as evaluated in time-lapse measurements of ethidium bromide uptake. Heterocellular coupling between NPCs and glial cells was evidenced in co-cultures of neurospheres with astrocytes (incidence of coupling: 91.0 ± 4.7%) or with microglia (incidence of coupling: 71.9 ± 6.7%). Dye coupling in neurospheres and in co-cultures was inhibited by octanol, a gap junction blocker. Altogether, these results suggest the existence of functional hemichannels and gap junction channels in postnatal subventricular zone neurospheres. In addition, they demonstrate that subventricular zone-derived NPCs can establish functional gap junctions with astrocytes or microglia. Therefore, cell-cell communication via gap junctions and hemichannels with host glial cells might subserve a role in the functional integration of NPCs after implantation in the damaged brain.

INTRODUCTION

Neurogenesis in the adult rodent brain persists during adulthood in two main neurogenic zones, the subgranular zone of the dentate gyrus in the hippocampus, and the subventricular zone (SVZ) lining the walls of the lateral ventricles. The postnatal and adult SVZ contains neural progenitor cells (NPCs) that give rise to transit-amplifying intermediate progenitors, which after several divisions differentiate into neuroblasts. SVZ neuroblasts migrate along the rostral migratory stream towards the olfactory bulb where they generate new interneurons (Gage, 2000; Anderson, 2001; Alvarez-Buylla *et al*., 2002). Gap junction intercellular communication has been described to occur in the SVZ at homocellular and heterocellular contacts (Menezes *et al*., 2000; Lacar *et al*., 2011). This type of cellular communication provides a mechanism for the coordination of metabolic and electrical activities (Bruzzone *et al*., 1996; Kumar and Gilula, 1996) that might play an active role in shaping the specific behavior of the SVZ cell population.

Gap junction channels are composed of two hemichannels, one on each of the communicating cells. Hemichannels in vertebrates can be constituted by two types of proteins: connexins or pannexins. There are 21 different connexins known to date, which differ primarily in their C-terminal domain, molecular weight and tissue specificity (Willecke *et al*., 2002). Among all connexins, Cx26 (molecular weight of 26 kDa), Cx43 and Cx45 are expressed by NPCs of different sources (Nadarajah *et al*., 1997; Duval *et al*., 2002; Cina *et al*., 2007; Freitas *et al*., 2012; Khodosevich *et al*., 2012). Specifically, Cx45 is involved in the modulation of proliferation and differentiation of NPCs from the postnatal SVZ (Khodosevich *et al*., 2012). Although the majority of connexin hemichannels are docked to function as gap junction channels, unapposed hemichannels have also been documented on the surface of different cell types (Chen *et al*., 2005; Retamal *et al*., 2006). These channels, when open, serve as a conduit between the intracellular space and the external environment allowing uptake of metabolic substrates and release of autocrine and paracrine signals. The presence and possible functional role of open connexin hemichannels in postnatal SVZ NPCs remains to be elucidated. Hemichannels formed by pannexins, in contrast to those formed by connexins, might not form gap junction channels (Dahl and Locovei 2006; D'hondt *et al*., 2009; MacVicar and Thompson, 2010). It has been recently reported that postnatal SVZ NPCs and their immature neuronal progeny express pannexin 1 (Panx1) as large

pore channels that mediate the release of ATP, which has been proposed to regulate NPC proliferation by interaction with purinergic P2 receptors (Wicki-Stordeur *et al*., 2012).

NPCs of the SVZ can be isolated and amplified *in vitro* in the form of floating aggregates termed neurospheres (Carpenter *et al*., 1999; Vescovi *et al*., 1999; Gage 2000). NPCs derived from SVZ neurospheres provide an interesting cell population to be used for transplantation purposes in different types of brain lesions, not only because of their capacity to integrate into the host tissue, contributing to the possible replacement of damaged cells, but also because of several bystander capacities such as tissue trophic support and immune regulation (Ben-Hur, 2008). The ability of implanted NPCs to integrate and exert benefitial effects to the lesioned host tissue depends on local interactions created in the microenvironment of the site of grafting in which communication between implanted and host cells are crucial (Martino and Pluchino 2006; Martino *et al*., 2011). For instance, Jäderstad *et al*. reported in 2010 that an early and essential step in the functional integration of grafted NPCs is cell-cell coupling via gap junctions with host neurons that permits exogenous NPCs to influence directly host network activity. In line with this, we have recently reported that implanted NPCs after mechanical brain injury establish gap junctional communication with host astrocytes and microglia (Talaverón *et al*., 2014).

As a further step, we have aimed to analyze whether gap junctions formed between NPCs and astrocytes or microglial cells are functional. For that purpose, we have performed dye coupling experiments in neurospheres and in co-cultures of SVZ-derived NPCs and primary astrocytes or microglia. Our results show that cells from SVZ neurospheres present hemichannel activity and are coupled via gap junctions. In addition, we describe that gap junctional communication is established between neurosphere-derived cells and astrocytes or microglia *in vitro*.

METHODS

Animals

Experiments were conducted on 1-day and 7-day postnatal Sprague-Dawley rats obtained from the animal facilities of the Faculty of Biological Sciences of the Pontificia Universidad Católica de Chile. All procedures were in accordance with the institutional guidelines and were approved by the Bioethic and Biosecurity Committee of the Pontificia Universidad Católica de Chile.

Cell culture reagents

Dulbecco's modified Eagle's medium (DMEM), minimum essential medium (MEM), DMEM- F-12 1:1 medium (DF-12) , HCO_3^--free F-12 medium, B-27 supplement, HEPES, GlutaMAX™, phosphate buffered saline (PBS), PBS without Ca^{2+} and Mg^{2+}, trypsin (0.5%-EDTA 5 mM), trypsin (2.5%), penicillin/streptomycin 100X, horse serum and fetal bovine serum were purchased from GIBCO (Life Technologies, Carlsbad, CA, USA). Bovine pancreas DNaseI, poly-D-lysine, DiI, La^{3+}, Lucifer yellow, ethidium bromide and octanol were purchased from Sigma-Aldrich (St. Louis, MO, USA). Epidermal growth factor (EGF) was purchased from Peprotech (London, UK) and basic fibroblast growth factor (FGF-2) from Millipore (Darmstadt, Germany). Coverslips were purchased from Marienfeld Laboratory Glassware (Lauda-Könighshofen, Germany). All plastic culture flasks and dishes were from Sarstedt Inc. (Nümbrecht, Germany).

Neural progenitor cell culture

NPCs were isolated from the SVZ of 7-day postnatal rats and were expanded in the form of neurospheres essentially as described before (Talaveron *et al*., 2013). Briefly, the lateral walls of the lateral ventricles were removed and enzymatically dissociated with 1 mg/ml trypsin at 37°C for 15 min. The tissue was then centrifuged at 150x g for 5 min, rinsed in DF-12 and centrifuged again in the same conditions. Then, cells were resuspended in DF-12 and mechanically disaggregated with a fire-polished Pasteur pipette. The dissociated cells were centrifuged, resuspended in neurosphere growth medium consisting in DF-12 added with B-27 supplement, GlutaMAX™, 100 units/ml penicillin and 100 µg/ml streptomycin, 20 ng/ml EGF and 10 ng/ml FGF-2, and maintained in an atmosphere of 5% CO_2, at 37°C. After 1-2 days, cell aggregates known

as neurospheres were formed. Cells were subcultured 48 hours after isolation and then every 3-4 days. Cells used in the experiments were obtained from neurospheres after a minimun of two and a maximum of 6 subcultures. For dye coupling and dye uptake experiments, neurospheres were slightly disaggregated and plated on poly-D-lysine-treated coverslips.

Detection of Cx26, Cx43, Cx45, and Panx1 mRNAs

Relative levels of Cx26, Cx43, Cx45, and Panx1 mRNA were determined by RT-PCR. Total RNA was isolated from 700,000 neurosphere-derived cells using TRIzol reagent (Ambion) according to the manufacturer´s instructions. A RNA (10 µg) aliquot was treated with RQ1 RNase free-DNase (Promega) for 30 min at 37°C and purified with a second round of TRIzol. cDNA was synthesized from 2 µg total RNA using SuperScript™ First-Strand Synthesis System for RT-PCR (Invitrogen) according to the manufacturer instructions using random hexamers and the oligo(dT) primer provided with the kit. For detection, PCR reactions for Cx26, Cx43, Cx45, and Panx1 were performed with 1 µL of cDNA in 25 µl of reaction and contained 1.5 mM $MgCl_2$, 160 µM dNTPs, 240 nM of each forward and reverse primers, 1X Green GoTaq reaction buffer (Promega) and 1 unit of GoTaq DNA polymerase (Promega). For the control gene GAPDH, PCR reaction was similar as for target genes with the exception of the primer concentration, which was 160 nM for each primer. Sequences of PCR primers were as follows, Cx26 (forward, GGAGATGAGCAAGCCGATTT; reverse, GAAGAAGATGCTGGTGGTGTAG), Cx43 (forward, ATCCTTACCACGCCACCA; reverse, GCTAATGGCTGGAGTTCATGTC), Cx45 (forward AAAGAGCAGAGCCAACCA; reverse, GAATGGTCCCAAACCCTAGAT), Panx1 (forward, GAGATATCCGAAAGCCACTTCA; reverse, GGCGTACACTAGGAGGTTAATG) and GAPDH (forward, ACCACAGTCCATGCCATCAC; reverse, TCCACCACCCTGTTGCTGTA). PCR products were resolved in 1.5% agarose/1x TAE buffer electrophoresis (Invitrogen) and stained with ethidium bromide (0.5µg/ml) for visualization.

Primary culture of astrocytes and microglia

Primary cultures of astrocytes and microglia were prepared from 1-day postnatal rat neocortex. After removal of meninges, cortices were dissected, minced in small pieces

and incubated at 37°C for 30 min in trypsin (0.5%) and EDTA (5 mM) prepared in MEM supplemented with antibiotics (100 units/ml penicillin and 100 µg/ml streptomycin). After removal of the enzyme solution, tissue was triturated in dissociation medium (MEM, 10% horse serum and antibiotics) added with 0.01 mg/ml DNase I from bovine pancreas with the use of a Pasteur pipette. Dissociated cells were pelleted, resuspended in dissociation medium and plated on plastic culture flasks at 37°C in a 5% CO_2/95% air atmosphere. After 24 h, the medium was removed and replaced by growth medium (DMEM supplemented with 10% fetal bovine serum and antibiotics).

For astrocyte culture, the medium was replaced every other day. Five days after plating, cells were detached by treatment with trypsin (0.5%) and EDTA (5 mM) in PBS without Ca^{2+} and Mg^{2+}. After detachment, cells were collected, centrifuged and plated on 15-mm diameter coverslips with growth medium at a density of 20,000 cells/coverslip. More than 95% of cells showed immunoreactivity for glial fibrillary acidic protein.

Flasks reserved for microglia culture were kept for 10-15 days without medium renewal to allow microglia proliferation in astrocyte-conditioned medium. Cultures were then rigorously agitated for 30 min in an orbital shaker (Lab-Line Instruments) at 70 rpm and 37°C to detach cells adhering to the astrocyte monolayer. Thereafter, detached cells were collected, plated on 15 mm coverslips (20,000 cells/coverslip) and maintained in growth medium. Close to 99% of the cells obtained after this procedure were immunopositive for the ED-1 antigen but were negative for glial fibrillary acidic protein, indicating a very high enrichment in microglia (Eugenín *et al*., 2001).

Co-culture of neurosphere-derived cells and glial cells

Coverslips having confluent primary cultures of astrocytes or microglia were labeled with a lipophilic dye before co-culturing them with neurosphere-derived cells. For that purpose, cells were incubated with DiI (5 µM) for 15 min at 37°C and washed three times with PBS. Thirty minutes later, neurospheres were subjected to a brief mechanical disaggregation and plated on coverslips containing the DiI-labeled astrocytes or microglial cells (20,000 neurosphere-derived cells/coverslip). Co-cultures were maintained at 37°C in a 5% CO_2/95% air atmosphere with neurosphere growth medium

for a minimum of 1 hour before experiments.

Dye coupling

The functional state of gap junctions was evaluated as previously described (Martínez and Sáez, 1999) in neurosphere-derived cells and in co-cultures of neurosphere-derived cells with astrocytes or microglia. Single NPCs were iontophoretically microinjected with a glass micropipette filled with 75 mM Lucifer yellow (LY, 5% w/v in 150 mM LiCl). Dye coupling index was calculated as the mean number of cells to which the dye spread occurred in 3 min. All microinjections were performed in HCO_3^--free F-12 medium buffered with 10 mM HEPES (pH 7.4) containing 200 μM La^{3+} to avoid cell leakage of the microinjected dye via hemichannels. Dye coupling was assessed in the absence and in the presence of 750 μM octanol. Fluorescent cells were observed using a Nikon inverted microscope equipped with epifluorescence illumination (Xenon arc lamp) and Nikon B filter to LY (excitation wavelength 450–490 nm; emission wavelength above 520 nm) and XF34 filter to DiI fluorescence (Omega Optical, Inc., Brattleboro, VT, USA). Photomicrographs were obtained using a CCD monochrome camera (CFW-1310M; Scion; Frederick, MD, USA). Five to ten experiments were performed for every type of culture and dye coupling was tested by microinjecting a minimum of 10 cells per experiment.

Dye uptake

Hemichannel activity in neurosphere-derived cells was evaluated by using the ethidium (Etd) bromide uptake method (Schalper *et al*., 2008). Neurospheres plated on 25-mm poly-D-lysine-treated coverslips were transferred to a 30-mm dish, coated with a thin layer of vaseline to immobilize the coverslips. Then, cells were washed twice with a recording solution [in mM: NaCl (148); KCl (5); $CaCl_2$ (1.8); $MgCl_2$ (1); glucose (5); HEPES (5), pH = 7.4] containing 5 μM Etd. Basal fluorescence intensity from selected regions of the cells was recorded for 5 min, and cells were subsequently exposed for 5 min to a recording solution without divalent cations (divalent cation-free solution, DCFS). To confirm that Etd uptake was mediated by hemichannels, the blocker La^{3+} (200 μM) was added at the end of each recording (Schalper *et al*., 2008) and fluorescence was recorded for another 5 min. Dye uptake was recorded in an Olympus BX51WI upright microscope using a 40x water immersion objective (Melville), and equipped with the image acquisition system Q Imaging, model Retiga 13001, fast-

cooled monochromatic digital camera (12-bit) (Qimaging, Burnaby, BC, Canada). Images were captured every 30 s (exposure time = 30 ms, gain = 0.5). Metafluor software (version 6.2R5, Universal Imaging Co., Downingtown, PA, USA) was used for off-line image analysis and fluorescence quantification. For data representation and calculation of uptake rates, the average of three independent background fluorescence intensity measurements (FB, expressed as arbitrary units, AU) was subtracted from the fluorescence intensity in each cell (F1). Results of this calculation (F1-FB), including at least 10 cells per experiment, were averaged and plotted against time (expressed in minutes). Dye uptake rates were calculated with Microsoft Excel software and expressed as AU/min. Microscope and camera settings remained constant in all experiments.

Statistics

Data are presented as mean ± standard error of the mean (SEM) and were analyzed in Sigma Plot 11 (Systat Software) by using the one-way analysis of variance (ANOVA) followed by a Tukey's post-hoc test or Student´s t test, as appropriate. Differences were considered significant at a level of $p < 0.05$.

RESULTS

Cells obtained from neurospheres express mRNAs for hemichannel and gap junction proteins.

RT-PCR measurements were performed to detect mRNAs for different connexins (Cx43, Cx45, Cx26) as wells as for Panx1 in neurospheres obtained from the postnatal rat SVZ. We sought to detect the mRNAs of these proteins based on previous reports showing evidence for a role of these connexins on NPC proliferation (Cheng *et al*., 2004; Kunze *et al*., 2009; Khodosevich *et al*., 2012). RT-PCR revealed the presence of Cx43, Cx45, Cx26 and Panx1 mRNA in neurosphere-derived cells (Figure 1).

Cell coupling in neurosphere-derived cells.

Neurospheres were slightly disaggregated and plated on 15-mm poly-D-lysine-treated coverslips. Both non-disaggregated neurospheres and small clusters of about 5-25 cells were observed after plating. LY was microinjected in a single cell and the dye transfer to adjacent cells was evaluated three minutes later.

All the LY microinjections performed in neurosphere-derived cells led to dye transfer to adjacent cells, therefore, the incidence of coupling was 100% (data from 52 cells from 5 different experiments). Figure 2B shows an example of LY transfer to neighboring cells in a non-disaggregated neurosphere. Dye coupling also occurred in the small groups of neurosphere-derived cells (see example in Figure 2D, the cell microinjected with LY shows the highest intensity of fluorescence). The index of coupling, calculated as the mean number of cells to which the dye was transferred in positive cases, was 3.0 ± 0.3 cells. In the presence of the gap junction opening inhibitor octanol (750 μM), dye coupling was completely abolished, indicating that intercellular dye transfer occurred indeed through gap junctional communication (an example is shown in Figure 2F).

Connexin-mediated hemichannel activity in neurosphere-derived cells.

Hemichannel activity was tested in neurosphere-derived cells by analyzing time-lapse measurements of Etd uptake in different experimental conditions. Both non-disaggregated neurospheres and small clusters of 5-25 cells from slightly disaggregated neurospheres were analyzed.

Cells from non-disaggregated neurospheres showed evident Etd uptake under basal

conditions (Figure 3A-E). Etd uptake occurred through connexin hemichannels since addition of the connexin hemichannel blocker La^{3+} to the bath solution completely abolished it (Figure 3D and 3E). Etd uptake in basal conditions was only evident short after neurosphere plating (up to ~1h) and disappeared as cells adhered to the substrate (data not shown). This suggests that, in floating neurospheres, hemichannels are open in resting conditions and are closed or removed from the cell surface once cells begin to adhere to a substrate, a condition that initiates cell differentiation towards neural phenotypes.

However, in the majority of cells from small groups of slightly disaggregated neurospheres, Etd uptake was very low under basal conditions (Figures 4A, 4B and 4D) which probably indicates that mechanical disaggregation induces hemichannel closing or hemichannel removal from the cell surface. Only few cells in every analyzed cell cluster showed high basal Etd uptake (brightest cells in Figure 4B). Replacement of the extracellular saline solution by DCFS to increase the open probability of connexin hemichannels (Schalper *et al*., 2008), induced a progressive increase in Etd uptake in all cells (Figure 4C, 4D and 4E), indicating that hemichannels were indeed located at the cells surface but presented very low open probability. Addition of the connexin hemichannel blocker La^{3+} (200 μM) in this condition significantly inhibited Etd uptake in all neurosphere-derived cells (Figure 4D and 4E). Inducible opening of hemichannels in neurosphere-derived cells was only achieved shortly after plating. After 2-3 hours of plating, change to DCFS did not induce Etd uptake, indicating a loss of activatable hemichannel probably due to removal from the cell membrane as a result of cell adhesion (data not shown).

Cell coupling between neurosphere-derived cells and astrocytes.

Neurosphere-derived NPCs were plated on astrocyte monolayers to analyze gap junctional communication between both cell populations. Astrocytes were pre-labeled with the lipophilic dye DiI to distinguish them from neurosphere-derived NPCs. One hour after setting the co-culture, dye coupling was evaluated by microinjecting LY in non-labeled NPCs and analyzing the dye transfer to adjacent DiI-labeled astrocytes. Most injected NPCs were coupled to astrocytes (incidence of coupling of 91.0 ± 4.7%; 96 cells from 9 independent experiments; Figures 5A-C) and LY injected in one cell diffused to a mean of 2.4 ± 0.3 adjacent astrocytes (index of coupling) (Figure 5G).

Blockade of gap junctions with octanol (750 μM) prevented diffusion of LY from injected NPCs to adjacent astrocytes (Figures 5D-F and G).

Cell coupling between neurosphere-derived cells and microglia.

Microglial cells from primary cultures were also pre-labeled with DiI before NPCs were plated on them. One hour after co-culture, LY microinjections were performed in non-labeled NPCs and diffusion to DiI-labeled microglial cells was analyzed. Experiments revealed that NPCs also coupled to microglial cells (Figures 6A-C and 6G). However, a lower incidence of coupling with respect to astrocyte co-cultures was observed (71.9 ± 6.7%; 99 cells from 10 independent experiments). The index of dye coupling was 1.0 ± 0.1, also significantly lower than the obtained in NPCs-astrocyte co-cultures ($p<0.05$; Student's t test). Again, octanol prevented LY transfer from injected cells to neighbouring cells indicating that blocking gap junctions eliminated dye coupling between NPCs and microglia (Figures 6D-F and 6G).

DISCUSSION

In this study, we show evidence of hemichannel activity in NPCs from postnatal rat SVZ neurospheres. In addition, we demonstrate the existence of functional heterocellular gap junctions between neurosphere-derived cells and astrocytes or microglia. As NPCs are widely used for transplantation purposes in brain lesion models, we propose that this type of direct NPC-glial cell communication might take place in the host tissue with relevant roles for survival and integration of NPCs after implantation.

We have previously described that NPCs from postnatal rat SVZ express Cx43 *in vitro* and after implantation in the lesioned brain (Talaverón *et al*., 2014). In the current study, we have demonstrated that SVZ neurosphere-derived NPCs also express the mRNA for Cx26, Cx43, Cx45 and Panx1. Indeed, different roles for these hemichannel/gap junction proteins have been described in the SVZ neurogenic niche. For instance, Cx45 modulates the proliferation of transit-amplifying cells and neuroblasts in the postnatal SVZ by inducing cell cycle reentry via ATP signaling (Khodosevich *et al*., 2012). Also Panx1, expressed by NPCs in the SVZ, regulates NPC proliferation through the release of ATP (Wicki-Stordeour *et al*., 2012). Cx43 expression by NPCs from embryonic tissue is involved in their maintenance in a proliferative state (Cheng *et al*., 2004; Lemcke and Kuznetsov, 2013). Therefore, all results published to date point to a determinant role of the communication mediated by these hemichannel/gap junction proteins in the proliferation rate of this population of progenitor cells.

In the neurogenic postnatal SVZ, NPCs and niche astrocytes form microdomains of gap junctional communication networks (Lacar, *et al*., 2011). The specific role of this functional connectivity has not yet been elucidated although it has been proposed that astrocytes could shape the behavior of NPCs through functional coupling and calcium waves. Direct homocellular communication via gap junctions among NPCs also takes place in the postnatal SVZ that is involved in cell migration throughout the rostral migratory stream (Menezes *et al*., 2000; Marins *et al*., 2009). We show, in this study, that the ability of postnatal SVZ NPCs to form functional gap junctions remains when they are isolated and are grown as neurospheres. Dye coupling in neurospheres occurred in the presence of extracellular La^{3+}, that blocks connexin hemichannels (D´hondt *et al*.,

2009), and it was abolished by octanol, a gap junction blocker that does not significantly affect pannexin hemichannels (D´hondt *et al*., 2009). This indicates that the coupling took place through gap junctions and was not due to cell leakage and reuptake via pannexin or connexin hemichannels.

Autocrine/paracrine communication via open hemichannels might also occur in SVZ neurospheres since, as described before, they express different connexins as well as Panx1. We have demonstrated that cells from floating non-disaggregated neurospheres present evident hemichannel activity mediated by connexin hemichannels since it was abolished by La^{3+}, which specifically blocks connexin and not pannexin hemichannels (Pelegrin and Surprenant, 2006). Interestingly, hemichannel activity ceases when neurospheres adhere to a substrate, a condition that initiates cell differentiation towards neural phenotypes (Talaveron *et al*., 2013). This suggests that signaling through hemichannels may intervene on the maintainance of SVZ NPCs in an undifferentiated and proliferative state within the neurosphere. To our knowledge, this is the first study describing connexin hemichannel activity in postnatal SVZ neurospheres although its precise physiological role will have to be solved in future experiments.

NPCs isolated from the postnatal SVZ can form gap junctions after implantation in the mechanically-lesioned brain (Talaverón *et al*., 2014). Remarkably, gap junctions were identified not only among implanted NPCs, but also between NPCs and host astrocytes and less frequently with host microglia at the lesion site (Talaverón *et al*., 2014). In co-culture experiments of SVZ-derived NPCs with astrocytes, we have demonstrated that NPCs form functional gap junctions with astrocytes with more than a 90% incidence of coupling. As it was mentioned before, NPCs and astrocytes establish cellular networks of gap junctional communication in the SVZ neurogenic niche (Lacar *et al*., 2011) so, it is not surprising that the ability to form gap junctions between these two cell types remains *in vitro*. Therefore, it is quite feasible that gap junctions formed between NPCs implanted in the damaged brain and host astrocytes could be functional and have specific roles in NPC integration and in NPC-induced beneficial effects.

The demonstration of gap junctional communication within microglial cells and between microglia and neurons has been documented in *in vitro* experiments. Thereby, two independent groups have demonstrated that microglial cells can form functional gap junctions among them after activation with pro-inflammatory conditions (Eugenín *et al.,*

2001; Garg *et al*., 2005). Also Dobrenis *et al*. (2006) showed that in co-cultures, microglia can communicate with neurons via gap junctions. In contrast, in a recent study performed *in vivo*, both in normal and in diseased animals, the authors failed to identify any evidence of dye transfer between microglial cells or between microglia and neurons (Wasseff and Scherer, 2014). It is important to point out that we have previously identified at ultrastructural level the existence of gap junctions between implanted NPCs and host microglial cells in animals lesioned by axotomy (Talaverón *et al*., 2014). Now, we report here for the first time evidence of dye coupling between NPCs and microglia *in vitro*. The ability of NPCs to form functional gap junctions with microglia can be both physiologically and pathologically relevant. In healthy conditions, close proximity between microglial cells and NPCs has been documented in the SVZ neurogenic niche (Goings *et al*., 2006; Gonzalez-Perez *et al*., 2012; Mosher *et al*., 2012). Indeed, microglia and SVZ NPCs establish a bilateral cross-talk that can affect both microglial activation state and also NPC proliferation and differentiation (Mathieu *et al*., 2010; Gonzalez-Perez *et al*., 2012; Mosher *et al*., 2012; Shigemoto-Mogami *et al*., 2014). We propose here that direct communication via gap junctions between microglia and NPCs might also occur physiologically in the SVZ neurogenic niche with roles in the physiology of both cell types. In pathological conditions, possible scenarios for NPCs-microglia interactions include the use of NPC implants in lesioned brain with microglia activation. The inflammatory response triggered by host microglial cells is known to preserve implanted NPCs in an undifferentiated state in which they can promote CNS tissue healing by the secretion of immunomodulatory and neuroprotective molecules (Martino and Pluchino, 2006). As we have demonstrated *in vitro* direct NPC-microglia coupling, we raise the possibility that functional gap junctions between implanted NPCs and host microglia in the lesioned tissue might also intervene on restorative mechanisms induced by the implants.

Altogether our results demonstrate that postnatal SVZ NPCs cultured as neurospheres present functional hemichannels and gap junctions. In addition, neurosphere-derived cells can establish gap junctional communication with astrocytes and with microglia *in vitro*. Gap junctional communication between NPCs and glial cells might be involved in the behavior of NPCs both in their natural niche and also after implantation in the injured brain.

ACKNOWLEDGMENTS

This work was funded by Chilean Science Millennium Institute (P09-022-F to JCS) and grants BFU2012-33975 (MINECO-FEDER) and CVI-6053 (Junta de Andalucía-FEDER) from Spain. Rocío Talaverón thanks Santander Universidades for a short term fellowship in Chile. We thank Teresa Vergara and Adam Aguirre for their help and technical support.

AUTHORS CONTRIBUTIONS

AMP, ERM and JCS designed research. RT, PF, RE and JCS performed research. RT, PF, RE, AMP, ERM and JCS analyzed data. ERM and JCS wrote the paper.

REFERENCES

Alvarez-Buylla, A, Seri, B, and Doetsch, F. (2002). Identification of neural stem cells in the adult vertebrate brain. *Brain Res. Bull*. 57, 751-758.

Anderson, D. J. (2001). Stem cells and pattern formation in the nervous system: The possible versus the actual. *Neuron* 30, 19–35. doi:10.1016/S0896-6273(01)00260-4.

Ben-Hur, T. (2008). Immunomodulation by neural stem cells. *J. Neurol. Sci.* 265, 102–104. doi:10.1016/j.jns.2007.05.007.

Bruzzone, R., White, T.W., and Paul, D.L. (1996). Connections with connexins: the molecular basis of direct intercellular signaling. *Eur. J. Biochem*. 238, 1-27.

Carpenter, M. K., Cui, X., Hu, Z. Y., Jackson, J., Sherman, S., Seiger, A., and Wahlberg, L. U. (1999). In vitro expansion of a multipotent population of human neural progenitor cells. *Exp. Neurol.* 158, 265–278. doi:10.1006/exnr.1999.7098.

Chen, Y., Deng, Y., Bao, X., Reuss, L., and Altenberg, G. (2005). Mechanism of the defect in gap-junctional communication by expression of a connexin 26 mutant associated with dominant deafness. *FASEB J.* 16, 9–12.

Cheng, A., Tang, H., Cai, J., Zhu, M., Zhang, X., Rao, M., and Mattson, M. P. (2004). Gap junctional communication is required to maintain mouse cortical neural progenitor cells in a proliferative state. *Dev. Biol.* 272, 203–216. doi:10.1016/j.ydbio.2004.04.031.

Cina, C., Bechberger, J.F., Ozog, M.A., and Naus, C.C.G. (2007). Expression of connexins in embryonic mouse neocortical development. *J. Comp. Neurol.* 504, 298-313.

D'hondt, C., Ponsaerts, R., De Smedt, H., Bultynck, G., and Himpens, B. (2009). Pannexins, distant relatives of the connexin family with specific cellular functions? *BioEssays* 31, 953–974. doi:10.1002/bies.200800236.

Dahl, G., and Locovei, S. (2006). Pannexin: to gap or not to gap, is that a question? *IUBMB Life* 58, 409–419. doi:10.1080/15216540600794526.

Dobrenis, K., Chang, H.-Y., Pina-Benabou, M.H., Woodroffe, A., Lee, S.C., Rozental, R., Spray, D.C., and Scemes, E. (2005). Human and mouse microglia express connexin36, and functional gap junctions are formed between rodent microglia and neurons. *J. Neurosci. Res.* 82, 306-315.

Duval, N., Gomès, D., Calaora, V., Calabrese, A., Meda, P., and Bruzzone, R. (2002). Cell coupling and Cx43 expression in embryonic mouse neural progenitor cells. *J. Cell Sci.* 115, 3241-3251.

Eugenín, E.A., Eckardt, D., Theis, M., Willecke, K., Bennett, M.V.L., and Sáez, J.C. (2001). Microglia at brain stab wounds express connexin 43 and in vitro form

functional gap junctions after treatment with interferon-γ and tumor necrosis factor-α. *Proc. Natl. Acad. Sci. U.S.A.* 98, 4190-4195.

Freitas, A. S., Xavier, A. L. R., Furtado, C. M., Hedin-Pereira, C., Fróes, M. M., and Menezes, J. R. L. (2012). Dye coupling and connexin expression by cortical radial glia in the early postnatal subventricular zone. *Dev. Neurobiol.* 72, 1482–1497. doi:10.1002/dneu.22005.

Gage, F. H. (2000). Mammalian neural stem cells. *Science* 287, 1433–1438. doi:10.1126/science.287.5457.1433.

Garg, S., Md Syed, M., and Kielian, T. (2005). Staphylococcus aureus-derived peptidoglycan induces Cx43 expression and functional gap junction intercellular communication in microglia. *J. Neurochem.* 95, 475–83. doi:10.1111/j.1471-4159.2005.03384.x.

Goings, G. E., Kozlowski, D. A., and Szele, F. G. (2006). Differential activation of microglia in neurogenic versus non-neurogenic regions of the forebrain. *Glia* 54, 329–342. doi:10.1002/glia.

Gonzalez-Perez, O., Gutierrez-Fernandez, F., Lopez-Virgen, V., Collas-Aguilar, J., Quinones-Hinojosa, A., and Garcia-Verdugo, J. M. (2012). Immunological regulation of neurogenic niches in the adult brain. *Neuroscience* 226, 270–281. doi:10.1016/j.neuroscience.2012.08.053.

Jäderstad, J., Jäderstad, L.M., Li, J, Chintawar, S., Salto, C., Pandolfo, M., Ourednik, V., Teng, Y.D., Sidman, R.L., Arenas, E., Snyder, E.Y., and Herlenius, E. (2010). Communication via gap junctions underlies early functional and beneficial interactions between grafted neural stem cells and the host. *Proc. Natl. Acad. Sci. U.S.A.* 107, 5184-5189.

Khodosevich, K., Zuccotti, A., Kreuzberg, M. M., Le Magueresse, C., Frank, M., Willecke, K., and Monyer, H. (2012). Connexin45 modulates the proliferation of transit-amplifying precursor cells in the mouse subventricular zone. *Proc. Natl. Acad. Sci. U. S. A.* 109, 20107–12. doi:10.1073/pnas.1217103109.

Kumar, N.M., and Gilula, N. (1996). The gap junction communication channel. *Cell* 84, 381-388.

Kunze, A., Rubenecia, M., Hartmann, C., Wallraff-beck, A., Hu, K., Bedner, P., Requardt, R., Seifert, G., Redecker, C., Willecke, K., et al. (2009). Connexin expression by radial glia-like cells is required for neurogenesis in the adult dentate gyrus. *Proc. Natl. Acad. Sci. U. S. A.* 106, 11336-11341.

Lacar, B., Young, S. Z., Platel, J. C., and Bordey, A. (2011). Gap junction-mediated calcium waves define communication networks among murine postnatal neural progenitor cells. *Eur. J. Neurosci.* 34, 1895–1905. doi:10.1111/j.1460-9568.2011.07901.x.

Lemcke, H., and Kuznetsov, S.A. (2013). Involvement of connexin43 in the EGF/EGFR signalling during self-renewal and differentiation of neural prgenitor cells. *Cell Signal.* 25, 2676-2684.

MacVicar, B. A., and Thompson, R. J. (2010). Non-junction functions of pannexin-1 channels. *Trends Neurosci.* 33, 93–102. doi:10.1016/j.tins.2009.11.007.

Marins, M., Xavier, A.L.R., Viana, N.B., Fortes, F.S.A., Fróes, M.M. and Menezes, J.R.L. (2009). Gap junctions are involved in cell migration in the early postnatal subventricular zone. *Develop. Neurobiol.* 69, 715-730.

Martínez, A. D., and Sáez, J. C. (1999). Arachidonic acid-induced dye uncoupling in rat cortical astrocytes is mediated by arachidonic acid byproducts. *Brain Res.* 816, 411–423. doi:10.1016/S0006-8993(98)01016-6.

Martino, G., and Pluchino, S. (2006). The therapeutic potential of neural stem cells. *Nat. Rev. Neurosci.* 7, 395–406. doi:10.1038/nrn1908.

Martino, G., Pluchino, S., Bonfanti, L., and Schwartz, M. (2011). Brain regeneration in physiology and pathology: the immune signature driving therapeutic plasticity of neural stem cells. *Physiol. Rev.* 91, 1281–304. doi:10.1152/physrev.00032.2010.

Mathieu, P., Battista, D., Depino, A., Roca, V., Graciarena, M., and Pitossi, F. (2010). The more you have, the less you get: the functional role of inflammation on neuronal differentiation of endogenous and transplanted neural stem cells in the adult brain. *J. Neurochem.* 112, 1368–85. doi:10.1111/j.1471-4159.2009.06548.x.

Menezes, J.R.L., Fróes, M.M., Moura Neto, V., and Lent, R. (2000). Gap junction-mediated coupling in the postnatal anterior subventricular zone. *Dev. Neurosci*. 22, 34-43.

Mosher, K. I., Andres, R. H., Fukuhara, T., Bieri, G., Hasegawa-Moriyama, M., He, Y., Guzman, R., and Wyss-Coray, T. (2012). Neural progenitor cells regulate microglia functions and activity. *Nat. Neurosci.* 15, 1485–7. doi:10.1038/nn.3233.

Nadarajah, B., Jones, A.M., Evans, W.H., and Parnavelas, J.G. (1997). Differential expression of connexins during neocortical development and neuronal circuit formation. *J. Neurosci.* 17, 3096-3111.

Pelegrin, P., and Surprenant, A. (2006). Pannexin-1 mediates large pore formation and interleukin-1beta release by the ATP-gated P2X7 receptor. *EMBO J.* 25, 5071–5082. doi:10.1038/sj.emboj.7601378.

Retamal, M. a, Cortés, C. J., Reuss, L., Bennett, M. V. L., and Sáez, J. C. (2006). S-nitrosylation and permeation through connexin 43 hemichannels in astrocytes: induction by oxidant stress and reversal by reducing agents. *Proc. Natl. Acad. Sci. U. S. A.* 103, 4475–4480. doi:10.1073/pnas.0511118103.

Schalper, K.A., Palacios-Prado, N., Orellana, J.A., and Sáez, J.C. (2008). Currently used methods for identification and characterization of hemichannels. *Cell Commun. Adhes.* 15, 207-218.

Shigemoto-Mogami, Y., Hoshikawa, K., Goldman, J. E., Sekino, Y., and Sato, K. (2014). Microglia enhance neurogenesis and oligodendrogenesis in the early postnatal subventricular zone. *J. Neurosci.* 34, 2231–43. doi:10.1523/JNEUROSCI.1619-13.2014.

Talaverón, R., Matarredona, E. R., de la Cruz, R. R., and Pastor, A. M. (2013). Neural progenitor cell implants modulate vascular endothelial growth factor and brain-derived neurotrophic factor expression in rat axotomized neurons. *PLoS One* 8, e54519. doi:10.1371/journal.pone.0054519.

Talaverón, R., Matarredona, E. R., de la Cruz, R. R., Macías, D., Gálvez, V., and Pastor, A. M. (2014). Implanted neural progenitor cells regulate glial reaction to brain injury and establish gap junctions with host glial cells. *Glia* 62, 623–638.

Vescovi, A. L., Parati, E. A., Gritti, A., Poulin, P., Ferrario, M., Wanke, E., Frölichsthal-Schoeller, P., Cova, L., Arcellana-Panlilio, M., Colombo, A., et al. (1999). Isolation and cloning of multipotential stem cells from the embryonic human CNS and establishment of transplantable human neural stem cell lines by epigenetic stimulation. *Exp. Neurol.* 156, 71–83. doi:10.1006/exnr.1998.6998.

Wasseff, S. K., and Scherer, S. S. (2014). Activated microglia do not form functional gap junctions in vivo. *J. Neuroimmunol.* 269, 90–93. doi:10.1016/j.jneuroim.2014.02.005.

Wicki-Stordeur, L. E., Dzugalo, A. D., Swansburg, R. M., Suits, J. M., and Swayne, L. (2012). Pannexin 1 regulates postnatal neural stem and progenitor cell proliferation. *Neural Dev.* 7, 11. doi:10.1186/1749-8104-7-11.

Willecke, K., Eiberger, J., Degen, J., Eckardt, D., Romualdi, A., Güldenagel, M., Deutsch, U., and Söhl, G. (2002). Structural and functional diversity of connexin genes in the mouse and human genome. *Biol. Chem.* 383, 725-737.

FIGURE LEGENDS

Figure 1. Detection of Cx43, Cx45, Cx26 and Panx1 mRNAs in SVZ neurosphere-derived cells. Two μg of total RNA from neurosphere-derived cells was analyzed by RT-PCR with specific primers designed to detect the presence of Cx43, Cx45, Cx26 and Panx1 mRNAs. Detection of the housekeeping GADPH mRNA was included as a loading control. Lane 1, 100-bp DNA ladder. Lanes labeled – RT are negative controls without reverse transcriptase enzyme. A representative agarose gel from 4 independent experiments is shown.

Figure 2. Dye coupling between cells in SVZ neurospheres. Examples of dye coupling 3 minutes after Lucifer yellow (LY) microinjection into a cell of a non-disaggregated neurosphere (A-B) or into a neurosphere-derived cell (C-D). After addition of the gap junction blocker octanol (750 μM), microinjected LY did not spread to neighboring neurosphere-derived cells (E-F). A, C and E show the corresponding phase-contrast views of the fields of the representative pictures of LY microinjections shown in B, D and F, respectively. Bar: 50 μm.

Figure 3. Floating SVZ neurospheres present high connexin hemichannel activity. Representative fluorescence images of a non-disaggregated floating neurosphere incubated in a solution containing 5 μM ethidium (Etd) for 3.5 min (B) and 3.5 min later (C). A shows the corresponding phase-contrast image. Bar: 25 μm. D: Time-lapse Etd uptake (in arbitrary units, AU) under basal conditions (Basal; first 7 min) and after addition of the connexin hemichannel blocker 200 μM La^{3+} (+La^{3+}, following 3.5 min). Each point corresponds to the mean of 20 cells from one experiment. E: Etd uptake rates (in AU/min) in cells of neurospheres under basal conditions and after La^{3+} addition (+La^{3+}). Data are presented as mean ± SEM of three independent experiments. * $p < 0.05$ compared to basal conditions (Student's t test).

Figure 4. Connexin hemichannel activity in SVZ neurosphere-derived cells.

Representative fluorescence images of a small cluster of neurosphere-derived cells incubated in a solution containing 5 μM ethidium (Etd) under basal conditions (B) and after bathing with divalent cation-free solution (DCFS) to increase the open probability of connexin hemichannels (C). A shows the corresponding phase-contrast image. Brightest cells in B are cells with high basal Etd uptake in contrast to the majority of

neurosphere-derived cells that presented very low basal Etd uptake. Bar: 25 µm. D: Time-lapse Etd uptake (in arbitrary units, AU) under basal conditions (Basal; first 5 min), after incubation in DCFS (DCFS, following 5 min) and after addition of the connexin hemichannel blocker 200 µM La^{3+} (La^{3+}, following 5 min). Each point corresponds to the mean of 10 cells with low basal Etd uptake from one experiment. E: Etd uptake rates (in AU/min) in neurosphere-derived cells measured under basal conditions (Basal), after incubation in DCFS (DCFS) and after La^{3+} addition (La^{3+}) in low basal Etd uptake cells and in high basal Etd uptake cells. Data are presented as mean ± SEM from three independent experiments. * $p < 0.05$ compared to basal conditions. # $p < 0.05$ compared to DCFS condition (one-way ANOVA followed by Tukey's *post-hoc* test).

Figure 5. Neurosphere-derived cells and astrocytes establish gap junctional communication. Photomicrographs showing examples of Lucifer yellow (LY) microinjections in co-cultures of neurosphere-derived cells and primary astrocytes. Astrocytes were labeled with the lipophilic dye DiI before the co-culture to allow their identification. LY was microinjected in neurosphere-derived cells and the transfer to adjacent DiI-labeled cells was evaluated three minutes later. A: Phase-contrast view of the fields shown in B and C. The asterisk denotes the cell microinjected with LY. B: LY microinjection in a neurosphere-derived cell and dye transfer to adjacent cells (arrowheads). C: DiI-labeled cells of the same field shown in B. Cells that received the dye are indicated with arrowheads. D: Phase-contrast view of the fields shown in E and F. The asterisk denotes the cell microinjected with LY. E: LY microinjection in a neurosphere-derived cell after addition of the gap junction blocker octanol (750 µM). A lack of dye transfer to adjacent cells is observed. F: DiI-labeled cells of the same field shown in E. Bar: 50 µm. G. Index of coupling, calculated as the mean number of cells that received LY in every injection, in co-cultures of neurosphere-derived cells and astrocytes in control conditions (-) and after addition of octanol to the extracellular saline solution (+). Results are the mean ± SEM of 96 cells from 9 independent experiments). *$p < 0.05$ compared to control conditions (Student's t test).

Figure 6. Neurosphere-derived cells and microglia establish gap junctional communication.

Photomicrographs showing examples of Lucifer yellow (LY) microinjections in co-cultures of neurosphere-derived cells and primary microglia. Microglial cells were

labeled with the lipophilic dye DiI before the co-culture to allow their identification. LY was microinjected in neurosphere-derived cells and the transfer to adjacent DiI-labeled cells was evaluated. A: Phase-contrast view of the fields shown in B and C. The asterisk denotes the cell microinjected with LY. B: LY microinjection in a neurosphere-derived cell and dye transfer to an adjacent cell (arrowhead). C: DiI-labeled cells of the same field shown in B. An example of a DiI-labeled cell that received LY is indicated with an arrowhead. D: Phase-contrast view of the fields shown in E and F. The asterisk denotes the cell microinjected with LY. E: LY microinjection in a neurosphere-derived cell after addition of the gap junction blocker octanol (750 μM). A lack of dye transfer to adjacent cells is observed. F: DiI-labeled cells of the same field shown in E. Bar: 50 μm. G. Index of coupling, calculated as the mean number of cells that received LY in every injection, in co-cultures of neurosphere-derived cells and microglia in control conditions (-) and after addition of octanol to the medium (+). Results are the mean ± SEM of 99 cells from 10 independent experiments). *$p < 0.05$ compared to control conditions (Student's t test).

Figure 1.TIF

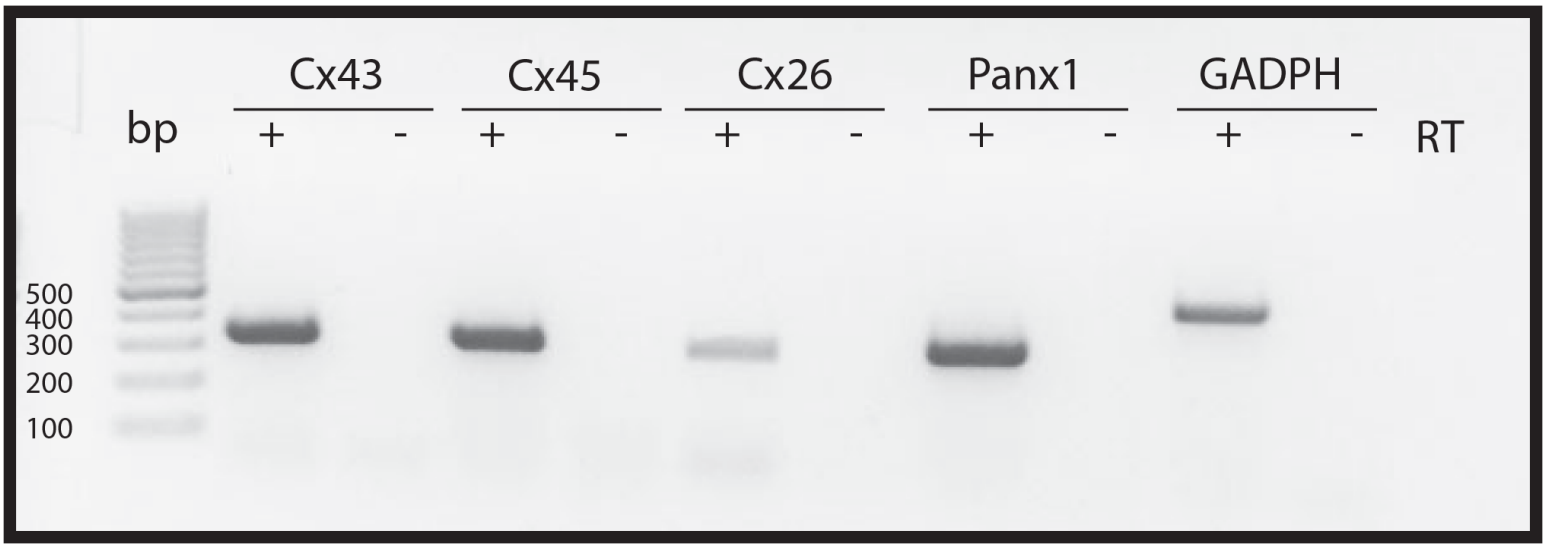

Figure 2.TIF

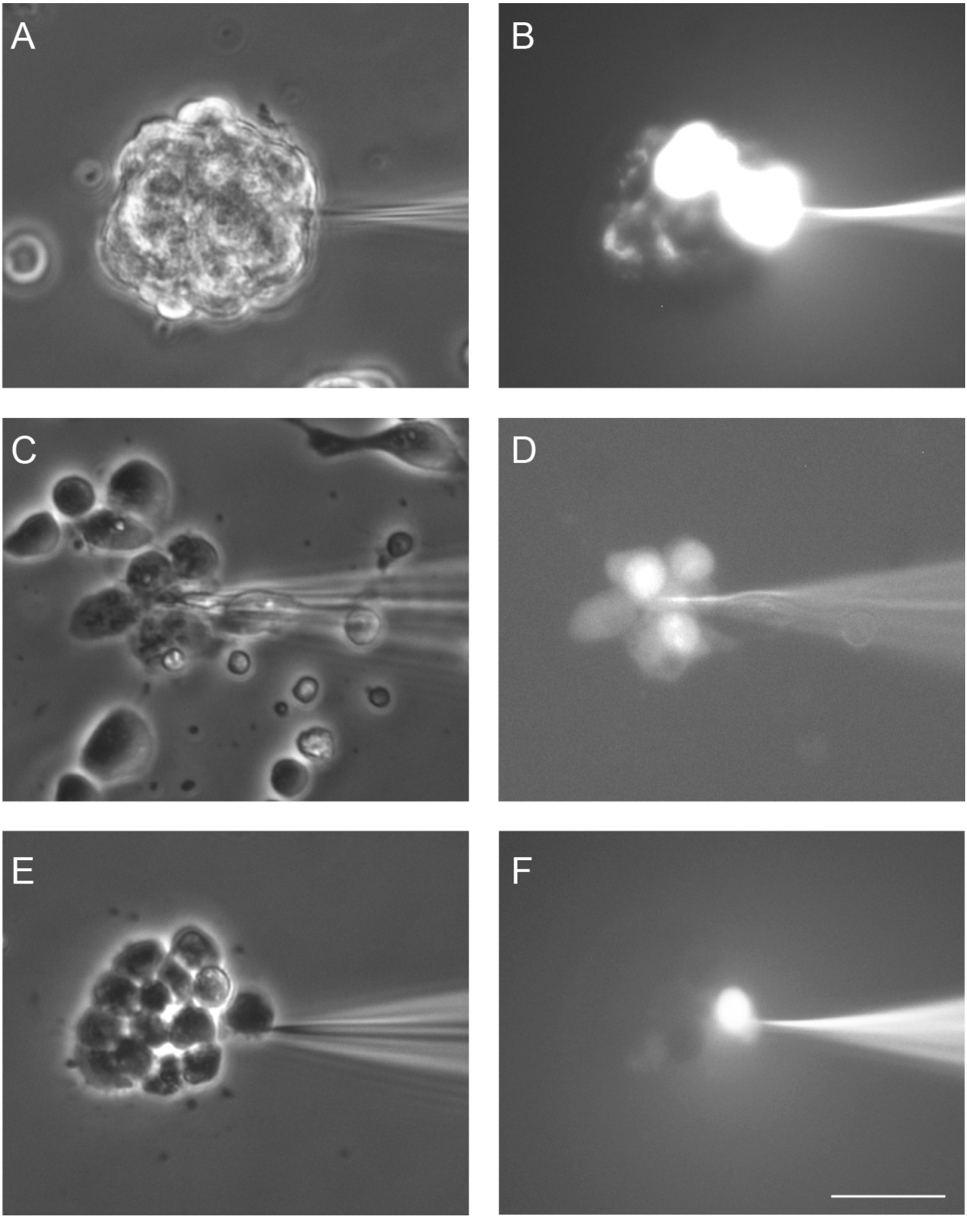

Figure 3.TIF

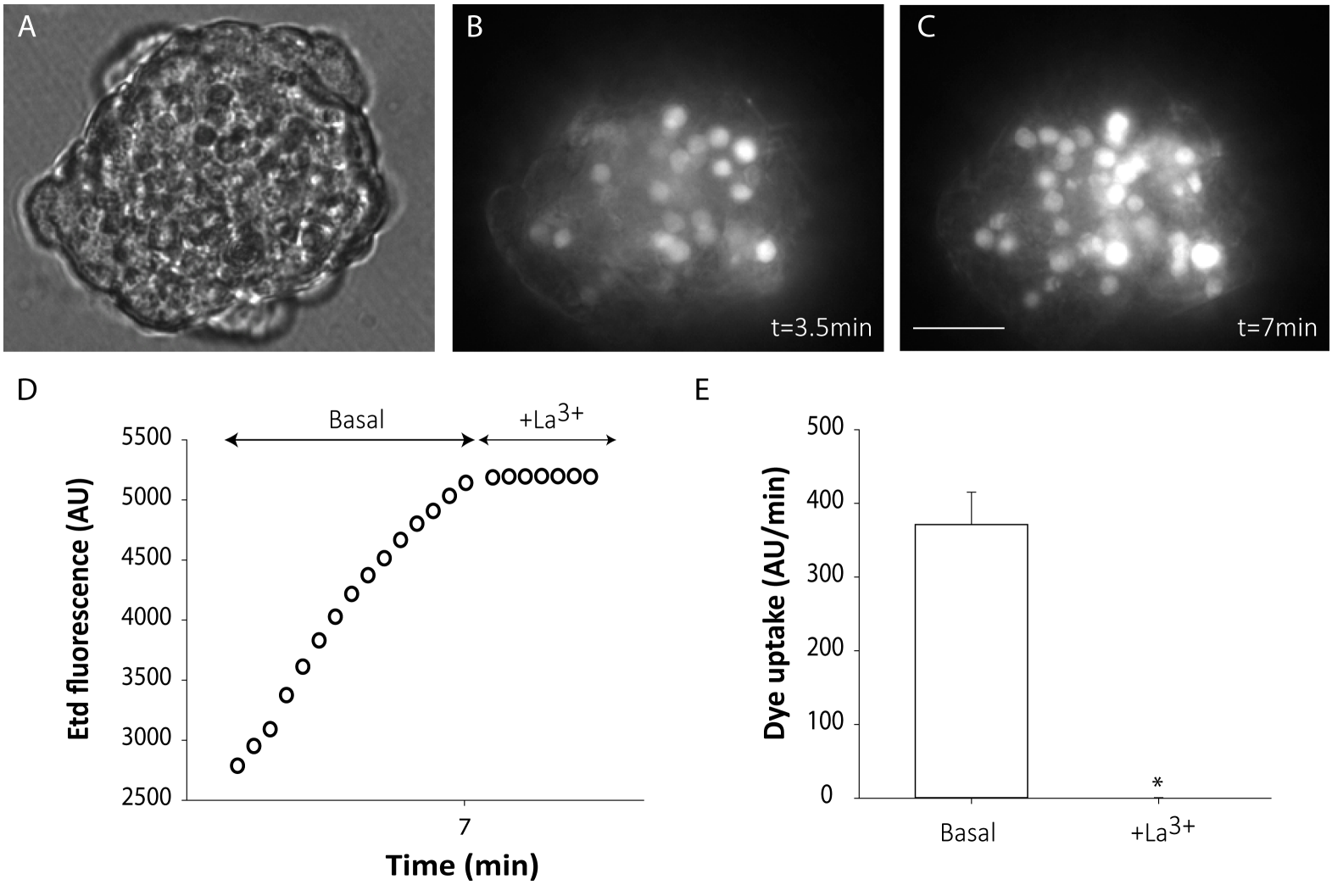
A
B
t=3.5min
C
t=7min
D
Basal
+La3+
5500
5000
4500
4000
3500
3000
2500
Etd fluorescence (AU)
7
Time (min)
E
500
400
300
200
100
0
Dye uptake (AU/min)
*
Basal
+La3+

Figure 4.TIF

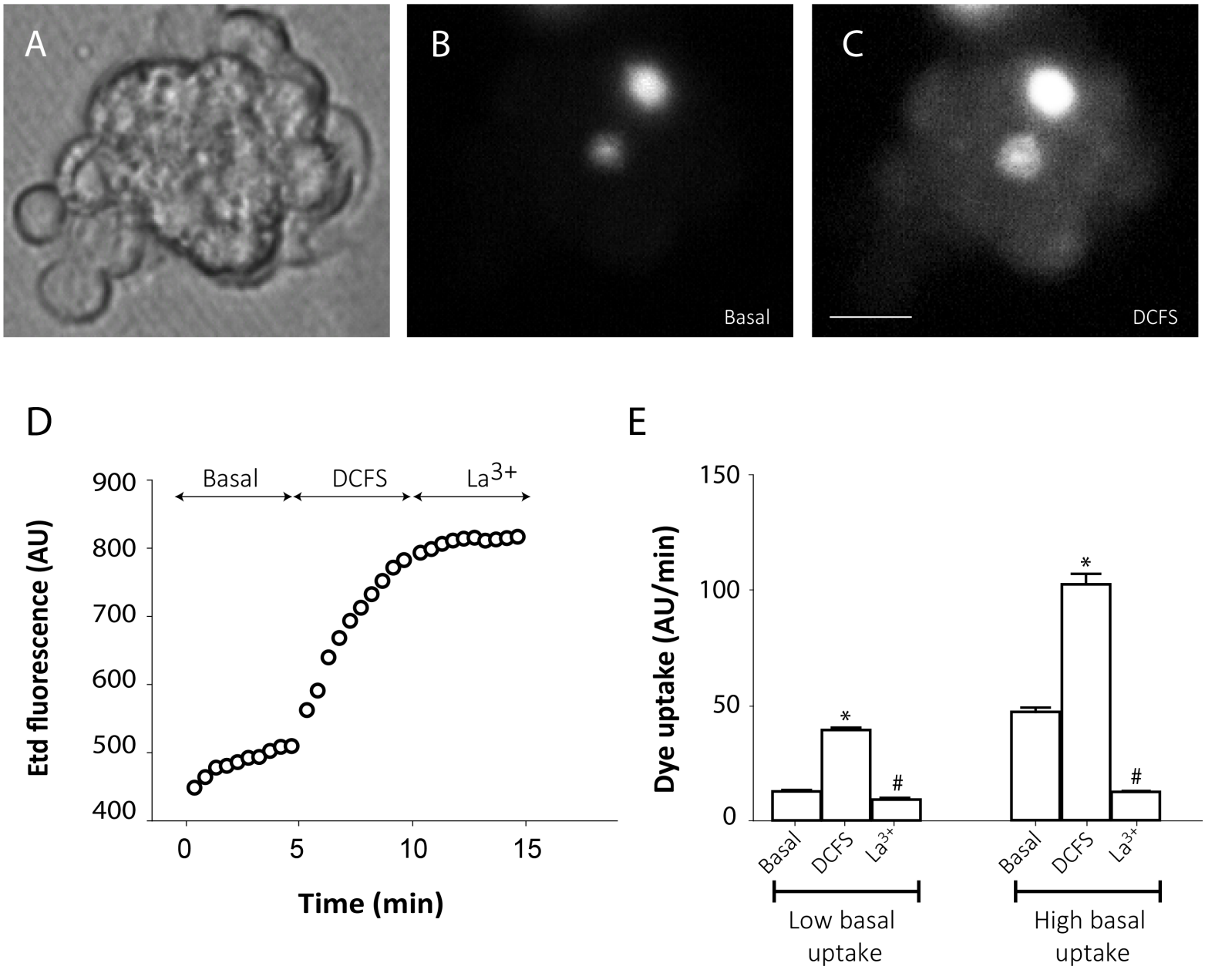
A
B
Basal
C
DCFS
D
Basal
DCFS
La3+
900
800
700
600
500
400
Etd fluorescence (AU)
0
5
10
15
Time (min)
E
150
100
50
0
Dye uptake (AU/min)
*
*
#
#
Basal
DCFS
La3+
Basal
DCFS
La3+
Low basal uptake
High basal uptake

Figure 5.TIF

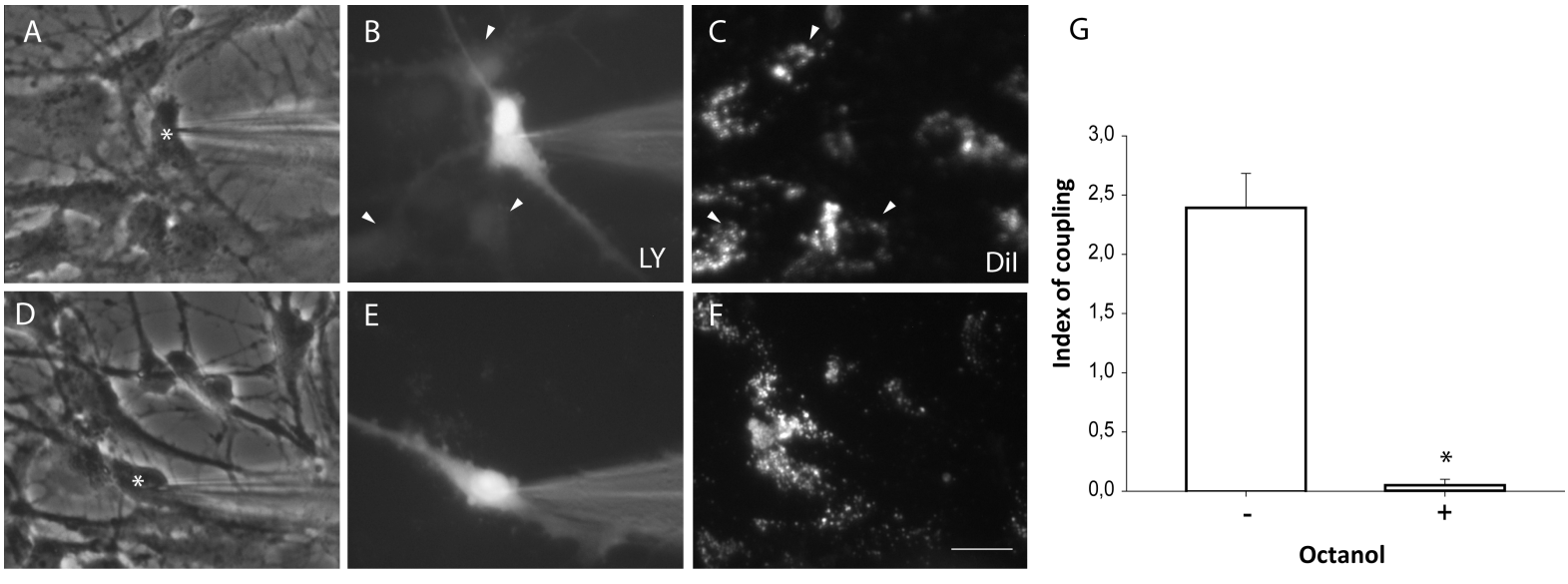

Figure 6.TIF

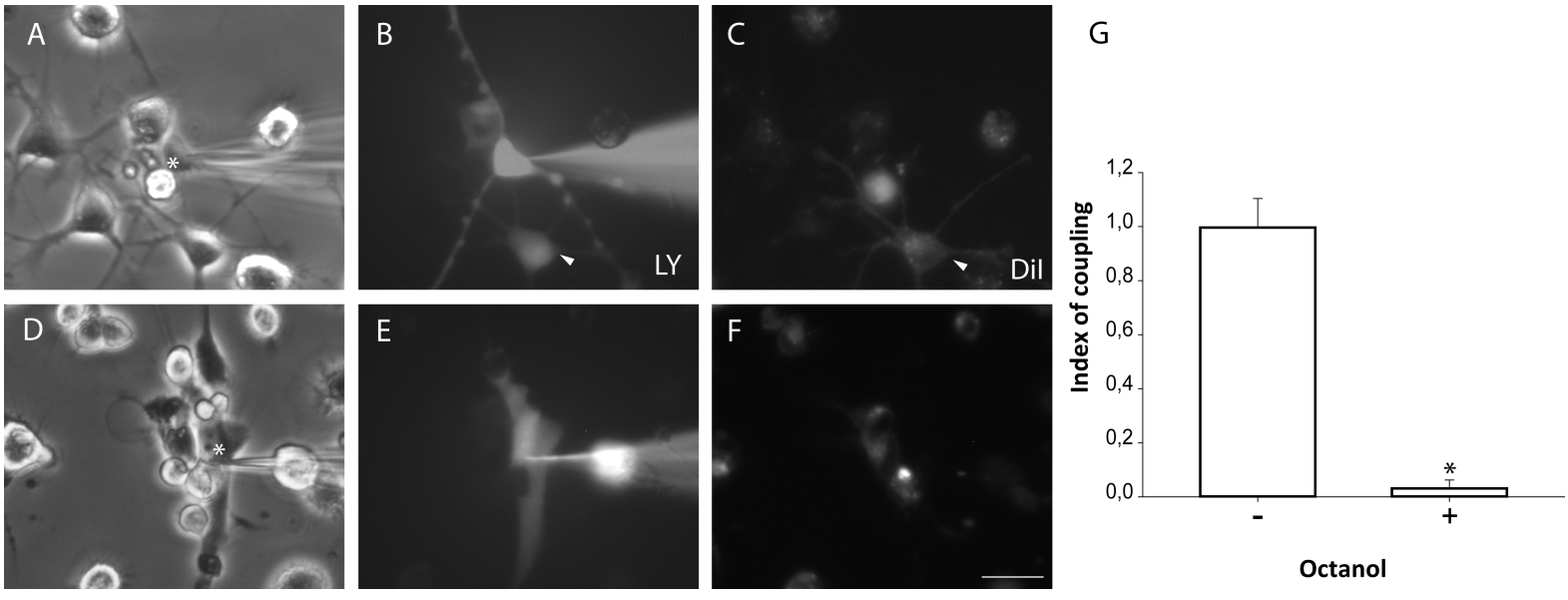

RESUMEN GLOBAL DE LOS RESULTADOS

1.- Resultados referentes al artículo

Neural Progenitor Cell Implants Modulate Vascular Endothelial Growth Factor and Brain-Derived Neurotrophic Factor Expression in Rat Axotomized Neurons. 2013. PLOS ONE, 8: e54519

En este artículo realizamos implantes de CPNs en ratas adultas tras la transección del FLM y analizamos la expresión de factores neurotróficos en la población de neuronas lesionadas, las neuronas internucleares del NMOE. El objetivo fue estudiar si la expresión de factores neurotróficos de las neuronas lesionadas se modificaba como consecuencia del implante. Mediante técnicas inmunocitoquímicas demostramos que la expresión de VEGF en las neuronas internucleares del NMOE no se vio afectada por la axotomía, pero incrementó significativamente cuando se realizaron implantes de CPNs en los animales lesionados. (Figura 3 del artículo).

Respecto al BDNF, la axotomía produjo un aumento de los niveles de esta neurotrofina en los somas de las neuronas lesionadas. Los animales que recibieron implantes de CPNs tras la lesión mostraron, sin embargo, niveles de expresión de BDNF similares a los de neuronas no lesionadas (Figura 3 del artículo).

Estos efectos del implante sobre la expresión de VEGF y BDNF se produjeron selectivamente en la población lesionada del NMOE (las neuronas internucleares), no detectándose ningún efecto sobre la otra población celular este núcleo, las motoneuronas (Figura 4 del artículo).

La expresión de las neurotrofinas NT-3 y NGF en los somas de las neuronas lesionadas no se modificó por efecto del implante (Figura 5 del artículo).

Por último, demostramos que las CPNs expresan VEGF tras su implante en el cerebro del hospedador (Figura 6 del artículo).

2.- Resultados referentes al artículo

*Implanted Neural Progenitor Cells Regulate Glial Reaction to Brain Injury and Establish Gap Junctions with Host Glial Cells.*2014. GLIA, 62:623-638

En este artículo analizamos la reacción glial del tejido hospedador tras la lesión por axotomía del FLM y el implante de CPNs en el lugar de la lesión. El objetivo fue

estudiar si la reacción glial se modificaba como consecuencia del implante de CPNs y analizar la interacción de las CPNs implantadas con las células de la glía hospedadora.

Mediante técnicas inmunocitoquímicas observamos un aumento en la densidad de astrocitos ocho semanas tras la lesión y que los animales que recibieron implantes mostraron un incremento similar a los que recibieron inyecciones de vehículo tras la lesión (Figura 2 del artículo). Sin embargo observamos que la densidad de células inmunorreactivas a un marcador de microglía activada aumentaba significativamente tras la lesión y se veía duplicada en animales con lesión e implante de CPNs (Figura2 del artículo). Además, las CPNs implantadas se disponían muy próximas tanto a astrocitos reactivos como a la microglía activada del hospedador (Figuras 3 y 5 del artículo).

No se detectaron cambios en la densidad de la glía positiva a NG2 en los animales lesionados, ni en los implantados con CPNs (Figura3).

Por otro lado demostramos que las CPNs eran inmunopositivas a la proteína de uniones gap Cx43, tanto in vitro cultivadas como neuroesferas como tras su implante en el cerebro lesionado. Identificamos también Cx43 en astrocitos reactivos de la zona de la lesión y en algunas células de microglía activada. Además, en algunos casos la Cx43 se disponía en la interfase entre las prolongaciones de las CPNs y los astrocitos reactivos del tejido hospedador o las ramificaciones de células de microglía (Figura7 del artículo).

Por último, mediante microscopía electrónica demostramos la presencia de uniones gap en el lugar de la lesión y el implante. Observamos estas uniones gap entre CPNs implantadas, entre CPNs implantadasy astrocitos y entre CPNs implantadas y microglía (Figura 8 del artículo).

3.- Resultados referentes al artículo

Neural Progenitor Cells Isolated from the Subventricular Zone Present Hemichannel Activity and Form Functional Gap Junctions with Glial Cells. 2015. Frontiers Cellular Neuroscience. En revisión.

El objetivo fue estudiar si las uniones gap que ya habíamos obsevado entre CPNs implantadas y glía sdel cerebro hospedador podían ser funcionales.

Para ello realizamos un estudio *in vitro* con cocultivos de CPNs en forma de neuroesferas y cultivos primarios de o con cultivos primarios de microglía. En primer lugar mediante la técnica de PCR cualitativa demostramos que las CPNs de la ZSV cultivadas en forma de neuroesferas presentan ARNm de las proteínas formadoras de hemicanales y uniones gap Cx26, Cx43, Cx45 y Panx1 (Figura 1 del artículo).

Mediante técnicas de acoplamiento de colorante demostramos que las CPNs en cultivo forman uniones gap funcionales entre ellas (Figura2 del artículo). Así, cuando se inyectaba el colorante hidrofílico Lucifer Yellow en una célula de la neuroesfera, éste se transfería a 1-4 células adyacentes. Esta trasferencia de colorante se veía impedida cuando se añadía al cultivo octanol, un bloqueante de las uniones gap.

Mediante técnicas de captación de colorante demostramos que las CPNs cultivadas como neuroesferas tienen además hemicanales funcionales formados por Cxs y que estos hemicanales pierden su funcionalidad cuando las CPNs de las neuroesferas comienzan a adherirse a un sustrato (Figuras 3 y 4 del artículo)

En los cocultivos de CPNs con astrocitos demostramos por la técnica de acoplamiento de colorante que las CPNs forman uniones gap funcionales con astrocitos (Figura 5 del artículo). La trasferencia de colorante desde CPNs a astrocitos también se inhibía al añadir octanol al medio de cultivo.

Por último, también demostramos trasferencia de Lucifer Yellow desde CPNs a células de microglía en cocultivos de ambos tipos celulares, aunque en estos casos el índice de acoplamiento (número de células a las que se trasfiere el colorante inyectado en una célula) fue significativamente menor que el de las CPNs y astrocitos (Figura 6 del artículo).

DISCUSIÓN

1.- Las células progenitoras neurales modulan la expresión de VEGF y BDNF en las neuronas axotomizadas

Al producirse una lesión por axotomía de las neuronas internucleares del NMOE, éstas quedan desconectadas de su diana natural, lo que produce una disminución de su frecuencia de disparo y la retirada de las aferencias sinápticas (de la Cruz et al. 2000; Pastor et al. 2000). El implante de CPNs provenientes de la ZSV en la zona seccionada, produjo una recuperación de las propiedades de disparo de las neuronas axotomizadas y de las aferencias sinápticas inhibidoras (Morado-Díaz et al., 2014). Numerosos trabajos han demostrado que las CPNs que se implantan tras una lesión son capaces de inducir cambios en la expresión de proteínas en las células lesionadas que podrían ser determinantes para su recuperación (Imitola et al., 2004; Capone et al., 2007; Madhavan et al., 2008). Uno de nuestros objetivos fue el de analizar si el contenido en factores neurotróficos de las neuronas axotomizadas se modificaba en animales que recibían implante de CPNs, ya que esto podría intervenir en la recuperación del patrón de disparo de estas neuronas y en el mantenimiento de las aferencias sinápticas inhibidoras.

Los resultados en la situación control, es decir en animales sin axotomía ni implante, demostraron que los somas de las neuronas internucleares del NMOE tenían una intensa inmunorreactividad tanto para VEGF como BDNF, mientras que para NGF y NT-3 la inmunorreactividad fue débil. Estas diferencias en el nivel de expresión sugieren un papel relevante del VEGF y del BDNF en el mantenimiento funcional de estas células.

Tras la axotomía, la inmunorreactividad al VEGF de las neuronas internucleares del NMOE se mantuvo igual que neuronas no lesionadas. Sin embargo, el contenido en VEGF aumentó significativamente en estas neuronas en animales que recibieron implantes de CPNs tras la lesión. Existen dos posibles explicaciones para este hallazgo. El VEGF podría ser captado por los axones lesionados y ser transportado retrógradamente hacia el soma o bien las neuronas lesionadas podrían haber aumentado la expresión de este factor como consecuencia de interacciones celulares en la zona del implante. Las neuronas internucleares del NMOE en el gato tienen el

receptor para VEGF Flk-1 (Morado-Díaz et al., 2014) lo que posibilita que puedan estar captando VEGF del ambiente extracelular y desde la zona del implante. No obstante, en el sitio de la lesión también hay astrocitos que son inmunopositivos a VEGF, de manera que si el VEGF les estuviese llegando a las células lesionadas por vía paracrina, en la situación de lesión también observaríamos un aumento en la expresión de VEGF, y éste no es el caso. Por lo que parece más factible que las células lesionadas aumenten su expresión de este factor como consecuencia de las interacciones celulares que tienen lugar en la zona de la lesión y el implante. Aunque no se puede descartar que las células capten el VEGF del medio. En cualquier caso, las neuronas lesionadas pueden beneficiarse del incremento de producción de este factor ya que se le conocen numerosas acciones neuroprotectoras (Azzouz et al. 2004; McCloskey et al. 2005; Wang et al. 2007 Nicoletti et al. 2008).

La axotomía produjo un aumento de la inmunorreactividad a BDNF y NT-3 en las neuronas lesionadas. Previamente se había demostrado que las neuronas internucleares del NMOE tienen receptores de BDNF y NT-3, TrkB y TrkC respectivamente (Benítez-Temiño et al., 2004). Por tanto, el aumento de la expresión de BDNF y NT-3 en las neuronas axotomizadas podría estar compensando la falta de soporte trófico a través de vías paracrinas y autocrinas (Venero et al., 2000; Lee et al., 2001). Sin embargo, tras el implante de CPNs la expresión de BDNF en los somas de las neuronas internucleares del NMOE disminuyó hasta valores similares a la situación control. Probablemente en el microambiente creado por el implante en el lugar de la lesión se estén liberando otras moléculas que sustituyan la dependencia trófica de estas neuronas al BDNF y en consecuencia se produzca una disminución de la expresión de este factor. Este no es el caso del NT-3, ya que su inmunorreactividad aumentó tanto en la lesión como tras el implante.

Es importante destacar que las motoneuronas del NMOE, que están entremezcladas con las interneuronas, no mostraron ningún cambio en la inmunorreactividad del VEGF ni del BDNF demostrándose así que los cambios observados en el contenido de estos factores neurotróficos tras el implante fueron exclusivos de la población de neuronas axotomizadas.

En conjunto, estos datos sugieren que el aumento en los niveles de VEGF de las neuronas lesionadas parece estar relacionado con la presencia del implante y que la dependencia trófica del BDNF que muestran las neuronas lesionadas desaparece también como consecuencia del implante.

2.- Las células progenitoras neurales implantadas expresan VEGF

Las CPNs podrían constituir una nueva fuente de factores tróficos para las neuronas axotomizadas. De hecho, las CPNs de la ZSV expresan VEGF en su nicho neurogénico y cuando son cultivadas en forma de neuroesferas (Tonchev et al., 2007; Pluchino et al., 2010). Quisimos averiguar por tanto si las células implantadas continuaban expresando VEGF o algún otro factor neurotrófico tras el implante en nuestro modelo de lesión por axotomía del FLM. Los resultados demostraron que el 25% de las CPNs eran inmunorreactivas para VEGF, pero no para BDNF, NT-3 ni NGF.

En resumen, en esta tesis demostramos que las CPN implantadas en el cerebro lesionado expresan VEGF dos meses después del implante y además son capaces de modular la expresión de VEGF y BDNF en las neuronas lesionadas. Nuestra hipótesis de trabajo es que el aumento del contenido en VEGF promovido por las CPNs en las neuronas lesionadas podría estar involucrado en los efectos beneficiosos de los implantes.

3.- El implante de células precursoras neurales modula la reacción glial en el sitio de lesión

Al producirse una lesión por axotomía se induce una fuerte reacción glial en la que intervienen astrocitos, que se activan y regulan a la alta la expresión de la proteína GFAP, y la proliferación de glía positiva a NG-2, y células microgliales, que adquieren morfología ameboide y actividad fagocítica, liberando citoquinas inflamatorias (Aldskogius and Kozlova, 1998).

La reacción glial a la axotomía del FLM ha sido caracterizada con anterioridad (Pastor et al., 2000). En este trabajo quisimos averiguar si ésta se veía modificada por el implante de CPNs. Hemos demostrado que en animales implantados se mantiene el aumento de la inmunorreactividad a GFAP que se induce por la lesión pero aumenta

significativamente la inmunorreactividad a OX-6, marcador de microglía reactiva. Por lo tanto, la presencia de CPNs en el tejido hospedador induce una alteración en la respuesta microglial a la lesión. Mosher y colaboradores describieron que 24 horas después del implante de CPNs en el cuerpo estriado de rata, tanto el número total de células de microglía como las que presentaban morfología activada fue significativamente mayor en el lugar del implante en comparación con los animales que recibieron solamente inyecciones del vehículo (Mosher et al., 2012). Nosotros hemos analizado la población microglial activada mediante marcadores inmunocitoquímicos (OX-6) en un período de tiempo mucho más largo (dos meses), observando una diferencia considerable en la activación microglial entre animales con lesión y animales con lesión e implante. Por tanto, hemos demostrado que las CPNs son capaces de regular la activación microglial después de una lesión cerebral y que este efecto se mantiene en el tiempo.

4.-Las CPNs implantadas se localizan muy próximas a células gliales activadas del hospedador

El análisis con microscopía confocal reveló una estrecha asociación entre las CPNs implantadas y células microgliales activadas en el lugar de la lesión. Observamos contactos muy cercanos entre prolongaciones de las CPNs y células de microglía y cómo los procesos de las CPNs ocasionalmente envolvían a las células de microglía. Esta relación anatómica nos sugería una posible comunicación entre ambos tipos celulares de forma directa a través de uniones de membrana tipo gap, o indirecta, y paracrina liberando factores difusibles al medio. Mosher y colaboradores demostraron que las CPNs que se implantan en cerebro lesionado liberan VEGF y que a su vez este VEGF está implicado en la regulación de la microglía del tejido hospedador (Mosher et al., 2012). Como se ha mencionado anteriormente, hemos demostrado que las CPNs provenientes de la ZSV implantadas en el FLM lesionado de ratas son inmunorreactivas a VEGF lo que sugiere la posibilidad de que este VEGF podría participar en la respuesta microglial tras el implante. Otros autores también han descrito la importancia de la interacción de las CPNs implantadas con las células de microglía en la recuperación funcional ante una lesión de la médula espinal (Pluchino y Martino, 2005; Ziv et al., 2006).

También observamos el contacto próximo entre CPNs implantadas y astrocitos del hospedador. El análisis a nivel ultraestructural nos confirmó la existencia de contactos directos entre CPNs implantadas con astrocitos y tambien en menor medida con microglía hospedadora, lo que nos llevó a interesarnos por la posibilidad de comunicación citoplásmica a través de uniones gap entre las CPNs con la glía del cerebro que recibe los implantes.

5.- Las CPNs implantadas y las células gliales del hospedador expresan Cx43

Hemos demostrado que las CPNs cultivadas en forma de neuroesferas provenientes de la ZSV son inmunorreactivas para Cx43. Estos datos concuerdan con estudios anteriores que mostraban expresión de esta conexina en células indiferenciadas provenientes de neuroesferas obtenidas de la ZSV embrionaria de ratón (Duval et al., 2002) lo que sugiere un papel activo de esta conexina en la proliferación y diferenciación de las CPNs. Cuando analizamos la expresión de Cx43 en las CPNs dos meses después de su implante en el cerebro lesionado, observamos que la mayor parte de las células implantadas (identificadas por su expresión de GFP) fueron inmunorreactivas para Cx43 y que además permanecían en un estado indiferenciado. Otros autores ya habían demostrado que cuando se implantan CPNs en el cerebro inflamado, se establece una comunicación entre las CPNs implantadas y las células inmunes tal que mantiene a las CPNs en un estado indiferenciado (Pluchino et al., 2005). En este estado, las CPNs poseen propiedades neuroprotectoras a través de mecanismos inmunomoduladores (Pluchino et al., 2005; Ziv et al., 2006). Por lo tanto, es posible que la respuesta inflamatoria asociada a la lesión por axotomía mantenga a las CPNs empleadas en nuestro estudio en un estado indiferenciado en el que siguen expresando Cx43 y en el que pudieran relacionarse mediante uniones gap entre ellas y/o con las células del hospedador.

Los astrocitos del hospedador en el lugar de la lesión fueron inmunopositivos a Cx43. Además, se observó inmunorreactividad a Cx43 en la interfase entre prolongaciones de las CPNs implantadas y procesos astrocíticos, datos que fueron corroborados a nivel ultraestructural. Estos resultados indican que las CPNs se pueden comunicar con los astrocitos del hospedador a través de uniones gap.

Con respecto a la microglía, nuestros datos muestran presencia de proteína Cx43 en algunas células microgliales reactivas del lugar de la lesión. Eugenín y colaboradores previamente demostraron *in vivo* que, en condiciones de reposo, la mayoría de las células de microglía no expresa Cx43 pero sí lo hacen tras una lesión mecánica (Eugenín et al. 2001). Como ocurrió con los astrocitos, también identificamos elementos inmunorreactivos a Cx43 localizados entre procesos de CPNs y ramificaciones microgliales indicando, por tanto, la posibilidad de formación de uniones gap entre ambas.

6.- Las CPNs implantadas establecen uniones gap con la glía del hospedador

En el análisis ultraestructural del tejido de animales con implantes de CPNs hemos demostrado la presencia de uniones gap entre CPNs implantadas, y también entre CPNs y astrocitos y microglía del hospedador. En 2010, Jäderstad y colaboradores mostraron que el acoplamiento a través de uniones gap entre CPNs implantadas y neuronas del tejido hospedador era esencial para la supervivencia y las acciones protectoras atribuidas a las células implantadas (Jäderstad et al., 2010). Las CPNs fueron implantadas en modelos mutantes de ratón en los que degeneraban las neuronas de Purkinje y demostraron que el acoplamiento celular temprano a través de uniones gap entre CPNs y neuronas de Purkinje del hospedador era esencial para rescatar a estas neuronas de la degeneración. En nuestro estudio, sin embargo, el modelo de lesión fue diferente y la evaluación de la presencia de uniones intercelulares se llevó a cabo mediante un estudio ultraestructural y dos meses después de la lesión.

Este es el primer estudio que demuestra la posibilidad de comunicación a través de uniones gap entre CPNs implantadas y la microglía activada del hospedador en vivo, en animales adultos, y después de un largo tiempo de una lesión. Por lo tanto, se sugiere que entre las CPNs implantadas y la glía hospedadora se puede establecer una comunicación de tipo paracrino pero también una comunicación directa mediante uniones gap, a través de las cuales pueden compartir pequeñas moléculas, iones o algunos metabolitos con un papel esencial en la neutralización de los procesos

patológicos, en la prevención de la muerte celular, o en el restablecimiento de funciones alteradas por la lesión.

7.- Las CPNs de las neuroesferas se comunican mediante uniones gap y hemicanales

Hemos demostrado que las CPNs de la ZSV, cultivadas como neuroesferas, expresan el ARNm de las conexinas Cx26, Cx43 y Cx45 y de la panexina Panx1. Estudios previos han descrito que estas proteínas intervienen en la proliferación de las CPNs. Por ejemplo, la Cx45 modula la proliferación celular en la ZSV (Khodosevich et al., 2012). Panx1, expresada por CPNs en la ZSV, regula también la proliferación de las CPNs a través de la liberación de ATP (Wicki-Stordeur et al., 2012). La expresión de Cx43 en CPNs de tejido embrionario de ratón está involucrada en el mantenimiento de las CPNs en un estado indiferenciado y proliferativo (Cheng et al., 2004; Lemcke y Kuznetsov, 2013). Por tanto, todos los datos publicados hasta el momento sugieren un papel determinante de la comunicación a través de uniones gap o a través de hemicanales en la proliferación de las CPNs.

En este estudio, hemos demostrado que las CPNs de neuroesferas obtenidas de la ZSV forman uniones gap funcionales entre ellas. Los experimentos de acoplamiento de colorante en estos cultivos de neuroesferas revelaron una incidencia de acoplamiento del 100%, es decir, la inyección de colorante en una célula siempre produjo la trasferencia del mismo a células vecinas. Este acoplamiento se inhibió con octanol, un bloqueante específico de uniones gap (D'hondt et al., 2009), lo que indica que el acoplamiento se realizó a través de uniones gap.

La comunicación autocrina/paracrina vía hemicanales también podría tener lugar en neuroesferas obtenidas de la ZSV, ya que expresan diferentes conexinas así como Panx1. Empleando la técnica de captación de colorante hemos demostrado que las células de neuroesferas no disgregadas presentan hemicanales funcionales, que se bloquearon con La^{3+}, un inhibidor específico de hemicanales de Cxs (Pelegrin y Surprenant, 2006). Curiosamente, observamos que la actividad de los hemicanales cesaba cuando las neuroesferas comenzaban a adherirse a un sustrato, una condición que inicia la diferenciación celular hacia fenotipos neurales. Estos resultados sugieren que la señalización a través hemicanales podría intervenir en el mantenimiento de las

CPNs en un estado indiferenciado y proliferativo, estado en el que se encuentran las CPNs al implantarlas en el FLM lesionado.

8.- Las CPNs de la ZSV forman uniones gap funcionales con astrocitos y microglía *in vitro*

Ya se ha mencionado que las CPNs obtenidas de la ZSV forman uniones gap con células gliales del hospedador cuando se implantan tras una lesión. Para averiguar si las uniones gap que se forman entre ambos tipos de células son funcionales, realizamos experimentos de acoplamiento de colorante en cocultivos de CPNs de la ZSV cultivadas en forma de neuroesferas y cultivos primarios de astrocitos o de microglía.

Con respecto a los cocultivos de CPNs con astrocitos, se observó que las células derivadas de las neuroesferas formaron uniones gap funcionales con ellos, con una incidencia del 90% de acoplamiento. En la ZSV, las CPNs establecen redes de comunicación a través de uniones gap con astrocitos (Benjamin Lacar et al., 2011), por lo que no es de extrañar que la capacidad de formar uniones gap entre estos dos tipos celulares se mantenga *in vitro*. Por tanto, es posible que las uniones gap formadas entre CPNs y astrocitos en la zona de la lesión y el implante puedan ser funcionales e intervengan en la integración de las CPNs y en los efectos beneficiosos del implante, aunque se precisan estudios adicionales para determinar esta funcionalidad.

Experimentos *in vitro* anteriores a este estudio habían demostrado la comunicación a través de uniones gap entre células de microglía y entre microglía y neuronas Así, dos grupos independientes demostraron que las células de microglía pueden formar uniones gap entre ellas cuando se inician procesos inflamatorios (Eugenín et al., 2001; Garg et al., 2005). También Dobrenis y colaboradores describieron en cocultivos que las células de microglía eran capaces de establecer uniones gap con neuronas (Dobrenis et al. 2006). Sin embargo, en un estudio reciente realizado *in vivo* tanto en animales sanos, como en condiciones patológicas, no se observó transferencia de colorante entre las células microgliales o entre células de microglía y neuronas (Wasseff and Scherer, 2014). En este trabajo sin embargo, sí hemos demostrado a nivel ultraestructural que las CPNs implantadas pueden formar uniones gap con la microglía que se activa tras la lesión.

En base a esto el siguiente objetivo planteado fue demostrar si las uniones gap entre CPNs y microglía podían ser funcionales. Para ello, realizamos experimentos de acoplamiento de colorante en cocultivos de CPNs y cultivos primarios de microglía. Las CPNs se acoplan con células de microglía con una incidencia de acoplamiento del 72%, y de nuevo, la trasferencia de colorante entre los dos tipos de células tuvo lugar mediante uniones gap, ya que el octanol inhibió por completo la trasferencia del colorante hacia las células de microglía. En el cerebro sano, existe proximidad física entre las CPNs de los nichos neurogénicos y las células de microglía (Goings et al., 2006; Gonzalez-Perez et al., 2012; Mosher et al., 2012). De hecho, la microglía y las CPNs de la ZSV establecen una comunicación bilateral que puede afectar al estado de activación microglial y a la proliferación y diferenciación de las CPNs (Mathieu et al., 2010; Gonzalez-Perez et al., 2012; Mosher et al., 2012; Shigemoto-Mogami et al., 2014). En condiciones patológicas, la respuesta inflamatoria que se produce por células microgliales del hospedador mantiene a las CPNs implantadas en un estado indiferenciado, en el que pueden promover la reparación del tejido dañado mediante la secreción de moléculas inmunomoduladoras y neuroprotectoras (Martino and Pluchino, 2006). Por lo tanto, pensamos que la comunicación directa a través de uniones gap entre CPNs y células microgliales en el tejido lesionado también podría intervenir en los mecanismos de recuperación inducidos por el implante, aunque de nuevo, se necesitan experimentos adicionales para confirmar esta hipótesis.

Este es el primer estudio que demuestra que las CPNs de la ZSV cultivadas como neuroesferas presentan hemicanales funcionales y uniones gap entre ellas. Además, es la primera vez que se demuestra también que las CPNs provenientes de las neuroesferas pueden establecer uniones gap funcionales con astrocitos y con microglía. La comunicación a través de uniones gap entre CPNs y células gliales podría estar involucrada en la proliferación y diferenciación de las CPNs, tanto en su nicho neurogénico como después del implante en el cerebro lesionado.

CONCLUSIONES

1.- El implante de CPNs tras la axotomía del FLM produce un aumento de la expression de VEGF en las células lesionadas.

2.- Las CPNs de la ZSV implantadas en el FLM lesionado expresan VEGF a largo plazo (dos meses) después de la lesion y el implante.

3.- El implante de CPNs en el FLM lesionado produce un aumento de la densidad de microglía activada en el sitio de lesión. Sin embargo no se ha observado que el implante modifique la densidad de astrocitos ni de glía positiva a NG2.

4.- Existen contactos directos entre las CPNs implantadas tras la axotomía y astrocitos y microglías reactivas del tejido hospedador. Además se observa localización de Cx43 entre procesos de células progenitoras y de células gliales (astrocitos o microglía) del tejido hospedador en el sitio de la lesión.

5.- Las CPNs implantadas forman uniones gap con astrocitos y células de microglía en el sitio de la lesión.

6.- Las CPNs de la ZSV cultivadas como neuroesferas establecen uniones gap funcionales entre ellas. Además muestran comunicación a través de hemicanales formados por conexinas.

7.-Las CPNs de la ZSV forman uniones gap funcionales con astrocitos y con microglía en cultivos conjuntos de estos tipos celulares

Tesis: Se propone que las interacciones celulares, paracrinas o directas, que ocurren en el sitio de la lesión e implante son determinantes para los efectos neuroprotectores de las CPNs implantadas y para su integración en el cerebro hospedador.

BIBLIOGRAFÍA

Aarum J, Sandberg K, Haeberlein SLB, Persson M a a. 2003. Migration and differentiation of neural precursor cells can be directed by microglia. Proc Natl Acad Sci U S A 100:15983–8.

Altman J, Das GD. 1965. Post-natal origin of microneurones in the rat brain. Nature 207:953–6.

Alvarez-Buylla a., Theelen M, Nottebohm F. 1990. Proliferation “hot spots” in adult avian ventricular zone reveal radial cell division. Neuron 5:101–109.

Alvarez-Buylla A, García-Verdugo JM. 2002. Neurogenesis in adult subventricular zone. J Neurosci 22:629–634.

Arévalo JC, Wu SH. 2006. Neurotrophin signaling: Many exciting surprises! Cell Mol Life Sci 63:1523–1537.

Azzouz M, Ralph GS, Storkebaum E, Walmsley LE, Mitrophanous K a, Kingsman SM, Carmeliet P, Mazarakis ND. 2004. VEGF delivery with retrogradely transported lentivector prolongs survival in a mouse ALS model. Nature 429:413–417.

Barbacid M. 1995. Structural and functional properties of the TRK family of neurotrophin receptors. Ann N Y Acad Sci 766:442–58.

Bath KG, Lee FS. 2010. Neurotrophic Factor Control of Adult SVZ Neurogenesis Kevin. 70:339–349.

Belachew S, Chittajallu R, Aguirre A a., Yuan X, Kirby M, Anderson S, Gallo V. 2003. Postnatal NG2 proteoglycan-expressing progenitor cells are intrinsically multipotent and generate functional neurons. J Cell Biol 161:169–186.

Benítez-Temiño B, De La Cruz RR, Pastor a. M. 2003. Grafting of a new target prevents synapse loss in abducens internuclear neurons induced by axotomy. Neuroscience 118:611–626.

Bergles DE, Roberts JD, Somogyi P, Jahr CE. 2000. Glutamatergic synapses on oligodendrocyte precursor cells in the hippocampus. Nature 405:187–191.

Bozoyan L, Khlghatyan J, Saghatelyan a. 2012. Astrocytes Control the Development of the Migration-Promoting Vasculature Scaffold in the Postnatal Brain via VEGF Signaling. J Neurosci 32:1687–1704.

Bruzzone R, Hormuzdi SG, Barbe MT, Herb A, Monyer H. 2003. Pannexins, a family of gap junction proteins expressed in brain. Proc Natl Acad Sci U S A 100:13644–13649.

Butt AM, Duncan A, Hornby MF, Kirvell SL, Hunter A, Levine JM, Berry M. 1999. Cells expressing the NG2 antigen contact nodes of ranvier in adult CNS white matter. Glia 26:84–91.

Butt AM, Hamilton N, Hubbard P, Pugh M, Ibrahim M. 2005. Synantocytes: The fifth element. J Anat 207:695–706.

Calvo C-F, Fontaine RH, Soueid J, Tammela T, Makinen T, Alfaro-Cervello C, Bonnaud F, Miguez A, Benhaim L, Xu Y, Barallobre M-J, Moutkine I, Lyytikkä J, Tatlisumak T, Pytowski B, Zalc B, Richardson W, Kessaris N, Garcia-Verdugo JM, Alitalo K, Eichmann A, Thomas J-L. 2011. Vascular endothelial growth factor receptor 3 directly regulates murine neurogenesis. Genes Dev 25:831–44.

Chao M V. 2003. Neurotrophins and their receptors: a convergence point for many signalling pathways. Nat Rev Neurosci 4:299–309.

Contreras JE, Sánchez HA, Véliz LP, Bukauskas FF, Bennett MVL, Sáez JC. 2004. Role of connexin-based gap junction channels and hemichannels in ischemia-induced cell death in nervous tissue. Brain Res Brain Res Rev 47:290–303.

Crouch EE, Liu C, Silva-Vargas V, Doetsch F. 2015. Regional and Stage-Specific Effects of Prospectively Purified Vascular Cells on the Adult V-SVZ Neural Stem Cell Lineage. J Neurosci 35:4528–4539.

Cummings BJ, Uchida N, T SJ, S DL, H M, S R, G FH, A AJ. 2005. Human neural stem cells differentiate and promote locomotor recovery in spinal cord-injured mice. Proc Natl Acad Sci U S A 102:14069–14074.

Cusimano M, Biziato D, Brambilla E, Doneg M, Alfaro-Cervello C, Snider S, Salani G, Pucci F, Comi G, Garcia-Verdugo JM, De Palma M, Martino G, Pluchino S. 2012. Transplanted neural stem/precursor cells instruct phagocytes and reduce secondary tissue damage in the injured spinal cord. Brain 135:447–460.

Davies a M, Thoenen H, Barde Y a. 1986. The response of chick sensory neurons to brain-derived neurotrophic factor. J Neurosci 6:1897–1904.

Davis-López de Carrizosa M a, Morado-Díaz CJ, Morcuende S, de la Cruz RR, Pastor AM. 2010. Nerve growth factor regulates the firing patterns and synaptic composition of motoneurons. J Neurosci 30:8308–8319.

Davis-López de Carrizosa M a, Morado-Díaz CJ, Tena JJ, Benítez-Temiño B, Pecero ML, Morcuende SR, de la Cruz RR, Pastor AM. 2009. Complementary actions of BDNF and neurotrophin-3 on the firing patterns and synaptic composition of motoneurons. J Neurosci 29:575–587.

Dechant G, Rodríguez-Tébar a, Kolbeck R, Barde Y a. 1993. Specific high-affinity receptors for neurotrophin-3 on sympathetic neurons. J Neurosci 13:2610–2616.

Delgado-Garcia JM, del Pozo F, Baker R. 1986a. Behavior of neurons in the abducens nucleus of the alert cat--I. Motoneurons. Neuroscience 17:929–52.

Delgado-Garcia JM, del Pozo F, Baker R. 1986b. Behavior of neurons in the abducens nucleus of the alert cat--II. Internuclear neurons. Neuroscience 17:953–73.

Dimou L, Götz M. 2014. Glial Cells as Progenitors and Stem Cells: New Roles in the Healthy and Diseased Brain. Physiol Rev 94:709–737.

Doetsch F, Alvarez-Buylla a. 1996. Network of tangential pathways for neuronal migration in adult mammalian brain. Proc Natl Acad Sci U S A 93:14895–14900.

Doetsch F, Caillé I, Lim D a, García-Verdugo JM, Alvarez-Buylla A. 1999. Subventricular zone astrocytes are neural stem cells in the adult mammalian brain. Cell 97:703–16.

Doetsch F, García-Verdugo JM, Alvarez-Buylla a. 1997. Cellular composition and three-dimensional organization of the subventricular germinal zone in the adult mammalian brain. J Neurosci 17:5046–5061.

Doetsch F, Petreanu L, Caille I, Garcia-Verdugo JM, Alvarez-Buylla A. 2002. EGF converts transit-amplifying neurogenic precursors in the adult brain into multipotent stem cells. Neuron 36:1021–1034.

Eriksson PS, Perfilieva E, Björk-Eriksson T, Alborn a M, Nordborg C, Peterson D a, Gage FH. 1998. Neurogenesis in the adult human hippocampus. Nat Med 4:1313–1317.

Ernfors P, Lee KF, Kucera J, Jaenisch R. 1994. Lack of neurotrophin-3 leads to deficiencies in the peripheral nervous system and loss of limb proprioceptive afferents. Cell 77:503–512.

Eugenín E a, Eckardt D, Theis M, Willecke K, Bennett MVL, Sáez JC. 2001. Microglia at brain stab wounds express connexin 43 and in vitro form functional gap junctions after treatment with interferon-γ and tumor necrosis factor. Proc Natl Acad Sci U S A 98:4190–4195.

Falkenberg T, Ernfors P, Persson H, Lindefors N. 1992. Cortical transynaptic activation of tyrosine kinase receptor trkB messenger RNA expression in rat hippocampus. Neuroscience 51:883–889.

Ferrara N, Gerber H-P, LeCouter J. 2003. The biology of VEGF and its receptors. Nat Med 9:669–676.

Ferrara N, Henzel WJ. 2012. Pituitary follicular cells secrete a novel heparin-binding growth factor specific for vascular endothelial cells. 1989. Biochem Biophys Res Commun 425:540–7.

García-Verdugo JM, Doetsch F, Wichterle H, Lim D a., Alvarez-Buylla A. 1998. Architecture and cell types of the adult subventricular zone: In search of the stem cells. J Neurobiol 36:234–248.

Garg S, Md Syed M, Kielian T. 2005. Staphylococcus aureus-derived peptidoglycan induces Cx43 expression and functional gap junction intercellular communication in microglia. J Neurochem 95:475–83.

Ghashghaei HT, Lai C, Anton ES. 2007. Neuronal migration in the adult brain: are we there yet? Nat Rev Neurosci 8:141–151.

Giaume C, Leybaert L, Naus CC, Sáez JC. 2013. Connexin and pannexin hemichannels in brain glial cells: Properties, pharmacology, and roles. Front Pharmacol 4:1–17.

Goings E.G, Kozlowski DA, Szele FG. 2006. Differential Activation of Microglia in Neurogenic VersusNon-neurogenic Regions of the Forebrain. Glia 54:329–342.

Goldmann T, Prinz M. 2013. Role of Microglia in CNS Autoimmunity 1. Clin Dev Immunol Volume 2013, Article ID 208093.

Han X, Chen M, Wang F, Windrem M, Wang S, Shanz S, Xu Q, Oberheim NA, Bekar L, Betstadt S, Silva AJ, Takano T, Goldman S a., Nedergaard M. 2013. Forebrain engraftment by human glial progenitor cells enhances synaptic plasticity and learning in adult mice. Cell Stem Cell 12:342–353.

Hayashida K-I, Clayton BA, Johnson JE, Eisenach JC. 2008. Brain derived nerve growth factor induces spinal noradrenergic fiber sprouting and enhances clonidine analgesia following nerve injury in rats. Pain 136:348–55.

Hempstead BL, Salzer JL. 2002. Neurobiology. A glial spin on neurotrophins. Science 298:1184–6.

Jabs R, Pivneva T, Hüttmann K, Wyczynski A, Nolte C, Kettenmann H, Steinhäuser C. 2005. Synaptic transmission onto hippocampal glial cells with hGFAP promoter activity. J Cell Sci 118:3791–3803.

Jalife J, Morley GE, Vaidya D. 1999. Connexins and impulse propagation in the mouse heart. J Cardiovasc Electrophysiol 10:1649–63.

Kaplan MR, Cho MH, Ullian EM, Isom LL, Levinson SR, Barres B a. 2001. Differential control of clustering of the sodium channels Nav1.2 and Nav1.6 at developing CNS nodes of Ranvier. Neuron 30:105–119.

Káradóttir R, Hamilton NB, Bakiri Y, Attwell D. 2008. Spiking and nonspiking classes of oligodendrocyte precursor glia in CNS white matter. Nat Neurosci 11:450–456.

Kettenmann H, Verkhratsky A. 2011. [Neuroglia--living nerve glue]. Fortschr Neurol Psychiatr 79:588–97.

Khodosevich K, Zuccotti A, Kreuzberg MM, Le Magueresse C, Frank M, Willecke K, Monyer H. 2012. Connexin45 modulates the proliferation of transit-amplifying precursor cells in the mouse subventricular zone. Proc Natl Acad Sci U S A 109:20107–12.

Kirschenbaum B, Goldman S a. 1995. Brain-derived neurotrophic factor promotes the survival of neurons arising from the adult rat forebrain subependymal zone. Proc Natl Acad Sci U S A 92:210–214.

Kolb B, Cote S, Ribeiro-Da-Silva a., Cuello a. C. 1997. Nerve growth factor treatment prevents dendritic atrophy and promotes recovery of function after cortical injury. Neuroscience 76:1139–1151.

Kornack DR, Rakic P. 2001. Cell proliferation without neurogenesis in adult primate neocortex. Science 294:2127–2130.

Kukley M, Capetillo-Zarate E, Dietrich D. 2007. Vesicular glutamate release from axons in white matter. Nat Neurosci 10:311–320.

de La Cruz RR, Delgado-García JM, Pastor ÁM. 2000. Discharge characteristics of axotomized abducens internuclear neurons in the adult cat. J Comp Neurol 427:391–404.

Lambrechts D, Storkebaum E, Morimoto M, Del-Favero J, Desmet F, Marklund SL, Wyns S, Thijs V, Andersson J, van Marion I, Al-Chalabi A, Bornes S, Musson R, Hansen V, Beckman L, Adolfsson R, Pall HS, Prats H, Vermeire S, Rutgeerts P, Katayama S, Awata T, Leigh N, Lang-Lazdunski L, Dewerchin M, Shaw C, Moons L, Vlietinck R, Morrison KE, Robberecht W, Van Broeckhoven C, Collen D, Andersen PM, Carmeliet P. 2003. VEGF is a modifier of amyotrophic lateral sclerosis in mice and humans and protects motoneurons against ischemic death. Nat Genet 34:383–394.

Levi-Montalcini R. 1982. Developmental neurobiology and the natural history of nerve growth factor. Annu Rev Neurosci 5:341–62.

Lewin GR, Carter BD. 2014. Neurotrophic factors. Preface. Handb Exp Pharmacol 220:v–vi.

Lim D a, Alvarez-buylla A. 2014. Adult neural stem cells stake their ground. Trends Neurosci 37:563–571.

Lim D a., Tramontin AD, Trevejo JM, Herrera DG, García-Verdugo JM, Alvarez-Buylla A. 2000. Noggin antagonizes BMP signaling to create a niche for adult neurogenesis. Neuron 28:713–726.

Lin S, Bergles DE. 2004. Synaptic signaling between GABAergic interneurons and oligodendrocyte precursor cells in the hippocampus. Nat Neurosci 7:24–32.

Lin SC, Huck JHJ, Roberts JDB, Macklin WB, Somogyi P, Bergles DE. 2005. Climbing fiber innervation of NG2-expressing glia in the mammalian cerebellum. Neuron 46:773–785.

Lois C, García-Verdugo JM, Alvarez-Buylla A. 1996. Chain migration of neuronal precursors. Science 271:978–81.

Luskin MB. 1993. Restricted proliferation and migration of postnatally generated neurons derived from the forebrain subventricular zone. Neuron 11:173–189.

Maisonpierre PC, Belluscio L, Friedman B, Alderson RF, Wiegand SJ, Furth ME, Lindsay RM, Yancopoulos GD. 1990. NT-3, BDNF, and NGF in the developing rat nervous system: parallel as well as reciprocal patterns of expression. Neuron 5:501–509.

Martino G, Martino G, Pluchino S, Pluchino S. 2006. The therapeutic potential of neural stem cells. Nat Rev Neurosci 7:395–406.

Mathieu P, Battista D, Depino A, Roca V, Graciarena M, Pitossi F. 2010. The more you have, the less you get: the functional role of inflammation on neuronal differentiation of endogenous and transplanted neural stem cells in the adult brain. J Neurochem 112:1368–85.

McCloskey, D. P., Croll, S. D., and Scharfman, H. E. (2005). Depression of synaptic transmission by vascular endothelial growth factor in adult rat hippocampus and evidence for increased efficacy after chronic seizures. *J. Neurosci.* 25:8889–97.

McCloskey DP, Hintz TM, Scharfman HE. 2008. Modulation of vascular endothelial growth factor (VEGF) expression in motor neurons and its electrophysiological effects. Brain Res Bull 76:36–44.

Menezes JR, Fróes MM, Moura Neto V, Lent R. 2000. Gap junction-mediated coupling in the postnatal anterior subventricular zone. Dev Neurosci 22:34–43.

Merkle FT, Tramontin AD, García-Verdugo JM, Alvarez-Buylla A. 2004. Radial glia give rise to adult neural stem cells in the subventricular zone. Proc Natl Acad Sci U S A 101:17528–17532.

Ming G, Song H. 2011. Adult Neurogenesis in the Mammalian Brain: Significant Answers and Significant Questions. Analysis 70:687–702.

Mirzadeh Z, Han Y, Soriano-navarro M, García- JM, Alvarez-buylla A. 2010. NIH Public Access. 30:2600–2610.

Mirzadeh Z, Merkle FT, Soriano-navarro M, García- JM, Alvarez-buylla A. 2009. NIH Public Access. 3:265–278.

Miyazaki S. 1985. Location of motoneurons in the oculomotor nucleus and the course of their axons in the oculomotor nerve. Brain Res 348:57–63.

Morado-Díaz CJ, Matarredona ER, Morcuende S, Talaverón R, Davis-López de Carrizosa M a, de la Cruz RR, Pastor AM. 2014. Neural progenitor cell implants in the lesioned medial longitudinal fascicle of adult cats regulate synaptic composition and firing properties of abducens internuclear neurons. J Neurosci 34:7007–17.

Morcuende S, Matarredona ER, Benítez-Temiño B, Muñoz-Hernández R, Pastor AM, de la Cruz RR. 2011. Differential regulation of the expression of neurotrophin receptors in rat extraocular motoneurons after lesion. J Comp Neurol 12: 2335-52.

Morcuende S, Silva-Hucha S, García-Hernández R, Benítez-Temiño B, de la Cruz RR, Pastor AM. Expression of vascular endothelial growth factor (VEGF) and its receptor Flk-1 in oculomotor system of the rat. 9th FENS Forum of Neuroscience, Milán, Italia, Julio 2014.

Mori T, Buffo A, Götz M. 2005. The novel roles of glial cells revisited: the contribution of radial glia and astrocytes to neurogenesis. Curr Top Dev Biol 69:67–99.

Mosher KI, Andres RH, Fukuhara T, Bieri G, Hasegawa-Moriyama M, He Y, Guzman R, Wyss-Coray T. 2012. Neural progenitor cells regulate microglia functions and activity. Nat Neurosci 15:1485–7.

Nottebohm F. 1985. Neuronal replacement in adulthood. Ann N Y Acad Sci 457:143–61.

Nowacka MM, Obuchowicz E. 2012. Vascular endothelial growth factor (VEGF) and its role in the central nervous system: A new element in the neurotrophic hypothesis of antidepressant drug action. Neuropeptides 46:1–10.

Oppenheim RW, Yin QW, Prevette D, Yan Q. 1992. Brain-derived neurotrophic factor rescues developing avian motoneurons from cell death. Nature 360:755–757.

Orellana J a, Sáez PJ, Shoji KF, Schalper K a, Palacios-Prado N, Velarde V, Giaume C, Bennett MVL, Sáez JC. 2009. Modulation of brain hemichannels and gap junction channels by pro-inflammatory agents and their possible role in neurodegeneration. Antioxid Redox Signal 11:369–99.

Pastor ÁM, Delgado-García JM, Martínez-Guijarro FJ, López-García C, De La Cruz RR. 2000. Response of abducens internuclear neurons to axotomy in the adult cat. J Comp Neurol 427:370–390.

Perea G, Araque A. 2010. GLIA modulates synaptic transmission. Brain Res Rev 63:93–102.

Pluchino S, Martino G. 2005. The therapeutic use of stem cells for myelin repair in autoimmune demyelinating disorders. J Neurol Sci 233:117–119.

Pluchino S, Zanotti L, Deleidi M, Martino G. 2005. Neural stem cells and their use as therapeutic tool in neurological disorders. Brain Res Rev 48:211–219.

Rackauskas M, Neverauskas V, Skeberdis VA. 2010. Diversity and properties of connexin gap junction channels. Medicina (Kaunas) 46:1–12.

Ray A, Zoidl G, Weickert S, Wahle P, Dermietzel R. 2005. Site-specific and developmental expression of pannexin1 in the mouse nervous system. Eur J Neurosci 21:3277–3290.

Reynolds B a, Tetzlaff W, Weiss S. 1992. A multipotent EGF-responsive striatal embryonic progenitor cell produces neurons and astrocytes. J Neurosci 12:4565–4574.

Rivers LE, Young KM, Rizzi M, Jamen F. 2013. Europe PMC Funders Group PDGFRA / NG2 glia generate myelinating oligodendrocytes and piriform projection neurons in adult mice. 11:1–24.

Rosenthal a, Goeddel D V, Nguyen T, Lewis M, Shih a, Laramee GR, Nikolics K, Winslow JW. 1990. Primary structure and biological activity of a novel human neurotrophic factor. Neuron 4:767–773.

Sabelström H, Stenudd M, Réu P, Dias DO, Elfineh M, Zdunek S, Damberg P, Göritz C, Frisén J. 2013. Resident neural stem cells restrict tissue damage and neuronal loss after spinal cord injury in mice. Science 342:637–40.

Saez JC, Berthoud VM, Branes MC, Martinez AD, Beyer EC. 2003. Plasma membrane channels formed by connexins: their regulation and functions. Physiol Rev 83:1359–1400.

Saijo K, Glass CK. 2011. Microglial cell origin and phenotypes in health and disease. Nat Rev Immunol 11:775–787.

Sathasivam S. 2008. VEGF and ALS. Neurosci Res 62:71–77.

Seri B, Herrera DG, Gritti a., Ferron S, Collado L, Vescovi a., Garcia-Verdugo JM, Alvarez-Buylla A. 2006. Composition and organization of the SCZ: A large germinal layer containing neural stem Cells in the adult mammalian brain. Cereb Cortex 16:i103-i111.

Shigemoto-Mogami Y, Hoshikawa K, Goldman JE, Sekino Y, Sato K. 2014. Microglia enhance neurogenesis and oligodendrogenesis in the early postnatal subventricular zone. J Neurosci 34:2231–43.

Siegel GJ, Chauhan NB. 2000. Neurotrophic factors in Alzheimer's and Parkinson's disease brain. Brain Res Brain Res Rev 33:199–227.

Sköld MK, Kanje M. 2008. Vascular endothelial growth factor in central nervous system injuries - a vascular growth factor getting nervous? Curr Neurovasc Res 5:246–59.

Snapyan M, Lemasson M, Brill MS, Blais M, Massouh M, Ninkovic J, Gravel C, Berthod F, Götz M, Barker P a, Parent A, Saghatelyan A. 2009. Vasculature guides migrating neuronal precursors in the adult mammalian forebrain via brain-derived neurotrophic factor signaling. J Neurosci 29:4172–4188.

Storkebaum E, Lambrechts D, Dewerchin M, Moreno-Murciano M-P, Appelmans S, Oh H, Van Damme P, Rutten B, Man WY, De Mol M, Wyns S, Manka D, Vermeulen K, Van Den Bosch L, Mertens N, Schmitz C, Robberecht W, Conway EM, Collen D, Moons L, Carmeliet P. 2005. Treatment of motoneuron degeneration by intracerebroventricular delivery of VEGF in a rat model of ALS. Nat Neurosci 8:85–92.

Tanaka Y, Tozuka Y, Takata T, Shimazu N, Matsumura N, Ohta A, Hisatsune T. 2009. Excitatory GABAergic activation of cortical dividing glial cells. Cereb Cortex 19:2181–2195.

Terenghi G. 1999. Peripheral nerve regeneration and neurotrophic factors. J Anat 194 Pt 1:1–14.

Tonchev a. B, Yamashima T, Guo J, Chaldakov GN, Takakura N. 2007. Expression of angiogenic and neurotrophic factors in the progenitor cell niche of adult monkey subventricular zone. Neuroscience 144:1425–1435.

Verkhratsky A, Butt A. 2007. Glial Neurobiology: A Textbook.

Wang Y, Mao XO, Xie L, Banwait S, Marti HH, David A. 2007. VEGF overexpression delays neurodegeneration and prolongs survival in ALS mice Yaoming. 27:304–307.

Whitman MC, Greer C a. 2010. Adult Neurogenesis and the Olfactory System Mary NIH Public Access. October 89:162–175.

Wicki-Stordeur LE, Dzugalo AD, Swansburg RM, Suits JM, Swayne L. 2012. Pannexin 1 regulates postnatal neural stem and progenitor cell proliferation. Neural Dev 7:11.

Widenfalk J, Lipson a., Jubran M, Hofstetter C, Ebendal T, Cao Y, Olson L. 2003. Vascular endothelial growth factor improves functional outcome and decreases secondary degeneration in experimental spinal cord contusion injury. Neuroscience 120:951–960.

Yamashita T, Ninomiya M, Hernández Acosta P, García-Verdugo JM, Sunabori T, Sakaguchi M, Adachi K, Kojima T, Hirota Y, Kawase T, Araki N, Abe K, Okano H, Sawamoto K. 2006. Subventricular zone-derived neuroblasts migrate and differentiate into mature neurons in the post-stroke adult striatum. J Neurosci 26:6627–6636.

Yano H, Chao M V. 2000. Neurotrophin receptor structure and interactions. Pharm Acta Helv 74:253–60.

Zappalà a., Cicero D, Serapide MF, Paz C, Catania M V., Falchi M, Parenti R, Pantò MR, La Delia F, Cicirata F. 2006. Expression of pannexin1 in the cns of adult mouse: Cellular localization and effect of 4-aminopyridine-induced seizures. Neuroscience 141:167–178.

Zhao M, Momma S, Delfani K, Carlen M, Cassidy RM, Johansson CB, Brismar H, Shupliakov O, Frisen J, Janson AM. 2003. Evidence for neurogenesis in the adult mammalian substantia nigra. Proc Natl Acad Sci U S A 100:7925–7930.

Zhu X, Hill R a, Nishiyama A. 2008. NG2 cells generate oligodendrocytes and gray matter astrocytes in the spinal cord. Neuron Glia Biol 4:19–26.

Zigova T, Pencea V, Wiegand SJ, Luskin MB. 1998. Intraventricular Administration of BDNF Increases the Number of Newly Generated Neurons in the Adult Olfactory Bulbin the Adult Olfactory Bulb. Mol Cell Neurosci 245:234–245.